Aus der II. Medizinische Klinik
der Medizinischen Fakultät Mannheim
(Direktor: Prof. Dr. med. Matthias Ebert)

Impact of Variant Notch Ligands on Chronic Liver Diseases

Inauguraldissertation
zur Erlangung des Doctor scientiarum humanarum (Dr. sc. hum.)
der
Medizinischen Fakultät Mannheim
der Ruprecht-Karls-Universität
zu
Heidelberg

vorgelegt von
Bedair Dewidar

aus
Al-Mahalla El-Kubra, Egypt
2018

Dekan: Prof. Dr. med. Sergij Goerdt
Referent: Prof. Dr. rer. nat. Steven Dooley

TABLE OF CONTENTS

Page

ABBREVIATIONS

α-SMA ..... α-smooth muscle actin
ACLF ..... Acute-on-chronic liver failure
ADAM ..... A desintegrin and metallopeptidase
AGS ..... Alagille syndrome
ALT ..... Alanine aminotransferase
AST ..... Aspartate aminotransferase
APAP ..... Acetaminophen
BDL ..... Bile duct ligation
bHLH ..... Basic helix loop helix
CADASIL ..... Subcortical infarcts and leukoencephalopathy
CBD ..... Common bile duct
CCA ..... Cholangiocarcinoma
CCl_4 ..... Carbon tetrachloride
cDNA ..... Complementary DNA
COUP-TFII... Chicken ovalbumin upstream promoter-transcription factor 2
CSL ..... CBF1/Su(H)/Lag-1
DAB ..... Diaminobenzidine
DEN ..... Diethylnitrosamine
DLL ..... Delta-like ligand
DMEM..... Dulbecco's Modified Eagle Medium
DOS ..... Delta and OSM-11
DR ..... Ductular reaction
DSL Delta-Serrate-Lag-2
ECD ..... Extracellular domain
ECM..... Extracellular matrix
EGF ..... Epidermal growth factor
ELISA ..... Enzyme-linked immunosorbent assay
EMT ..... Epithelial-mesenchymal transition
GSI ..... γ-secretase inhibitors
H&E ..... Hematoxylin and eosin
HBV ..... Hepatitis B virus
HCC ..... Hepatocellular carcinoma
HCs..... Hepatocytes
HD ..... Hetero-dimerization domain
Hes ..... Hairy enhance of split
Hey ..... Hairy enhancer of spit related
HGF ..... Hepatocytes growth factor
HNF ..... Hepatocyte nuclear factor
HRP ..... Horseradish peroxidase
HSCs ..... Hepatic stellate cells
ICC ..... Immunocytochemistry
ICD ..... Intracellular domain
IF ..... Immunofluorescence
IHC ..... Immunohistochemistry
INF-γ..... Interferon-γ
Irf6 ..... Interferon regulatory factor 6
JAG..... Jagged

KCs..... Kupffer cells
KO ..... Knockout
Ldlr ..... Low-density lipoprotein receptor
LPCs..... Liver progenitor cells
LPS..... Lipopolysaccharide
LSECs ..... Liver sinusoidal endothelial cells
MAM ..... Mastermind complex
MCD ..... Methionine-choline-deficient
MDB ..... Maximum diameter of bile infarcts
NEXT ..... Notch extracellular truncation
NFκB..... Nuclear factor kappa B
NICD..... Notch intracellular domain
NRE..... Notch-responsive element
Nrf2..... Nuclear factor erythroid 2–related factor 2
NRR..... Negative regulatory region
NTC ..... Notch transactivation complex
OVA ..... Ova albumin
PBS ..... Phosphate buffered saline
PDAC..... Pancreatic ductal adenocarcinoma
PDGFRB..... Platelet derived growth factor receptor-β
PEST ..... Proline (P), glutamic acid (E), serine (S) and threonine (T) domain
PH ..... Partial hepatectomy
qPCR..... Quantitative real-time PCR
RAM..... RBPJκ-associated module
RBPJκ ..... Recombination signal binding protein Jκ
rCcl2 ..... Recombinant chemokine ligand 2
rDll4 ..... Recombinant DLL4
rJag-1 ..... Recombinant JAG1
RT ..... Room temperature
SIR ..... Systemic inflammatory response syndrome
SOX9 ..... SRY (Sex-Determining Region Y)-Box 9
TAC ..... Transactivation complex
TACE..... Tumor necrosis factor α converting enzyme
TAD ..... Transactivation domain
T-ALL..... T-cell acute lymphoblastic leukemia
TGF-β ..... Transforming growth factor-β
TLR ..... Toll-like receptor
TNF-α ..... Tumor necrosis factor-α
TRAIL ..... TNF-related apoptosis-inducing ligand
Treg ..... T regulatory cells
TSS ..... Transcription start site
UTR ..... Untranslated region
VEGFR ..... Vascular endothelial growth factor receptor

1 INTRODUCTION

Notch signaling is conserved among different species and mediates short-range cell-cell communications. Notch gene was firstly discovered in *Drosophila melanogaster* in 1914 where it was responsible for notches in their wings (Lobry et al., 2014; Metz and Bridges, 1917). In mid-1980, the gene coding for transmembrane Notch receptor was cloned (Artavanis-Tsakonas et al., 1983). Subsequently, Notch family orthologues were identified in numerous organisms including mammals. The Notch signaling mediates a variety of fundamental physiological and biological processes, e.g., cell fate specification, organ development, cell differentiation, proliferation and apoptosis (Fiuza and Arias, 2007; Geisler and Strazzabosco, 2015; Miele, 2006; Morell et al., 2013).

1.1 Structure of Notch receptors and ligands

In comparison to Drosophila (*Drosophila melanogaster*) and Nematoda (*Caenorhabditis elegans*) that have one and two Notch receptors respectively, mammals have four Notch receptors namely NOTCH1, 2, 3, and 4 and five canonical ligands called Delta-like ligand (DLL)1, 3, and 4 and Jagged (JAG)1, and 2 (Fiuza and Arias, 2007). Notch receptors are produced from a single protein precursor that is first cleaved by furin-like convertase in Golgi apparatus (S1 cleavage). This cleavage creates two domains: Notch extracellular domain (ECD) bound non-covalently to transmembrane and intracellular Notch domains (NTMD, and NICD respectively). ECD contains 29-36 epidermal growth factor (EGF)-like repeats that are important in ligand binding. NTMD consists of three cysteine-rich repeat (LIN-12) and two hetero-dimerization units (HD) forming a negative regulatory region (NRR). NRR keeps the second cleavage site (S2) hidden from proteolytic enzymes until the receptor is activated by a Notch ligand. NICD comprises seven Ankyrin repeats, RAM (RBPJκ-associated module) domains, Transactivation domain (TAD) (absent in NOTCH3 and NOTCH4), and PEST (rich in proline (P), glutamic acid (E), serine (S), and threonine (T) residues) domain. RAM domain is crucial for binding to CSL (CBF1/Su(H)/Lag-1) DNA binding proteins and coactivators. Similarly, Notch ligands are heterodimer consisting of ECD and short intracellular domain (ICD) (Figure 1.1) (Carrieri and Dale, 2017; Gil-García and Baladrón, 2016; Kopan and Ilagan, 2009). ECD of Notch ligands contains DSL domain (Delta-Serrate-Lag-2). In addition, DOS

domain (Delta and OSM-11-like proteins) exists only in DLL1 and JAG1/2. Both of these domains are important for binding to EGF-like repeats of Notch receptors. Interestingly, Delta-like non-canonical Notch ligands (DLK1 and DLK2) do not have DSL domain. DLK1 and DLK2 are inhibitors of canonical Notch signaling pathway (Gil-García and Baladrón, 2016) which highlights the importance of DSL domain in the activation of Notch signaling. In comparison to DLL ligands, JAG ligands have specific cysteine-rich regions and more EGF-like repeats in their ECD (Blair, 2000; Chillakuri et al., 2012). ICD domain of Notch ligands are short and not homologous and contains PDZ domain (PDZ domain exists only in JAG1 and DLL1/4) which is necessary for binding to PDZ ligand. Noteworthy, truncated Notch ligands which lacks ICD function as inhibitors of Notch signaling (Hoyne, 2012).

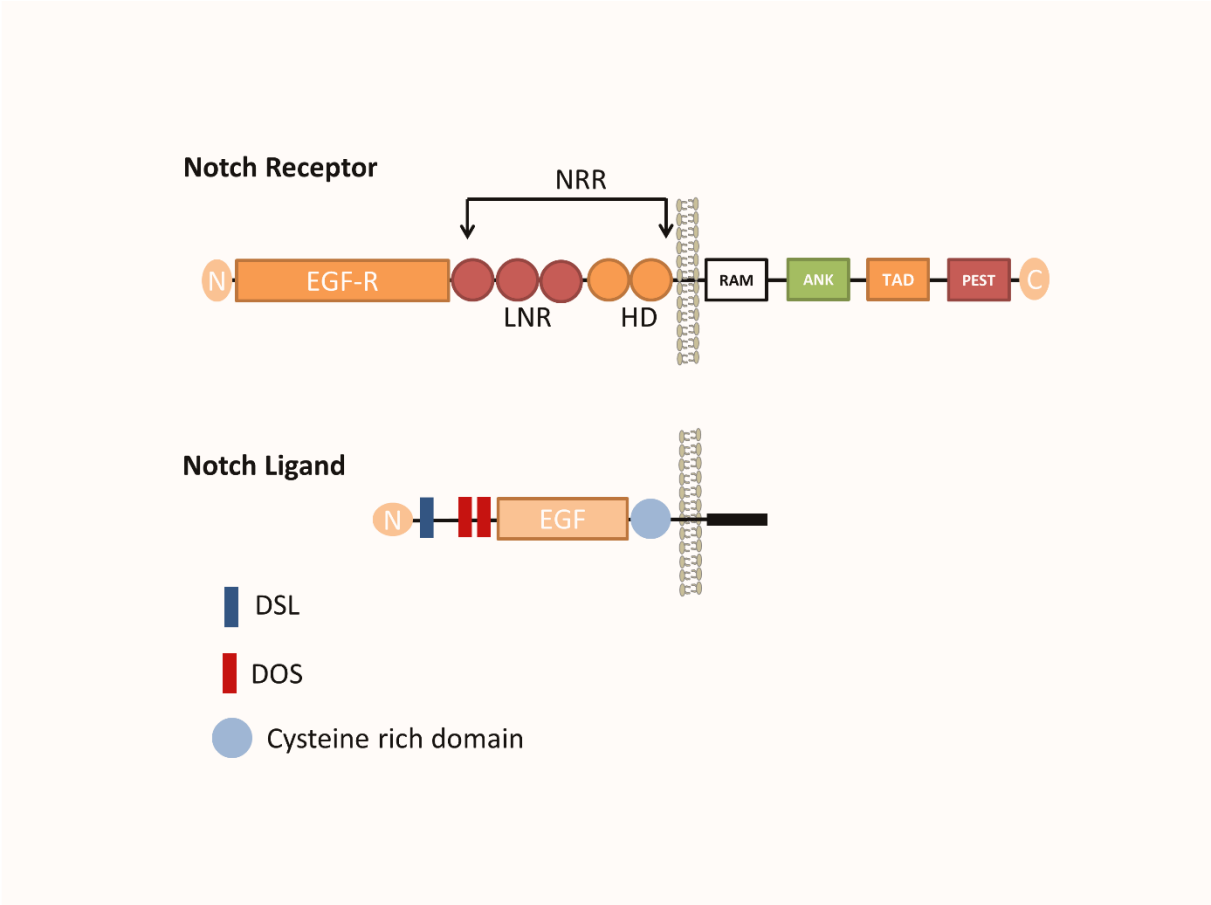

Figure 1.1 Structure of Notch receptors and ligands. NRR, negative regulatory region; LNR: LIN-12 Notch repeat; HD: hetero-dimerization units; EGF: epidermal growth factor (EGF)-like repeats; RAM: RBPJκ-associated module domain; ANK: Ankyrin repeats; TAD: Transactivation domain; PEST: rich in proline (P), glutamic acid (E), serine (S), and threonine (T) residues domain; DSL: Delta-Serrate-Lag-2; DOS: Delta and OSM-11-like proteins. N and C represent the amino- and carboxy-terminus of the protein. Modified from Kopan and Ilagan, 2009.

1.2 Mechanism of canonical Notch signaling

Canonical Notch signaling starts with the binding of a Notch ligand to a Notch receptor expressed on neighboring cells. This kind of binding is called *TRANS* activation. In contrary, when Notch ligands and receptors expressed on the same cells, their binding can lead to Notch inhibition instead of activation. The later type of binding is described as *CIS* inhibition (del Álamo et al., 2011). The *TRANS* binding facilitates uncovering S2 cleavage site and makes it susceptible to proteolytic cleavage by a disintegrin and metallopeptidase (ADAM10/17). S2 cleavage generates Notch extracellular truncation (NEXT) which is rapidly cleaved by transmembrane γ-secretase enzyme complex (S3) using presenilin catalytic subunit. S3 cleavage releases NICD, which translocates into the nucleus where it binds to $RBPJ_k$ (also known as CSL, CBF1/Su(H)/Lag-1) displacing corepressors and attracting coactivators as histone acetylase P300 and Mastermind complex (MAM) forming together Notch transactivation complex (NTC) (Figure 1.2). Noteworthy, $RBPJ_k$ binds to a unique sequence in DNA (CGTGGGAA) which is known as Notch-responsive element (NRE) and exists in the promoters of different Notch target genes (Tun et al., 1994). After transmitting the signal, NICD is quickly phosphorylated at PEST domain followed by ubiquitinylation and degradation (Kopan and Ilagan, 2009).

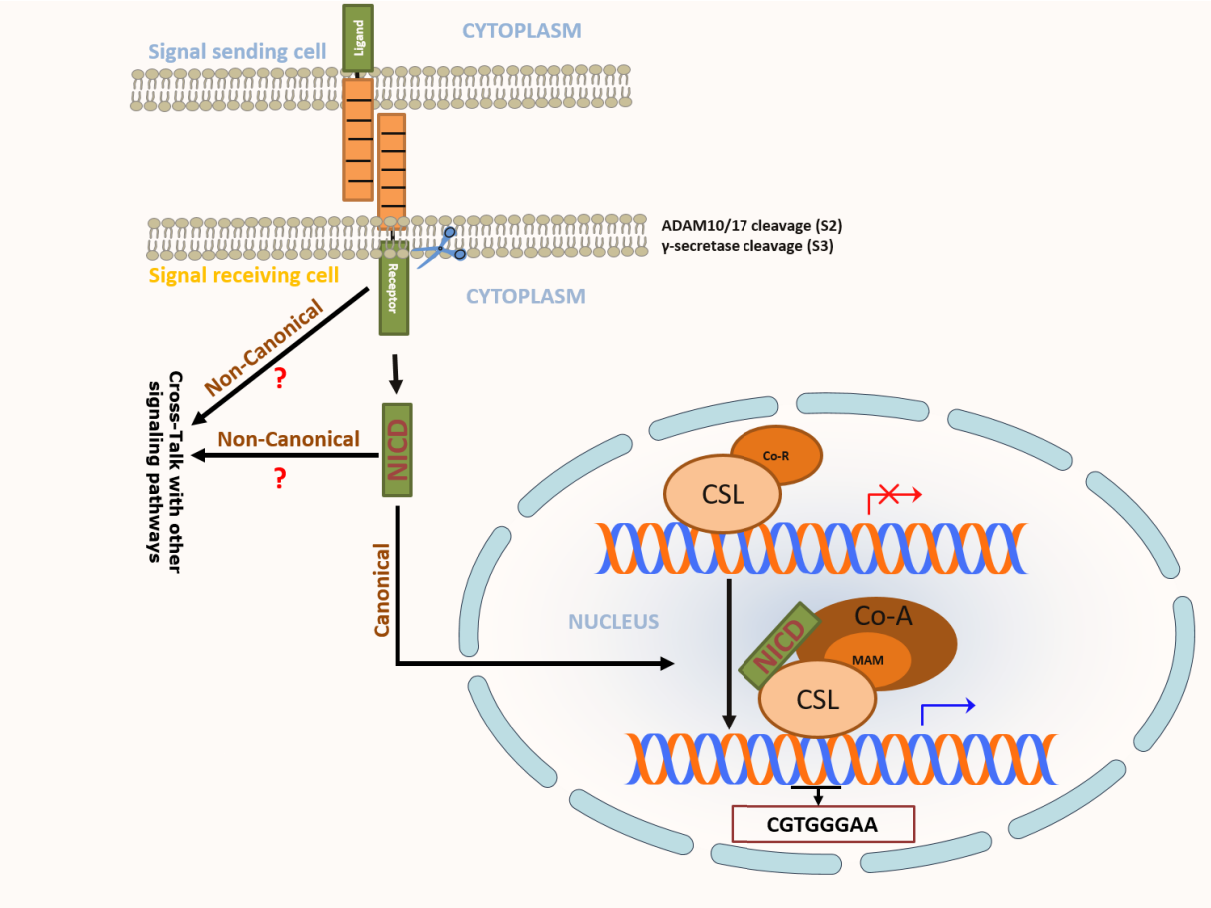

Figure 1.2 Canonical and non-canonical Notch signaling pathway Canonical Notch signaling starts with binding of a Notch ligand to a Notch receptor in *TRANS* activating series of proteolytic activities (S2 and S3) which generate NICD that translocates to the nucleus where it binds CSL protein forming transactivation complex (TAC) and stimulating the expression of Notch target genes. The intracellular part of Notch receptor can interact non-canonically (independent on CSL protein) with other signaling pathways. Non-canonical signaling is not well-characterized and represents an active area of current research. CGTGGGAA represents the DNA-binding site of CSL protein. Co-R, co-repressors; Co-A, co-activators; MAM, mastermind complex. Modified from Andersen et al., 2012; Kopan and Ilagan, 2009.

1.3 Non-canonical Notch signaling pathway

In addition to canonical pathway, Notch signaling could be stimulated by numerous non-canonical signals. Here, we highlight three of them. First, Notch signaling is modulated through a myriad of non-canonical ligands such as DLK1 and DLK2 (Wang, 2011). Non-canonical ligands are defined as secreted or membrane-bound proteins that have EGF-like repeats similar to canonical ligands but lack DSL domain leading to non-optimal binding to Notch receptors and subsequent inhibition of Notch signaling (Wang, 2011). Second, Notch receptors mediate signaling through interacting with different downstream proteins of other signaling pathways. This mechanism could be either Notch ligand-dependent or –independent (Figure 1.2) (Andersen et al., 2012). Third, $RBPJ_k$ forms NICD-independent TAC. For example,

viral proteins such as adenovirus 13SE1A or Epstein-Barr Virus EBNA2 could form TAC with $RBPJ_k$ and stimulate Notch target genes (Siebel and Lendahl, 2017).

1.4 Notch target genes:

The best-characterized Notch target genes are *Hes* (Hairy enhance of split) and *Hey* (Hairy enhancer of spit related) proteins which belong to basic helix loop helix (bHLH) family and act as transcription repressors (Fischer and Gessler, 2007). In addition, Notch signals induce other genes involved in **A**) cells proliferation, e.g. *cyclin D* (Joshi et al., 2009), and *Myc* (Krejcí et al., 2009), **B**) apoptosis and cell cycle arrest, e.g. *Bcl-2* (Deftos et al., 1998) and *p21* (Rangarajan et al., 2001), **C**) Notch pathway itself creating a positive and negative feedback loop to control its activity, e.g. *Nrarp* and *Numb* (Krejcí et al., 2009) and **D**) other signaling pathways that facilitate cross-talking, e.g. *Lip1* and *NfκB* (Krejcí et al., 2009; Osipo et al., 2008). The output of the Notch signaling is highly context-dependent.

1.5 Regulation of Notch signaling

To achieve optimal activity, Notch signaling is regulated by different mechanisms including **I)** Positive and negative feedback loops. Expression of Notch ligands, e.g. DLL1, and JAG1 and receptors, e.g. NOTCH1, and NOTCH3, are controlled by Notch signaling. The increase of ligands and receptors augment Notch signaling, thus creating a positive feedback loop. In additional conditions, Notch ligands could negatively regulate Notch signaling through binding Notch receptors expressed on the same cells, which is defined as "*CIS"* inhibition. Moreover, ICD of JAG1 can inhibit Notch activity through promoting the degradation of NICD. Alternatively, the classical Notch target genes *Hes1* and *Hey1* are transcriptional repressors that suppress the transcription of several Notch genes (Borggrefe and Liefke, 2012). **II)** microRNAs (miRNAs)-mediated regulation. miRNAs are short non-coding nucleotide sequences that bind 3´- untranslated region (UTR) region of specific mRNAs leading to their degradation (Cech and Steitz, 2014). Through targeting several members of Notch family, miRNA-34a mimics induce cell cycle arrest in a rat model of partial hepatectomy (PH) (Wang et al., 2017). Also, miRNA-30 targets *Dll4* expression during angiogenesis leading to enhanced sprouting and branching of blood vessels (Rostama et al., 2014). **III)** rapid degradation of NICD is also a basic regulatory mechanism to keep Notch signal transient. After transporting the Notch signal to the nucleus, CycC:CDK8 enzyme phosphorylate the PEST and TAD domains of NICD,

which is followed by degradation by Fbw7/Sel10 ubiquitin ligase (Fryer et al., 2004). These diverse mechanisms might explain why small alterations in Notch signaling create complex biological outcomes.

1.6 Expression of Notch ligands and receptors in the liver

Different Notch receptors (Nijjar et al., 2001) are expressed in distinct liver cells in a healthy liver. NOTCH1 and 2 are mainly expressed in cholangiocytes and liver progenitor cells (LPCs) (Morell et al., 2013). NOTCH3 and 4 are expressed in mesenchymal and endothelial cells of the liver (Morell et al., 2013). Liver injury alters the expression of Notch receptors. For example, quiescent hepatic stellate cells (qHSCs) express mainly NOTCH1 and low levels of NOTCH3 (Morell et al., 2013). During transactivation process, NOTCH1 is downregulated while NOTCH3 is upregulated (Chen et al., 2012; Sawitza et al., 2009). NOTCH1 and 2 are upregulated in cholangiocytes during a biliary injury (Boulter et al., 2012a). These results suggest a potential role of distinct NOTCH receptors in different liver diseases.

JAG1 and DLL4 are main Notch ligands expressed in the liver. JAG1 localize in biliary cells, liver progenitor cells (LPCs) and smooth muscle cells of the portal vein (Hofmann et al., 2010; Spee et al., 2010), while DLL4 expression is limited to endothelial cells (Loomes et al., 2002).

1.7 Notch signaling in development

Notch signaling plays central roles in tissue and organ development, i.e. stem cell maintenance and differentiation. Lateral inhibition is a specific differentiation program in which Notch signaling can specify two different cell populations from identical parent cell population. Notch signaling can keep the balance between these cellular fates. These processes are important in the development of many organs such as skeletal muscle, lung, nervous system, cardiac tissue, pancreas, and liver (Siebel and Lendahl, 2017).

1.7.1 Notch signaling in liver development:

Mutations of *JAG1* in patients with Alagille syndrome (AGS) gave the first evidence of the involvement of Notch signaling in liver development (Li et al., 1997). AGS is a multi-organ disorder characterized by ductopenia in the liver (Morell et al., 2013). Subsequent studies showed the importance of Notch signaling in stimulating

bipotential hepatoblasts to commit biliary cell fate and to express biliary-specific markers such as hepatocyte nuclear factor (HNF)-1β and SRY (Sex-Determining Region Y)-Box (SOX)9 (Morell et al., 2013; Zong et al., 2009). The role of Notch signaling in the morphogenesis of intrahepatic bile duct was elegantly confirmed by knockout (KO) mouse models of different components of Notch pathway, e.g. *Hes1* (Kodama et al., 2004), *Rbpjκ* (Sparks et al., 2010), *Notch1*, *Notch2* (Geisler et al., 2008; Morell et al., 2013).

1.8 Notch signaling in diseases

Several genetic disorders caused by gene mutations of Notch signaling pathway due to its central roles in the development of various organs (Aster et al., 2017; Mašek and Andersson, 2017). Mutations in *NOTCH3* cause subcortical infarcts and leukoencephalopathy (CADASIL), a hereditary condition characterized by stroke and dementia (Joutel et al., 1996). Similarly, infantile myofibromatosis is caused by mutations in Platelet Derived Growth Factor Receptor beta (*PDGFRB)* and *NOTCH3*, which lead to the development of tumors in skin, bone, muscle, and viscera (Martignetti et al., 2013). Other genetic disorders caused by mutations in Notch genes were summarized in Table 1.1.

Table 1.1 Genetic disorders caused by mutations in Notch-related genes. Modified from Aster et al., 2017; Mašek and Andersson, 2017.

Genetic Disorder	Mutated Gene(s)	Involved Organs	References
subcortical infarcts and leukoencephalopathy (CADASIL)	*NOTCH3*	cerebral arteries	Joutel et al., 1996
Alagille syndrome (AGS)	*JAG1* *NOTCH2*	cardiac tissues, liver, and bone	McDaniell et al., 2006; Oda et al., 1997
Spondylocostal dysostosis (Levin syndrome)	*DLL3*	Vertebrae and ribs	Bulman et al., 2000
Aortic valve disease	*NOTCH1*	Heart	Garg et al., 2005
Adams-Oliver syndrome	*DLL4* *NOTCH1* *RBPJ$_k$*	Skull and limbs	Hassed et al., 2012; Meester et al., 2015; Southgate et al., 2015
Hajdu-Cheney syndrome	*NOTCH2*	Bone tissue	Simpson et al., 2011
Infantile Myofibromatosis	*NOTCH3*	Tumors in multiple organs	Martignetti et al., 2013

Furthermore, Notch signaling is active in adult diseases, e.g. cancer (Aster et al., 2017), inflammation and injury (Geisler and Strazzabosco, 2015; Morell and Strazzabosco, 2014; Morell et al., 2013), fibrosis (Chen et al., 2012), metabolic disorders (Geisler and Strazzabosco, 2015), and others (Siebel and Lendahl, 2017).

The role of Notch signaling in different types of cancers received special attention due to its evident role in controlling cell cycle and cellular proliferation. In fact, Notch signaling plays complex roles in cancer, which could be oncogenic, a tumor suppressor, or both (Nowell and Radtke, 2017) (Table 1.2). Although the exact underlying mechanisms remain to be elucidated, oncogenic mechanisms were related to the ability of Notch pathway to activate genes of cell growth such as *Myc* (Palomero et al., 2006) and PI3K-Akt (Palomero et al., 2007) and cell survival as *Nfκb* (Shin et al., 2006; Vacca et al., 2006). On the other hand, Notch can suppress tumors by mediating antigrowth and pro-differentiation effects through controlling cell

cycle regulator *p21* (Rangarajan et al., 2001), or interferon regulatory factor (*Irf*) 6 (Restivo et al., 2011).

Table 1.2 Tumor promoting and suppressive role of Notch pathway in cancer. Modified from Giovannini et al., 2016; Lobry et al., 2011.

Cancer	Involved Notch R	Role	References
T-cell acute lymphoblastic leukemia (T-ALL)	NOTCH1	🟢	Weng et al., 2004
Skin tumors	NOTCH1	🔴	Nicolas et al., 2003
Squamous cell carcinomas	NOTCH1	🔴	Zhang et al., 2016a
Forebrain tumor	NOTCH1 NOTCH2	🔴	Giachino et al., 2015
pancreatic ductal adenocarcinoma (PDAC)	NOTCH1 NOTCH2	🔴 🟢	Hanlon et al., 2010; Mazur et al., 2010
Gastric cancer	NOTCH2	🟢	Tseng et al., 2012
Colorectal cancer	NOTCH1	🟢	Ishiguro et al., 2017
Breast cancer	NOTCH1 NOTCH2 NOTCH3 NOTCH4	🟢	Fu et al., 2010; Gallahan and Callahan, 1997; Klinakis et al., 2006; Yamaguchi et al., 2008
Ovarian cancer	NOTCH3	🟢	Park et al., 2006
Prostate cancer	NOTCH1	🟢	Ye et al., 2012
Bladder cancer	NOTCH2	🟢	Hayashi et al., 2016
Hepatocellular carcinoma (HCC)	NOTCH1 NOTCH2 NOTCH3	🟢	Giovannini et al., 2013, 2016b
Cholangiocarcinoma (CCA)	NOTCH1	🟢	Huntzicker et al., 2015

🔴 Tumor suppressive 🟢 Oncogenic

1.8.1 Notch signaling in liver cancer

The mutation of Notch genes in liver cancer was not yet demonstrated; however, there are many reports showing the dysregulation of Notch signaling in liver

carcinogenesis (Geisler and Strazzabosco, 2015). For example, NOTCH1 and NOTCH2 mediate oncogenic role in hepatocellular carcinoma (HCC) and cholangiocarcinoma (CCA). The overexpression of N1ICD and N2ICD in hepatoblasts induces HCC and CCA formation in mice (Dill et al., 2013; Villanueva et al., 2012). In the presence of tumor-inducing agents such as diethylnitrosamine (DEN), or thioacetamide, tumor formation shifts mainly to CCA (Dill et al., 2013; Sekiya and Suzuki, 2012). Several studies reported as well oncogenic role for NOTCH3 in HCC and CCA (Guest et al., 2014; Hu et al., 2013). However, NOTCH3 inhibition did not influence tumor burden in mice (Huntzicker et al., 2015).

Furthermore, DLL4 ligand regulates tumor angiogenesis. Interestingly, the activation and the inhibition of DLL4-mediated Notch signaling inhibit tumor growth by inducing tumor hypoxia (Noguera-Troise et al., 2006; Segarra et al., 2008).

Tumor suppressive roles have been attributed as well to Notch signaling in liver malignancies. For example, NOTCH1 sensitizes HCC cells to TNF-related apoptosis-inducing ligand (TRAIL)-induced apoptosis by interfering with the proteasomal degradation of p53 (Wang et al., 2009).

1.8.2 Notch signaling in liver regeneration

The effects of Notch signaling on liver injury and regeneration were extensively investigated in acute and chronic liver diseases. Köhler et al. reported nuclear accumulation of NICD in hepatocytes of rats 15 minutes (min) following PH (Köhler et al., 2004). In addition, silencing of *Jag1* and *Notch1* significantly reduced the proliferative capacity of hepatocytes of animals receiving PH (Köhler et al., 2004). Notch signaling exerts its effect in liver regeneration in cooperation with numerous growth factors such as hepatocytes growth factor (HGF) and EGF, and cytokines such as tumor necrosis factor (TNF)-α, and tumor growth factor (TGF)-β (Best et al., 2015).

The regenerative capacity of the liver is unique, by which a rodent liver can restore lost mass in 7 days (d) after 70% PH (Libbrecht, 2006). Regeneration in a healthy liver mainly depends on hepatocytes replication. In patients with chronic or severe liver diseases, regeneration occurs in the presence of continuous injuring insult such as virus and toxic drugs. Upon loss of more than 50% hepatocytes, the regenerative capacity of hepatocytes is compromised. In this situation, liver progenitors cells (LPCs)-based regeneration initiates (Best et al., 2015; Katoonizadeh et al., 2006).

LPCs are bi-potential liver stem cells localizing inside the canal of Herring and able to differentiate into hepatocytes or cholangiocytes (Lukacs-Kornek and Lammert, 2017). Microenvironment surrounding LPCs orchestrates the direction of their differentiation exploiting Notch and Wnt signaling. After the biliary injury, JAG1 expressed on myofibroblasts activates LPCs to differentiate to cholangiocytes (Boulter et al., 2012a). On the other side, when hepatocytes are the main damaged cells, infiltrated macrophages release WNT3A upon phagocytosis of the dead hepatocytes. WNT3A is a ligand of Wnt signaling pathway, which inhibits Notch signaling in LPCs by upregulating NUMB protein. Inhibition of Notch signaling stimulates the differentiation of LPCs to hepatocytes (Boulter et al., 2012b; Strazzabosco and Fabris, 2013). These results suggest that Notch signaling is the default inducer of biliary differentiation. In line with these results, the inhibition of Notch signaling by γ-secretase inhibitors (GSI) decreases the number of LPCs and ductular reaction (DR) in mice models with experimentally-induced biliary damage (Fiorotto et al., 2013). Noteworthy, this attractive idea could not be confirmed in a later study of lineage tracing. Both genetic inhibition of Notch signaling and activation of Wnt signaling were required for effective biliary maturation and expansion of DR, but failed to instruct the cells of 3,5-diethoxycarbonyl-1,4-dihydrocollidine (DDC)-induced DR to differentiate to hepatocytes (Jörs et al., 2015).

Beside the role of Notch signaling in liver regeneration, it could protect liver cells by upregulating Nuclear factor (erythroid-derived 2)-like 2 (Nrf2) signaling pathway. The protective functions of Nrf2 signaling are linked to its ability to stimulate the synthesis of various antioxidant enzymes that defense against oxidative stress-mediated cellular toxicity (Nguyen et al., 2009). Wakabayashi et al. reported that transient and stable expression of NICD in mouse hepatocytes protects the liver against paracetamol (APAP)-induced hepatotoxicity by inducing *Nrf2* expression. (Wakabayashi et al., 2014). In summary, Notch can cross-talk with different signaling pathways to direct liver regeneration or afford cytoprotection.

1.8.3 Notch signaling and liver fibrosis

Liver fibrosis is a scarring healing response characterized by the production of a large amount of extracellular matrix (ECM) which disturbs the normal function of the liver and could progress to liver cirrhosis and cancer in advanced stages (Friedman, 2008; Hernandez-Gea and Friedman, 2011).

Notch signaling plays crucial roles in the fibrosis of various organs such as liver, kidney, peritoneum, and heart (Bielesz et al., 2010; Chen et al., 2012; Nistri et al., 2017; Zhu et al., 2010). HSCs, the main producer of ECM in the liver, upregulate NOTCH3 and JAG1 during activation and trans-differentiation to myofibroblasts (Chen et al., 2012). Incubation of primary stellate cells with profibrogenic cytokine TGF-β induces *Jag1* expression (Morell et al., 2017), whereas HSCs stimulated with JAG1 increases α-smooth muscle actin (α-SMA) and collagen production (Geisler and Strazzabosco, 2015).

In vivo inhibition of Notch signaling with GSI protected hepatocytes against apoptosis and improved liver fibrosis in rats or mice with carbon tetrachloride (CCl_4) (Bansal et al., 2015; Chen et al., 2012), bile duct ligation (BDL) (Zhang et al., 2016b), and methionine-choline-deficient (MCD) diet administration (Morell et al., 2017).

In patients, Notch signaling is activated in severe liver fibrosis caused by different etiologies (He et al., 2015). On the other hand, AGS patients rarely develop liver fibrosis (Fabris et al., 2007). Taken together, Notch signaling might mediate profibrogenic functions in the liver.

1.8.4 Notch signaling and inflammation

Notch pathway can modulate inflammatory responses by stimulating M1 polarization of macrophages, which represent the inflammatory subtype of macrophage population (Xu et al., 2012). Thus, inhibition of Notch signaling suppressed M1 macrophage, increased anti-inflammatory M2 macrophage, and prevented HSC activation (Bansal et al., 2015). *Notch1* heterozygous KO mice have a reduced inflammatory response to lipopolysaccharide (LPS) and interferon (INF)-γ treatments (Outtz et al., 2010).

In vitro, the incubation of RAW264.7 macrophage cell line with LPS and INF-γ increased the expression of NOTCH1 and JAG1 (Monsalve et al., 2006), whereas N1ICD overexpression increased TNF-α and IL-6 expression (Shang et al., 2016) suggesting a positive feedback loop between inflammation and Notch signaling.

Several reports showed the interdependence between inflammation and liver fibrosis. For example, HSCs are highly responsive to LPS and inflammatory cytokines. Furthermore, secreted inflammatory cytokines keep the activated state of HSCs and maintain their survival (Seki and Schwabe, 2015). Additionally, targeting hepatic inflammation could stabilize and reverse liver fibrosis (Czaja, 2014). Considering its

roles in liver inflammation and fibrosis, Notch signaling might be a promising therapeutic target in inflammation-driven liver fibrosis.

1.9 JAG1- versus DLL4-mediated pathobiological effects

DLL4 and JAG1 are two Notch ligands expressed in the liver. Although both Notch ligands share similar binding sites, they mediate distinct biological functions. The molecular mechanisms remain obscure. In certain scenarios, it might be related to the expression pattern of such ligands on different cellular compartments. In other cases, the opposite biological functions are because of the differential affinity of Notch receptors to those ligands.

In asthma for example, DLL4 and JAG1 can produce opposite effects. JAG1 expressed on bone marrow-derived dendritic cells (DCs) activate Notch receptors on $CD4^+$ T-Cells stimulating IL-4 production and lead to airway hyper-responsiveness. On the other hand, DLL4 expressed on regulatory T cells (Treg) cells decreased the number of lung vessels which improved airway hyper-responsiveness (Huang et al., 2009; Okamoto et al., 2009). Recently, these results were confirmed in animal model of ova albumin (OVA)-induced allergic asthma (Huang et al., 2017). Moreover, upregulated *Jag1* facilitated fibrogenesis, whereas *Dll4* was downregulated in an animal model of bleomycin-induced pulmonary fibrosis (Yin et al., 2017).

During angiogenesis, DLL4- and JAG1-mediated effects antagonize each other. NOTCH1-DLL4 mediated signaling inhibits the sprouting of endothelial tip cells. JAG1 antagonizes DLL4-mediated effects mainly because of posttranslational modification of NOTCH1 receptor by Fringe enzyme. The Fringe-modified NOTCH1 receptor has a higher affinity for DLL4 than JAG1. When both ligands expressed on the same cells, JAG1 interfere with binding of DLL4 to NOTCH1 receptor and enhances sprouting. Furthermore, DLL4 reduce vascular endothelial growth factor receptor (VEGFR)2 while JAG1 induce VEGFR3 expression (Benedito et al., 2009; Liu et al., 2014). Recently, vimentin, an intermediate filament protein, was reported to balance JAG1 and DLL4 signaling in angiogenesis. Vimentin enhances JAG1 mediated signaling by supporting ligand-receptor trans-endocytosis, while it decreased DLL4 mediated signaling through inhibition of expression of Fringe proteins (Antfolk et al., 2017).

In the liver, DLL4 and JAG1 differentially regulate chicken ovalbumin upstream promoter-transcription factor 2 (COUP-TFII), an orphan nuclear receptor involved in HSCs activation and trans-differentiation. Fibrotic human and mouse liver have high

expression of COUP-TFII. In cultured HSCs, JAG1, but not DLL4, suppress COUP-TFII in *Hey1*-dependent mechanisms (Ceni et al., 2017).
In addition, inflammatory cytokines differentially regulate DLL4 and JAG1 expression. In primary macrophages, IFN-γ augmented LPS-induced JAG1 expression, whereas it downregulated DLL4 (Foldi et al., 2010). TNF-α induced JAG1, but not DLL4 expression in mouse aortic endothelial cells (Nus et al., 2016).

1.10 The aim of the current study:

Although Notch signaling plays crucial roles in liver injury and fibrosis, the contribution of individual Notch ligands is still not well-defined. The current knowledge of Notch signaling in liver fibrosis is based mainly on animal models receiving GSI administration. GSI have several side effects including gastrointestinal toxicity because of the vital role of Notch signaling in gastrointestinal hemostasis. Furthermore, the γ-secretase enzyme impacts expression of other important molecules such as CD44, cadherins, and ERBB4 (Andersson and Lendahl, 2014). These effects result in non-Notch signaling-dependent biological responses. To avoid these side effects, the current study investigates the effects of DLL4 and JAG1 on liver damage in patients with hepatitis B virus (HBV)-induced liver cirrhosis, and two mouse models induced by CCl_4 and BDL, respectively. In addition, how DLL4 and JAG1 exert their effects was investigated in isolated primary liver cells and cell lines.

2 MATERIALS AND METHODS

2.1 Reagents

The reagents, chemicals, cytokines, recombinant proteins, and antibodies used in the current study were listed in Table 2.1 and Table 2.2.

Table 2.1 Reagents

Reagent	Order Nr.	Company
4-(2-hydroxyethyl)-1-piperazineethanesulfonic acid (HEPES)	H4034-100G	Sigma-Aldrich, Munich, Germany
5x HOT FIREPol EvaGreen qPCR Mix Plus (ROX)	08-24-00020	Solis Biodyne, Tartu, Estonia
Acid Fuchsin	F8129-25G	Sigma-Aldrich, Munich, Germany
Acrylamide/Bis-acrylamide, 30% solution	10688.02	SERVA, Heidelberg, Germany
Agar	5210.1	Carl Roth, Mannheim, Germany
Ammonium persulfate (APS)	A3678-25G	Sigma-Aldrich, Munich, Germany
Bouin's solution	HT10132-1L	Sigma-Aldrich, Munich, Germany
Bovine Serum Albumin (BSA)	11930	SERVA, Heidelberg, Germany
Bromophenol blue	APP3640A/0.005	Armin Baack, Schwerin, Germany
Calcium chloride dihydrate ($CaCl_2.2\ H_2O$)	C3306-500G	Sigma-Aldrich, Munich, Germany
CD11b MicroBeads, human and mouse	130-049-60	Miltenyi, Gladbach, Germany
CHAPS	1479.3	Carl Roth, Mannheim,

		Germany
Collagen	11 179 179 001	Roche, Mannheim, Germany
Collagenase type II, CLSII	C2-22	Merck, New Jersey, USA
complete protease inhibitor cocktail tablets	4693132001	Roche, Mannheim, Germany
Dako Dual Endogenous Enzyme Block	S200389-2	DAKO, Glostrup, Denmark
DAKO Fluorescent Mounting Medium	S3023	DAKO, Glostrup, Denmark
DAPI	D9542-5MG	Sigma-Aldrich, Munich, Germany
Deoxycholic acid sodium salt (DOC)	18330.03	SERVA, Heidelberg, Germany
Dexamethasone	D1159-100MG	Sigma-Aldrich, Munich, Germany
D-Glucose	G8270-1KG	Sigma-Aldrich, Munich, Germany
Direct Red 80 (sirius red)	365548-5G	Sigma-Aldrich, Munich, Germany
Dithiothreitol (DTT)	A1101,0010	AppliChem, Darmstadt, Germany
DMEM medium	BE12-709F/12-M	Lonza, Basel, Switzerland
DMEM/F-12	21331-020	Thermo Fischer Scientific, Massachusetts, USA
DNase I	A3778	AppliChem, Darmstadt, Germany
dNTP Mix, 10 mM each, 0.2 mL	R0191	Thermo Fischer Scientific, Massachusetts, USA
DPBS	9124.1	Carl Roth, Mannheim, Germany
DRAQ5	4084L	New England Biolabs, Massachusetts, USA
Easycoll	L6145	Merck, New Jersey, USA

Eosin	1098441000	Merck, New Jersey, USA
Ethanol 99%	T171.4	Carl Roth, Mannheim, Germany
Ethanol absolute	LC40451	neoLab, Heidelberg, Germany
Ethylene glycol-bis(β-aminoethyl ether)-N,N,N',N'-tetraacetic acid (EGTA)	E3889-25G	Sigma-Aldrich, Munich, Germany
Ethylenediaminetetraacetic acid (EDTA)	324503	Calbiochem, San Diego, USA
Fetal Bovine Serum (FBS)	10270	Thermo Fischer Scientific, Massachusetts, USA
Glycerol	G5516-500ml	Sigma-Aldrich, Munich, Germany
Hanks' BSS (1X)	882012	Biozym, Oldendorf, Germany
Hematoxylin solution A according to Weigert	X906.1	Carl Roth, Mannheim, Germany
Hematoxylin solution according to Meyer	MHS16-500ML	Sigma-Aldrich, Munich, Germany
Hematoxylin solution B according to Weigert	X907.1	Carl Roth, Mannheim, Germany
HiSpeed Plasmid Midi Kit (25)	12643	Qiagen, Hilden, Germany
Histodenz	D2158-100G	Sigma-Aldrich, Munich, Germany
Human recombinant DLL4	1506-D4-050-CF	R&D, Minneapolis, USA
Human recombinant JAG1	1277-JG	R&D, Minneapolis, USA
Hydrogen peroxide (H_2O_2)	1072102500	Merck, New Jersey, USA
Insulin-Transferrin-Selenium (ITS -G) (100X)	41400045	Thermo Fischer Scientific, Massachusetts, USA
JSH-23 (NfκB inhibitor)	J4455-5MG	Sigma-Aldrich, Munich, Germany

Ketaminhydrochlorid 100 mg / ml	Hostaket ®	Parke-Davis, Freiburg, Germany
L-Alanine	A7627-100G	Sigma-Aldrich, Munich, Germany
L-Asparagine	A0884-25G	Sigma-Aldrich, Munich, Germany
L-Aspartic Acid	A6558-25G	Sigma-Aldrich, Munich, Germany
LB Broth (Miller)	X968.1	Carl Roth, Mannheim, Germany
L-Citrullin	C7629-25G	Sigma-Aldrich, Munich, Germany
L-Cysteine	168149-25G	Sigma-Aldrich, Munich, Germany
L-Glutamic Acid	G1251-100G	Sigma-Aldrich, Munich, Germany
L-Glutamine	G3126-100G	Sigma-Aldrich, Munich, Germany
L-Glutamine 200mM	G7513	Sigma-Aldrich, Munich, Germany
L-Glycine	G7126-100G	Sigma-Aldrich, Munich, Germany
L-Histidine	H-6034	Sigma-Aldrich, Munich, Germany
Light green	L5382-10G	Sigma-Aldrich, Munich, Germany
Lipopolysaccharide (LPS)	L3012-5mg	Sigma-Aldrich, Munich, Germany
L-Isoleucine	I7403-25G	Sigma-Aldrich, Munich, Germany
L-Leucine	L-8912	Sigma-Aldrich, Munich, Germany
L-Lysine	L5501-25G	Sigma-Aldrich, Munich, Germany

L-Methionine	M9625-25G	Sigma-Aldrich, Munich, Germany
L-Ornithine	O6503-25G	Sigma-Aldrich, Munich, Germany
L-Phenylalanine	P2126-100G	Sigma-Aldrich, Munich, Germany
L-Proline	P-5607	Sigma-Aldrich, Munich, Germany
L-Serine	S4311-25G	Sigma-Aldrich, Munich, Germany
L-Threonine	T8625-25G	Sigma-Aldrich, Munich, Germany
L-Tryptophane	T8941-25G	Sigma-Aldrich, Munich, Germany
L-Tyrosine	T3754-50G	Sigma-Aldrich, Munich, Germany
Luciferase assay reagent	E1483	Promega, Mannheim, Germany
Luminol	09253-25G	Sigma-Aldrich, Munich, Germany
L-Valine	V0513-25G	Sigma-Aldrich, Munich, Germany
Magnesium Chloride, Hexahydrate ($MgCl_2$. $6H_2O$)	5980-500GM	Sigma-Aldrich, Munich, Germany
Magnesium sulfate heptahydrate ($MgSO_4$ .7 H_2O)	63138-250G	Sigma-Aldrich, Munich, Germany
Malinol oil	3c-242	Waldeck, Münster, Germany
Methanol	4627.2	Carl Roth, Mannheim, Germany
Mouse CCL2/JE/MCP-1 DuoSet ELISA kit	DY479-05	R&D, Minneapolis, USA
Mouse recombinant CCL2	479-JE-010	R&D, Minneapolis, USA

Mouse recombinant DLL4	1389-D4-050-CF	R&D, Minneapolis, USA
N,N,N′,N′-Tetramethylethylenediamine (TEMED)	T9281-25ML	Sigma-Aldrich, Munich, Germany
Nonidet P40	11754599001	Sigma-Aldrich, Munich, Germany
Nycodenz	1002424	Progen Biotechnik, Heidelberg, Germany
Page Ruler Plus (prestained protein ladder)	26620	Thermo Fischer Scientific, Massachusetts, USA
p-Coumaric Acid	C9008-5G	Sigma-Aldrich, Munich, Germany
Penicillin-Streptomycin 100x (P/S)	P0781	Sigma-Aldrich, Munich, Germany
Percoll	GEHE17-0891-01	Sigma-Aldrich, Munich, Germany
Phosphatase inhibitors cocktail	P5726	Sigma-Aldrich, Munich, Germany
Phosphate buffer saline (PBS) powder	L182-50	Merck, New Jersey, USA
Phosphomolybdic acid	4440.3	Carl Roth, Mannheim, Germany
Phosphotungstic acid hydrate	2635.2	Carl Roth, Mannheim, Germany
Ponceau Xylidine	P2395-25G	Sigma-Aldrich, Munich, Germany
Potassium chloride (KCl)	P9333-500G	Sigma-Aldrich, Munich, Germany
Potassium phosphate dibasic (KH_2PO_4)	P2222-100G	Sigma-Aldrich, Munich, Germany
Pronase E	1.07433.005	Merck, New Jersey, USA
Proteinase K	S300402-2	DAKO, Glostrup, Denmak
Random Hexamer EA	SO142	Thermo Fischer Scientific, Massachusetts, USA

Recombinant Human CCL2/MCP-1	279-MC-010	R&D, Minneapolis, USA
Recombinant murine TNF-α	315-01A	Peprotech, Hamburg, Germany
Reporter Lysis Buffer 5X	E3971	Promega, Mannheim, Germany
RevertAid H Minus Reverse Transcriptase	EP0451	Thermo Fischer Scientific, Massachusetts, USA
RNA extraction kit	1060100300	Stratec, Birkenfeld, Germany
Roti Histofix (4% buffered formaldehyde solution)	5666.2	Carl Roth, Mannheim, Germany
Saturated aqueous solution of picric acid (1.3% in H_2O)	P6744-1GA	Sigma-Aldrich, Munich, Germany
Sodium bicarbonate ($NaHCO_3$)	S5761-500G	Sigma-Aldrich, Munich, Germany
Sodium chloride (NaCl)	P029.3	Carl Roth, Mannheim, Germany
Sodium dodecyl sulfate (SDS)	2326.2	Carl Roth, Mannheim, Germany
Sodium phosphate dibasic (Na_2HPO_4)	255793-10G	Sigma-Aldrich, Munich, Germany
Sodium phosphate monobasic monohydrate (NaH_2PO_4. H_2O)	71507-250G	Sigma-Aldrich, Munich, Germany
Subcloning Efficiency™ DH5α™ Competent Cells	18265017	Thermo Fischer Scientific, Massachusetts, USA
Sucrose	S0389-500G	Sigma-Aldrich, Munich, Germany
TGF-β	240-B-010	R&D, Minneapolis, USA
TRIS	5429.5	Carl Roth, Mannheim, Germany
Trisodium citrate dihydrate	S1804-500G	Sigma-Aldrich, Munich, Germany

Triton X-100	T-9284	Sigma-Aldrich, Munich, Germany
Trypsin-EDTA solution 10X	T4174-100M	Sigma-Aldrich, Munich, Germany
Tween 20	1247ML500	neoLab, Heidelberg, Germany
Viromer red	VR-01LB-01	Lipocalyx, Halle, Germany
William's E medium	W1878-6X500ML	Sigma-Aldrich, Munich, Germany
Xylazine hydrochloride 20 mg / ml	Rompun ®	Bayer, Leverkusen, Germany
Xylene	9713.2	Carl Roth, Mannheim, Germany
β-Mercaptoethanol	A4338,0250	AppliChem, Darmstadt, Germany

Table 2.2 Primary and secondary antibodies used in the current study. * antigen retrieval with citrate buffer. For antigen retrieval without *, EDTA buffer was used.

Antibody name	**Host**	**Product number**	**Dilution**	**Application**	**Company**
Primary antibodies					
α-SMA	mouse	M0851	1:500	IHC/IF	DAKO
Ccl-2	rabbit	LS-C211039-100	1:200	IHC	LS-Bio
CD16	mouse	Ab74512	Ready to use	IF	Abcam
CD45	rabbit	ab10558	1:50	IHC*	Abcam
Cleaved-caspase-3	rabbit	9664	1:100	IHC*	Cell Signaling
Desmin	rabbit	ab15200	1:100	IF	Abcam
Dll1	rabbit	sc-9102	1:100	IHC	Santa Cruz
Dll3	rabbit	sc-67269	1:100	IHC	Santa Cruz

Dll4	rabbit	sc-28915	1:100	IHC	Santa Cruz
F4/80	rat	ab6640	1:150	IHC*	Abcam
F4/80	rat	14-4801-81	1:100	IF	eBioscience
GAPDH	rabbit	Ab9485	1:2500	WB	Abcam
Histone H1	mouse	Sc-8030	1:500	WB	Santa Cruz
HNF-4α	rabbit	3113	1:100	IF	Cell signaling
Jagged1	goat	sc-6011	1:500	IHC	Santa Cruz
Jagged2	rabbit	sc-5604	1:50	IHC	Santa Cruz
Ly-6B	rat	MCA771GA	1000	IHC *	AbD Serotec
Myeloperoxidase	rabbit	AB45977	1:50	IHC *	Abcam
Notch1	goat	sc-6014	1:100	IHC	Santa Cruz
Notch2	rabbit	ab8926	1:200	IHC	Abcam
Notch3	rabbit	sc-5593	1:100	IHC	Santa Cruz
Notch4	rabbit	ab23427	1:50	IHC	Abcam
p50	mouse	Sc-8414	1:500	WB	Santa Cruz
p65	rabbit	Sc-372	1:500	WB	Santa Cruz
Stabilin2	mouse	MAB3645	1:25	IF	R & D
Secondary antibodies					
Polyclonal anti-Rabbit / HRP	swine	P0217	1:200	IHC	Dako
Polyclonal anti-mouse / HRP	goat	P0447	1:200	IHC	Dako
Polyclonal Anti-Rat / HRP	rabbit	P0450	1:200	IHC	Dako
Alexa Fluor® 488 Anti-Rat	Donkey	712-546-150	1:200	IF	Jackson ImmunoResearch
Alexa Fluor® 488 Anti-Rabbit	Donkey	711-546-152	1:200	IF	Jackson ImmunoResearch
Alexa Fluor® 488 Anti-Mouse	Donkey	715-545-150	1:200	IF	Jackson ImmunoResearch
Cy™ Anti-Mouse	Donkey	715-225-150	1:200	IF	Jackson ImmunoResearch
Cy™2 Anti-	Donkey	711-225-	1:200	IF	Jackson

Rabbit		152			ImmunoResearch
Cy™2 Anti-Rat	Donkey	712-225-153	1:200	IF	Jackson ImmunoResearch
Cy™3 Anti-Rat	Donkey	712-165-153	1:200	IF	Jackson ImmunoResearch
Cy™3 Anti-Mouse	Donkey	715-165-150	1:200	IF	Jackson ImmunoResearch
Cy™3 Anti-Rabbit	Donkey	711-165-152	1:200	IF	Jackson ImmunoResearch
Anti-Mouse / HRP	goat	sc-2063	1:3000	WB	Santa Cruz
Anti-Rabbit / HRP	goat	sc-2301	1:3000	WB	Santa Cruz

2.2 Patients' liver tissue specimen

Liver tissues from 31 patients, 5 with hepatolithiasis, and 26 with HBV-induced cirrhosis (10 with compensated cirrhosis and 16 with acute-on-chronic liver failure (ACLF)) were obtained from The First Affiliated Hospital, College of Medicine, Zhejiang University, China. In addition, 5 liver samples from patients undergoing liver resection due to hepatic hemangioma were included as a healthy control. Informed written consents were collected from all patients or relatives. The study was approved by the Ethics Committee of The First Affiliated Hospital, College of Medicine, Zhejiang University.

2.3 Cells

Primary mouse liver cells, e.g. hepatocytes (HCs), Kupffer cells (KCs), and hepatic stellate cells (HSCs) and cell lines, e.g. mouse HSCs (JS-1), mouse HCs (AML-12), and mouse macrophage (RAW264.7) were used in the current study. JS-1 cell line (Guo et al., 2010) was kindly provided by Dr. Scott Friedman (Mount Sinai School of Medicine, New York, USA). RAW264.7 cells were a kind gift from Dr. Astrid Schmieder (Heidelberg University, Germany). AML-12 cell line was purchased from ATCC cell bank (Virginia, USA). Cells were cultured in described mediums (Table 10.1) in a humidified incubator at 37 C° with 5% CO_2.

2.3.1 Isolation and treatment of primary HSCs:

HSCs were isolated according to Mederacke et al., 2015 with minor modifications. Briefly, 5-7 months old C57BL/6N mice were anesthetized with a commercial combination of xylazine and ketamine (Hostaket ® and Rompun ®), the liver was exposed and perfused through vena cava with three different sequential solutions: EGTA, pronase E, and collagenase D (Appendix 10.1.7.14). Next, the portal vein was cut to drain out the perfusion solutions and to reduce the internal liver pressure. Later, the liver was minced gently, and filtered through 100 µM cell strainer (Corning, Wiesbaden, Germany). Finally, HSCs were separated from the top layer of Nycodenz gradient (8.27%). After three days of culture with TGF-β (5 ng/ml) and/or recombinant Dll4 (rDll4) (500 ng/ml), the RNA was collected for analysis of HSC activation markers, e.g. *α-Sma*, collagen 1α1 (*Col1α1*), and collagen 1α2 (*Col1α2*).

2.3.2 Isolation and treatment of primary HCs and KCs:

Isolation of mouse HCs and KCs were carried out according to Hengstler et al., 2000; and Hu et al., 2014 with minor modifications. Similar to HSCs isolation, 16 weeks old C57BL/6N were anesthetized and the liver was exposed and perfused sequentially through vena cava with EDTA and collagenase solutions. Next, the liver was minced gently in suspension buffer and filtered through 100 µM cell strainer (Corning, Wiesbaden, Germany). Hepatocytes were separated by centrifugation at 50g for 2 min. The viable HCs were enriched by percoll density gradient and used for activated caspase-3 assay. KCs were isolated from non-parenchymal cell fraction using CD11b microbeads according to Hu et al., 2014. KCs were cultured in KC medium and stimulated with LPS (20 ng/ml) for 16 hours (h). Then, the cells were incubated with LPS for 6 h with/without rDll4 (500 ng/ml). RNA was collected for further analysis. All used buffers and mediums were described in Appendix 10.2 and 10.1.7. The purity of isolated primary HCs, KCs, and HSCs was checked by immunofluorescence staining with specific cell markers, hepatocyte nuclear factor (HNF)-4α, F4/80, and DESMIN respectively (Figure 2.1).

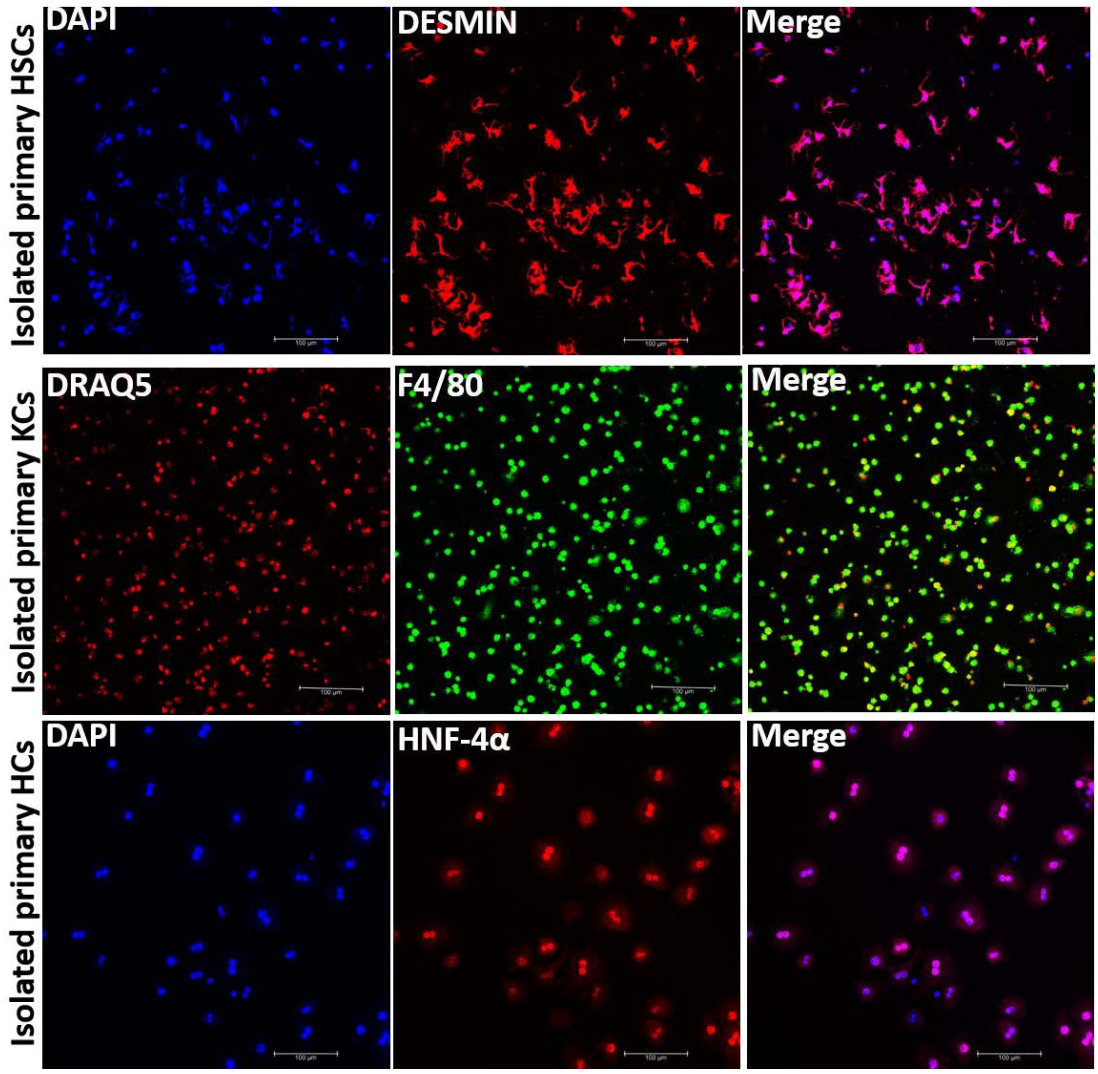

Figure 2.1 Primary isolated HSCs, KCs, and HCs stained with DESMIN, F4/80, and HNF-4α respectively. Nuclei were stained with either DRAQ5 or DAPI.

2.4 Animal models

Male 10-15 weeks old C57BL/6N wild-type mice were used for CCl_4 treatment and BDL surgery in Hangzhou. Guidelines for animal care were approved by the Animal Care Committee of Zhejiang University and were followed in all mentioned animal protocols. The paraffin blocks of carbon tetrachloride (CCl_4)-treated and bile duct ligation (BDL)-operated animals were kindly provided by our Chinese collaboration group (Shen et al., Zhejiang University, China).

2.4.1 CCl_4-induced liver fibrosis animal model:

Animals were divided into six groups: sham, rDll4, rJag-1, CCl_4, CCl_4+rDll4, and CCl_4+rJag-1 (six animals per group). CCl_4 was diluted in mineral oil (1:4) and was

injected intraperitoneal (I.P) in the dosage of 0.5 ml/kg twice weekly for 4 weeks. rDll4 (6.25 µg/kg) and rJag-1 (6.25 µg/kg) were injected I.P twice weekly 1 day (d) after CCl_4 administration. Twenty-four hours after the last injection, the animals were sacrificed. Blood and liver samples were collected for further analysis (Figure 2.2). Sham animals were injected only with mineral oil.

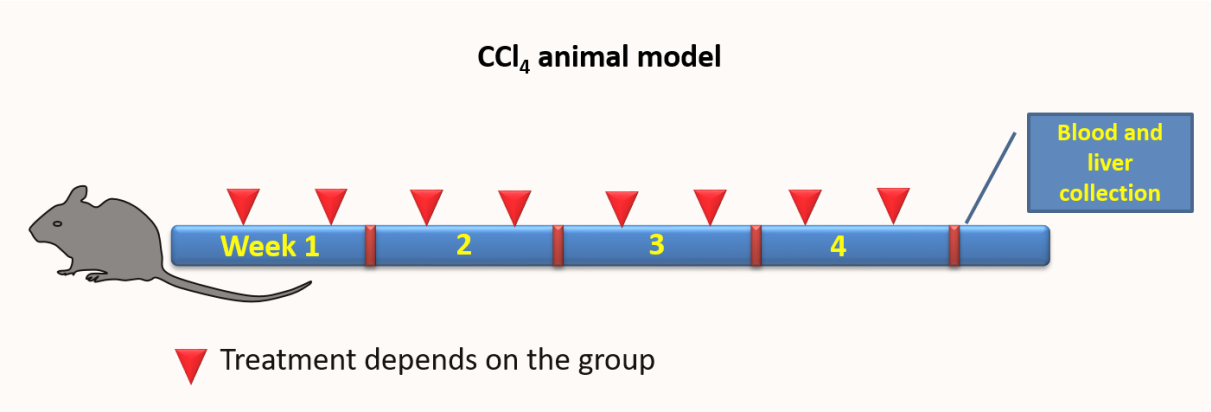

Figure 2.2 Treatment plan of CCl_4 animal model.

2.4.2 BDL-induced liver damage animal model:

Mice were divided into 3 groups (n=6): BDL, BDL+rDll4, and BDL+rJag-1. BDL operation was performed according to previous description (Miyoshi et al., 1999; Tag et al., 2015). After anesthesia, the abdominal cavity was explored and common bile duct (CBD) was exposed. CBD was double ligated and cut in between. BDL+rDll4 or BDL+rJag-1 groups (n=6 per group) were injected with 6.25 µg/kg rDll4 or 6.25 µg/kg rJag-1 twice weekly, 1 d after BDL operation. For rescue experiments, the animals were injected with two different dosages of recombinant chemokine ligand 2 (rCcl2) (1 and 5 µg/kg) 24 h after rDll4 or rJag-1 administration. Blood and liver samples were collected once the animals died or 2 weeks following BDL, the end point of study (Figure 2.3).

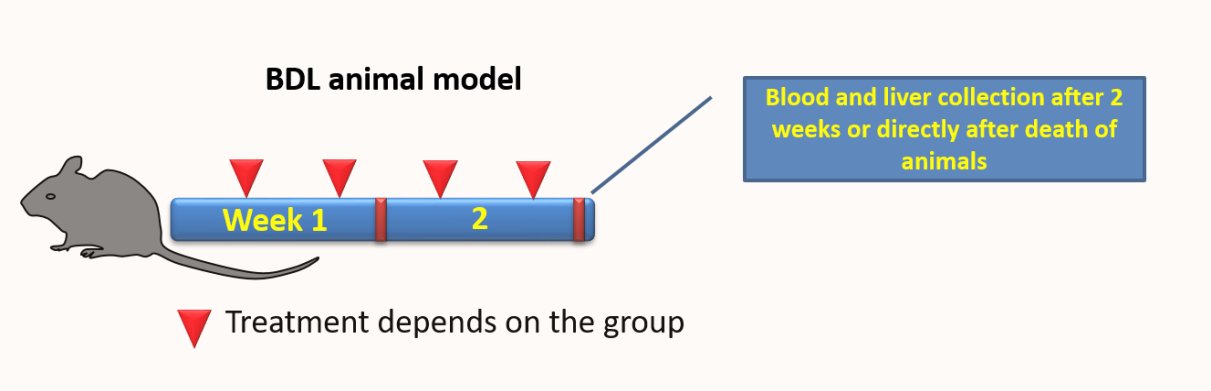

Figure 2.3 Treatment plan of BDL animal model.

2.5 Histological and immune-histological analysis:

Liver tissues were fixed in 4% paraformaldehyde and embedded in paraffin. Later, the tissues were sectioned at 4 µm and used for staining.

2.5.1 Histology:

Liver tissues were deparaffinized in a series of xylene and ethanol solutions respectively. After deparaffinization, the tissues were stained for hematoxylin and eosin (H&E), sirius red, and Masson's trichrome as described below.

A. H&E staining:

   We followed the protocol of Fischer et al. (2008) with minor modifications. Briefly, deparaffinized slides were stained with Meyer's modified hematoxylin for 3 min followed by washing in cold H_2O for 10 min. Excess hematoxylin was removed by washing the slides in 0.1% HCl (diluted in 70% ethanol) for 5 seconds. After washing the slides in warm H_2O for 10 min, the slides were incubated with eosin for 3 min. Finally, the slides were washed with tap water for 2 min, dehydrated by passing through series of ethanol and xylene solutions respectively, mounted with resinous oil, covered, and left for drying.

B. Sirius red staining:

   Deparaffinized slides were incubated with picro-sirius red solution for 20 min at room temperature (RT). Then, the slides were washed twice with absolute ethanol, mounted and covered (Junqueira et al., 1979). The solutions were described in Appendix 10.1.1.3.

C. Masson's trichrome staining:

   Deparaffinized slides were fixed in Bouin's Solution to improve staining quality. Then, nuclei were stained with Weigert's iron hematoxylin solution. After a wash in distilled water, the slides were incubated in solution A for 10 min, solution B for 5 min, and solution C for 10 min respectively. Finally, the slides were dehydrated and mounted as previously described. The used solutions were described in Appendix 10.1.1.4. Detailed procedure was described by Bancroft and Layton, 2013.

2.5.2 Immunohistochemistry (IHC) staining:

IHC protocol was used as previously described by Weng et al., 2009. After paraffin removal, the slides were washed by distilled water and antigens are unmasked by heating the sample at 99 C° in EDTA buffer (0.1 mM, pH=8.4) or citrate buffer (10

mM, pH=6) for 10 min (Table 2.2). After cooling the slides to RT, the slides are washed 3 times with PBS and incubated with DAKO dual peroxidase blocker for 20 min at RT to block endogenous peroxidase activity. Then, the slides were washed 3 times with PBS and the tissues were incubated with primary antibody at 4 C° overnight (Table 2.2). Next day, slides were washed 3 times with PBS to remove excess primary antibody and incubated with horseradish peroxidase (HRP)-labelled secondary antibody (Table 2.2) for 30 min at RT. After washing 3 times in PBS, the brown color was developed by incubating the slide with HRP substrate, diaminobenzidine (DAB), for less than 10 min. Then, nuclei were counterstained with Meyer`s modified hematoxylin. Lastly, the slides were dehydrated, mounted, and left for drying. Later, the staining was analyzed by Leica microscope (Leica Microsystem, Wetzlar, Germany). For quantification purposes, pictures were taken from at least five non-overlapping fields (100x) per slide and analyzed by ImageJ software version 1.50b (NIH, Maryland, USA). Tissue sections treated only with secondary antibodies were used as a negative control.

2.5.3 Immunofluorescence (IF) staining:

We followed the same protocol as IHC except that slides were incubated with fluorescent-labeled secondary antibodies for 1 h at RT (Table 2.2). After washing in PBS, the nuclei were counterstained with 4',6-diamidino-2-phenylindole (DAPI) (1:3000) or DRAQ5® (1:1000) for 5 min at RT. Finally, the tissues were covered with fluorescent mounting medium (DAKO) and examined under Leica confocal microscope TCS SP8 (Leica Microsystem, Wetzlar, Germany). Tissue sections without primary antibodies were used as a negative control. This protocol was modified from Weng et al., 2009.

2.5.4 Immunocytochemistry (ICC):

The protocol of Abcam (Cambridge, UK) was followed with minor modifications. Initially, RAW264.7 cells were grown on coverslips at $2x10^5$ cells per well in 12-well plate overnight. Then, cells were incubated with LPS (1000 ng/ml) with/without rDll4 (500 ng/ml), or rJag-1 (500 ng/ml) for 25 min in starvation medium. Afterward, the cells were washed twice with PBS and fixed in 4% buffered formaldehyde solution for 15 min at RT. Then, the cells were washed twice in wash buffer and incubated with blocking buffer for 45 min at RT. After removal of the blocking buffer, the cells were incubated with primary antibodies following the previously described IF protocol. The

wash and blocking buffers were described in Appendix 10.1.2.3 and 10.1.2.4 respectively.

2.6 RNA isolation, and quantitative real-time PCR (qPCR)

After treatment, the cells were washed twice with Hanks' balanced salt solution (Hanks'BSS) (Biozym, Oldendorf, Germany), and were lysed by lysis solution TR containing β-Mercaptoethanol (1%) as RNase inhibitor. Total RNA was extracted according to manufacturer's protocol (Stratec, Birkenfeld, Germany). Briefly, DNA was removed using a DNA-binding spin filter. Then, the binding properties of RNA were optimized by adding 70% ethanol. Next, RNA was bound to RTA spin filter and washed one time with wash buffer R1 and twice with R2. Finally, RNA was eluted with elution buffer R and stored immediately on ice. RNA concentration was determined by measuring the absorbance of isolated RNA at λ=260 nm (A260). The ratio between A260 and A280 estimated the purity of RNA. Next, 500 ng RNA was converted into complementary DNA (cDNA) with RevertAid H Minus Reverse Transcriptase (Thermo Fischer Scientific, Massachusetts, USA). cDNA was used for qPCR following the instructions of EvaGreen qPCR Mix (Solis Biodyne, Tartu, Estonia). The transcripts number in each sample was quantified in triplicate. The sequences of primers were described in Table 2.3. For data analysis, the $2^{-\Delta Ct}$ method was used (Schmittgen and Livak, 2008).

Table 2.3 Primers used for qPCR

Gene	Forward sequence	Reverse sequence
β-actin	5'-GTGCTATGTTGCTCTAGACTTCG-3'	5'-ATGCCACAGGATTCCATACC-3'
α-Sma	5'-GGACGTACAACTGGTATTGTGC-3'	5'-CGGCAGTAGTCACGAAGGAAT-3'
Ccl-2	5'-CTTCTGGGCCTGCTGTTCA-3'	5'-CAGCCTACTCATTGGGATCA-3'
Ccl5	5'-AGATCTCTGCAGCTGCCCTCA-3'	5'-GGAGCACTTGCTGCTGGTGTAG-3'
Ccl8	5'-TCTACGCAGTGCTTCTTTGCC-3'	5'-AAGGGGGATCTTCAGCTTTAGTA-3'
Col1a1	5'-CATGTTCAGCTTTGTGGACCT-3'	5'-GCAGCTGACTTCAGGGATGT-3'
Col1a2	5'-AAGGGTGCTACTGGACTCCC-3'	5'-TTGTTACCGGATTCTCCTTTGG-3'
Cxcl10	5'-AAATCATCCCTGCGAGCCTATC-3'	5'-GGAGCCCTTTTAGACCTTTTTTGG-3'
Cxcl9	5'-TGGGCAGAAGTTCCGTCTTG-3'	5'-ATTACCGAAGGGAGGTGGACAACG-3'
Hes1	5'-AGAAGAGGCGAAGGGCAAGAAT-3'	5'-AGGTCATGGCGTTGATCTGG-3'
Hes5	5'-CGCATCAACAGCAGCATAGAG-3'	5'-TGGAAGTGGTAAAGCAGCTTC-3'
Il-1α	5'-CGAAGACTACAGTTCTGCCATT-3'	5'-GACGTTTCAGAGGTTCTCAGAG-3'
Il-10	5'-TCTTTCAAACAAAGGACCAGC-3'	5'-ACCCAGGGAATTCAAATGC-3'
Il-6	5'-CTGCAAGAGACTTCCATCCAG-3'	5'-AGTGGTATAGACAGGTCTGTTGG-3'
ppia	5'-GAGCTGTTTGCAGACAAAGTT-3'	5'-CCCTGGCACATGAATCCTGG-3'
Tgf-β	5'-GCAACAACGCCATCTATGAG-3'	5'-ACGCCAGGAATTGTTGCTAT-3'
Tnf-α	5'-CTGAACTTCGGGGTGATCG-3'	5'-GGCTACAGGCTTGTCACTCG-3'

2.7 Subcellular fractionation and Immunoblot analysis

RAW264.7 cells were seeded at $2x10^6$ cells per well in 6-well plate overnight. Then, cells were incubated with LPS (1000 ng/ml) with/without rDll4 (500 ng/ml), or rJag-1 (500 ng/ml) for 25 min in starvation medium. Afterward, the cellular lysate was fractionated according to GeneTex's instructions (Irvine, USA).

2.7.1 Subcellular fractionation:

The cells were washed twice with cold PBS and scrapped in 1 ml PBS/1 mM EDTA solution. Then, the cells were pelleted and lysed using Harvest Buffer containing a cocktail of proteases and phosphatases inhibitors. After centrifugation, the supernatant contained cytoplasmic/membrane proteins while the pellet had nuclear proteins. The pellets were washed several times with Buffer A and were loosen by

Buffer C. After centrifugation, nuclear protein was collected from the supernatant. The used buffers were described in Appendix 10.1.4.

2.7.2 Immunoblot analysis:

After subcellular fractionation, the protein concentration was measured using DC protein assay (Bio-Rad, Munich, Germany). Then, the protein in SDS-containing loading buffer (4X) was denatured by heating at 90 C° for 10 min. Twenty µg per sample were separated using polyacrylamide gel (12%). After electrophoresis, protein was transferred to nitrocellulose membrane (Pierce, Rockford, IL) and blocked with 5% milk solution in Tris-buffered saline with Tween 20 (TBST) buffer for 1 h at RT. Next, the membrane was incubated with primary antibodies at 4 C° overnight. In the second day, non-bound primary antibodies were removed by washing with TBST buffer and the membrane was incubated with HRP-conjugated secondary antibody (Santa Cruz) for 1 h at RT (Table 2.2). The membrane was developed using enhanced chemiluminescence (ECL) solution. GAPDH (Abcam, Cambridge, UK) and Histone H1 (Santa Cruz, Heidelberg, Germany) were used as internal loading control for cytoplasmic and nuclear fraction, respectively. The density of bands was quantified using ImageJ software version 1.50b (NIH, Maryland, USA). The composition of gel and buffers were described in Appendix 10.1.5. This protocol was done following Mahmood and Yang, 2012 with minor modifications.

2.8 Luciferase assay and plasmid transfection:

Ccl2 promoter reporter ampicillin-resistant plasmid (pcDNA3.1-CCL2-Luc) was kindly provided by Dr. Sze-Kwan Lin (National Taiwan University Hospital, Taipei, Taiwan) (Kok et al., 2009). The pcDNA3.1-CCL2-Luc construct was amplified in DH5α™ Competent Cells (Thermo Fischer Scientific, Massachusetts, USA) and extracted following HiSpeed Plasmid Midi Kit instructions (Qiagen, Hilden, Germany). The construct contains 540-bp of the mouse *Ccl2* promoter starting from 20-bp downstream of transcription start site (TSS) linked to luciferase reporter enzyme. For measuring luciferase activity, RAW264.7 cells were seeded at 5 x 10^5 cells per well in 6-well plate. After reaching 80-90% confluency, the cells were transfected with pcDNA3.1-CCL2-Luc construct using Viromer red (Lipocalyx, Halle, Germany) according to manufacturer's instructions. After 4 h, the medium was replaced with serum-free medium. Next day, the cells were treated with LPS (20 ng/ml) or LPS+rDll4 (500 ng/ml). Six hours later, the cells were lysed with reporter lysis buffer

(5X) (Promega, Mannheim, Germany). Firefly luciferase activity was measured by adding 50 µl firefly luciferase substrate from Promega into 30 µl cellular lysate in 96-well white plate and measuring luminescence using Tecan infinite M200 microplate reader (Thermo Scientific, Waltham, MA, USA). The activity of firefly luciferase was normalized to protein concentration of each sample.

2.9 Enzyme-linked Immunosorbent Assay (ELISA):

RAW264.7 cells were seeded at 2 x 10^5 cells per well in 12-well plate. Then, cells were treated with LPS (20 ng/ml) for 16 h before they received rDll4 (500 ng/ml) for 6 h. CCL2 concentration in the culture supernatant was determined using Mouse CCL2/JE/MCP-1 DuoSet ELISA kit following the manufacturer's instructions (R&D, Minneapolis, MN). Briefly, 96-well microplate (R&D Systems, order # DY990) were covered with 100 µl anti-Ccl2 capture antibody overnight at RT. After washing with wash buffer, each well was covered with 300 µl diluent buffer for 1 h at RT. Then, plate wash was repeated, 100 µl of diluted standard (seven point 2-fold serial dilution starting from 3.91 pg/ml to 250 pg/ml) and diluted supernatant were added in duplicate, and incubated for 2 h at RT. Afterward, 100 µl anti-Ccl2 biotinylated goat anti-mouse detection antibody was added after plate washing and incubated for additional 2 h at RT. Then, 100 µl Streptavidin-HRP was added and the plate is sealed and incubated for 20 min at RT in the dark. The color was developed by adding 100 µl substrate tetramethylbenzidine (Abcam, ab171529) for 20 min and stopped by 100 µl stop acidic solution (Abcam, ab171529). Absorbance was measured at λ=450 nm using Tecan infinite M200 microplate reader (Thermo Scientific, Waltham, MA, USA). Absorbance at λ=540 nm was used to correct for optical imperfections in the plate. The average absorbance value of the standard was plotted against the concentration (pg/ml) using four-parameter logistic (4-PL) curve-fit created by Excel software (Windows office, 2010). The concentration of the diluted supernatants was determined from the curve and multiplied by the dilution factor to determine the original concentration of CCL2. Buffers were described in Appendix 10.1.3.

2.10 Activated caspase-3 assay:

The activity of caspase-3 enzyme was determined fluorometrically as previously described with minor modifications (Murillo et al., 2005). The principle of the assay depends on the specific proteolytic cleavage of a cell-permeable fluorogenic

substrate N-Acetyl-Asp-Glu-Val-Asp-7-amido-4-Trifluoromethylcoumarin (AC-DEVD-AFC, Biomol) by activated caspase-3, which release free fluorescent 7-amino-4-trifluoromethylcoumarin (AFC) with an excitation wavelength at λ=400 nm and an emission wavelength at λ=505 nm that correlates with the amount of activated caspase-3 in the cellular extract. Primary hepatocytes were seeded at 150,000 cells/well in the collagen-coated 12-well plate and were treated with TGF-β (5 ng/ml) or TNF-α (20 ng/ml) with/without rDll4 (500 ng/ml) or rJag-1 (500 ng/ml) at 37 C° in medium 3 (Table 10.1). After 24 h, the cells were washed with Hank's BSS solution and were lysed with lysis buffer (Appendix 10.1.6). Protein concentration was determined using DC protein assay (Bio-Rad, Munich, Germany). The reaction was set up in white 96-well flat-bottom plate by adding 70 µl assay buffer (Appendix 10.1.6), 20 µl cell extract, and 10 µl AC-DEVD-AFC (diluted 1:20 in assay buffer with a final concentration of 0.05 mg/ml). After incubation for 60 min at 37 C° in the dark, the fluorescence was measured with Tecan infinite M200 microplate reader (Thermo Scientific, Waltham, MA, USA). Blank values were subtracted from the measured fluorescence values and the obtained values were normalized to protein content of each sample.

2.11 Statistics

Results were presented as mean ± standard error of the mean (SEM) unless specially indicated. Two-tailed unpaired Student t-test was used to analyze parametric data. Survival data were analyzed using Kaplan-Meier method and Mantel-Cox-Log rank test. Statistical analyses were performed mainly using GraphPad Prism version 6.0 for Windows (GraphPad Software Inc). Probability value (*P*-value) < 0.05 was considered significant and depicted graphically as one or more stars depending on its value (**P* < 0.05, ** *P* < 0.01, *** *P* < 0.001, **** *P* < 0.0001).

3 RESULTS

3.1 *In vivo* investigation of DLL4

3.1.1 Expression of Notch family members in patients' livers

Twenty liver tissue specimens (10 from patients with HBV-related cirrhosis, 5 with hepatolithiasis, and 5 controls with hemangioma) were used to perform IHC for detecting the expression of Notch receptors (NOTCH1, NOTCH2, NOTCH3, and NOTCH4) and ligands (DLL1, DLL3, DLL4, JAG1, and JAG2). Except JAG1 expressed in cholangiocytes, no additional Notch family members were detectable by IHC in control liver tissues (Table 3.1). Neither Notch ligands nor receptors were detected in sinusoidal cells of hepatolithiasis patients (Table 3.1). However, JAG1, DLL4, and NOTCH1 expressed in sinusoidal cells of patients with cirrhosis (Figure 3.1).

Table 3.1 Expression of Notch ligands and receptors in patients with HBV-associated cirrhosis, hepatolithiasis, and hepatic hemangioma.

Protein	Liver cells	Hemangioma (n=5)	Hepatolithiasis (n=5)	Cirrhosis (n=10)
JAG1	Hepatocytes	-	-	-
	Cholangiocytes	+ (5)	+ (5)	+ (10)
	Sinusoidal cells	-	-	+ (8)
JAG2	Hepatocytes	-	-	-
	Cholangiocytes	-	-	-
	Sinusoidal cells	-	-	-
DLL1	Hepatocytes	-	-	-
	Cholangiocytes	-	-	-
	Sinusoidal cells	-	-	-
DLL3	Hepatocytes	-	-	+ (4)
	Cholangiocytes	-	-	-
	Sinusoidal cells	-	-	-
DLL4	Hepatocytes	-	-	-
	Cholangiocytes	-	-	-
	Sinusoidal cells	-	-	+ (4)
NOTCH1	Hepatocytes	-	-	-
	Cholangiocytes	-	+ (5)	+ (7)
	Sinusoidal cells	-	-	+ (5)
NOTCH2	Hepatocytes	-	-	-
	Cholangiocytes	-	+ (5)	+ (10)
	Sinusoidal cells	-	-	-
NOTCH3	Hepatocytes	-	-	+ (6)
	Cholangiocytes	-	-	+ (8)
	Sinusoidal cells	-	-	-
NOTCH4	Hepatocytes	-	-	+ (3)
	Cholangiocytes	-	-	+ (6)
	Sinusoidal cells	-	-	-

(): number of positive samples

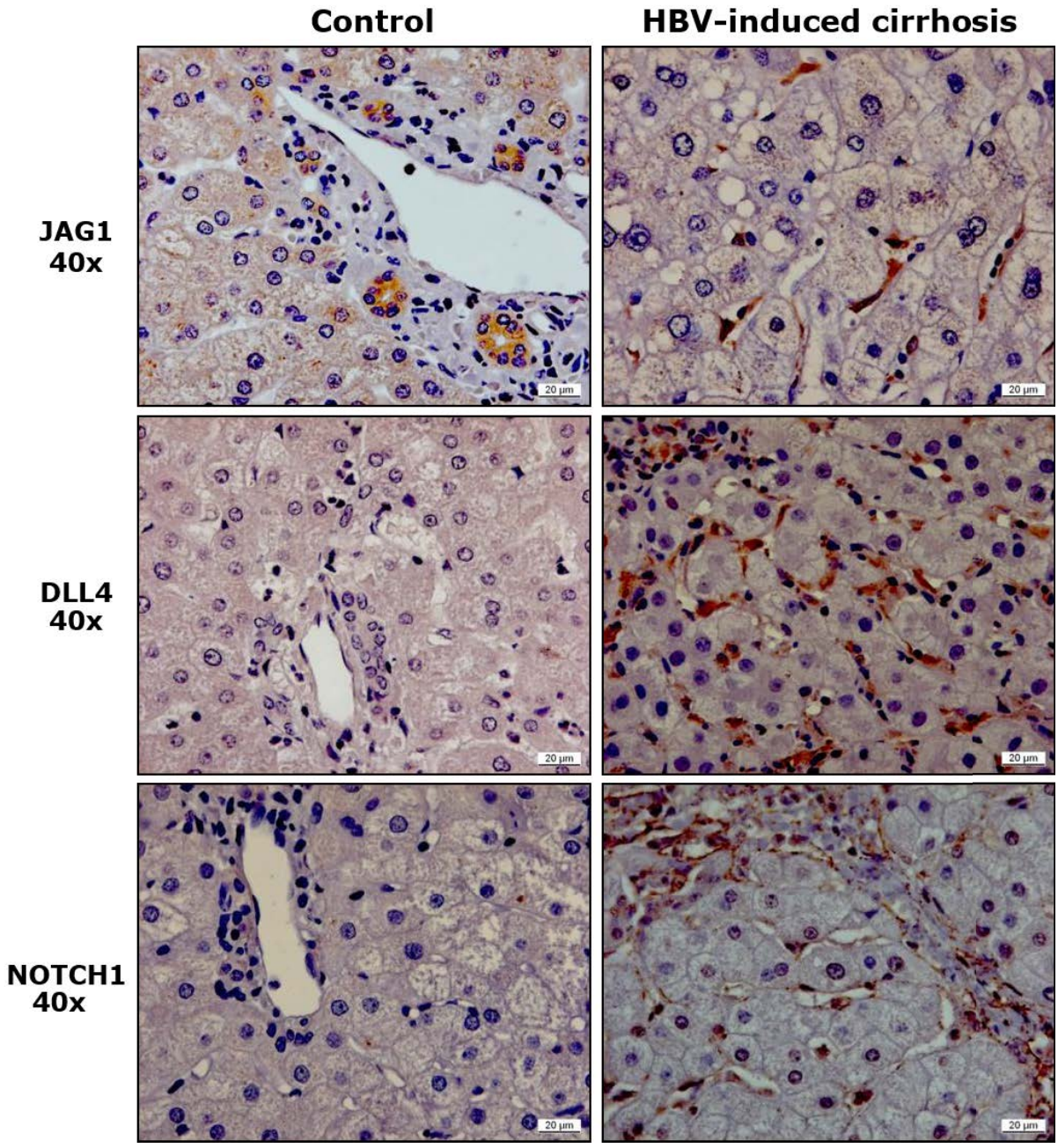

Figure 3.1 Immunostaining shows that JAG1, DLL4, and NOTCH1 localize in sinusoidal cells of a representative HBV patient with cirrhosis.

3.1.2 DLL4 expression in sinusoidal cells

Sinusoids are areas, where HSCs, KCs, and liver sinusoidal endothelial cells (LSECs) reside. To determine which cells express DLL4, Co-IF staining for DLL4 and α-SMA/CD68/CD16, the marker of HSCs, KCs and LSECs, respectively, were performed in 4 cirrhotic patients with high DLL4 positivity in sinusoidal cells. In all detected specimens, DLL4 positive sinusoidal cells did not express α-SMA, indicating that myofibroblasts are not the cellular source of DLL4 (Figure 3.2 A). In 2 patients, DLL4 expression was localized in CD68 positive KCs (Figure 3.2 B). In the other 2

patients, DLL4 positive sinusoidal cells did not express CD68 but were CD16 positive (Figure 3.2 C and D). These results suggest that DLL4 expressed in KCs and/or LSECs of different patients.

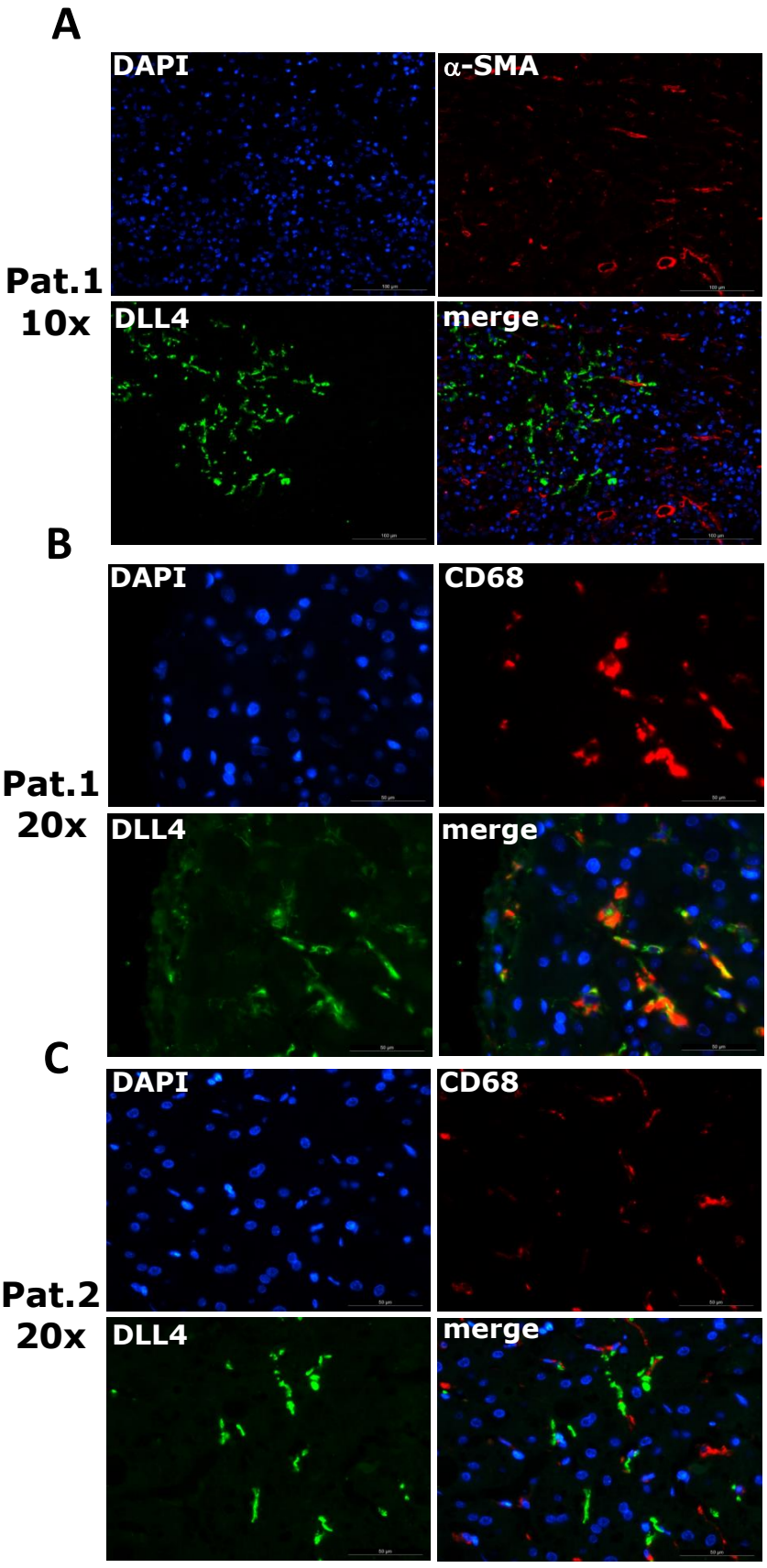

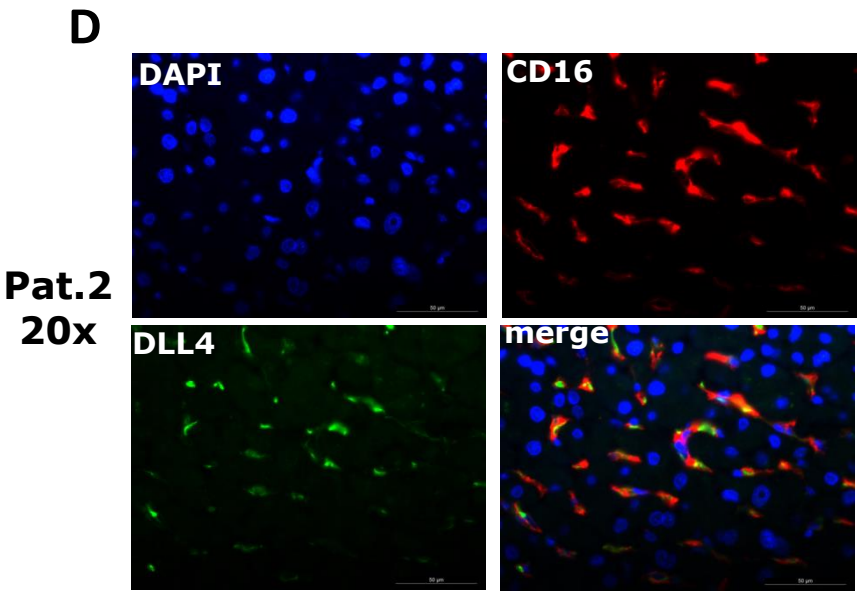

Figure 3.2 Co-staining for (**A**) DLL4 and α-SMA, (**B-C**) DLL4 and CD68 and (**D**) DLL4 and CD16 were performed in representative patients.

3.1.3 rDll4 administration improved liver fibrosis in CCl_4-challenged mice

Next, effects of rDll4 were examined in 2 animal models of liver injury i) hepatotoxicant model induced by CCl_4 injection and ii) cholestasis-driven model by BDL. In the CCl_4 animal model, treatment of mice with rDll4 increased *Hes1 and Hes5* mRNA expression (Figure 3.3 A), indicating active Notch signal following rDll4 administration. IHC for α-SMA and sirius red staining showed that rDll4 treatment significantly decreased CCl_4-induced α-SMA expression and collagen deposition (Figure 3.3 B and C). rDll4 alone had no significant effects on α-SMA and collagen deposition (Figure 3.3 C).

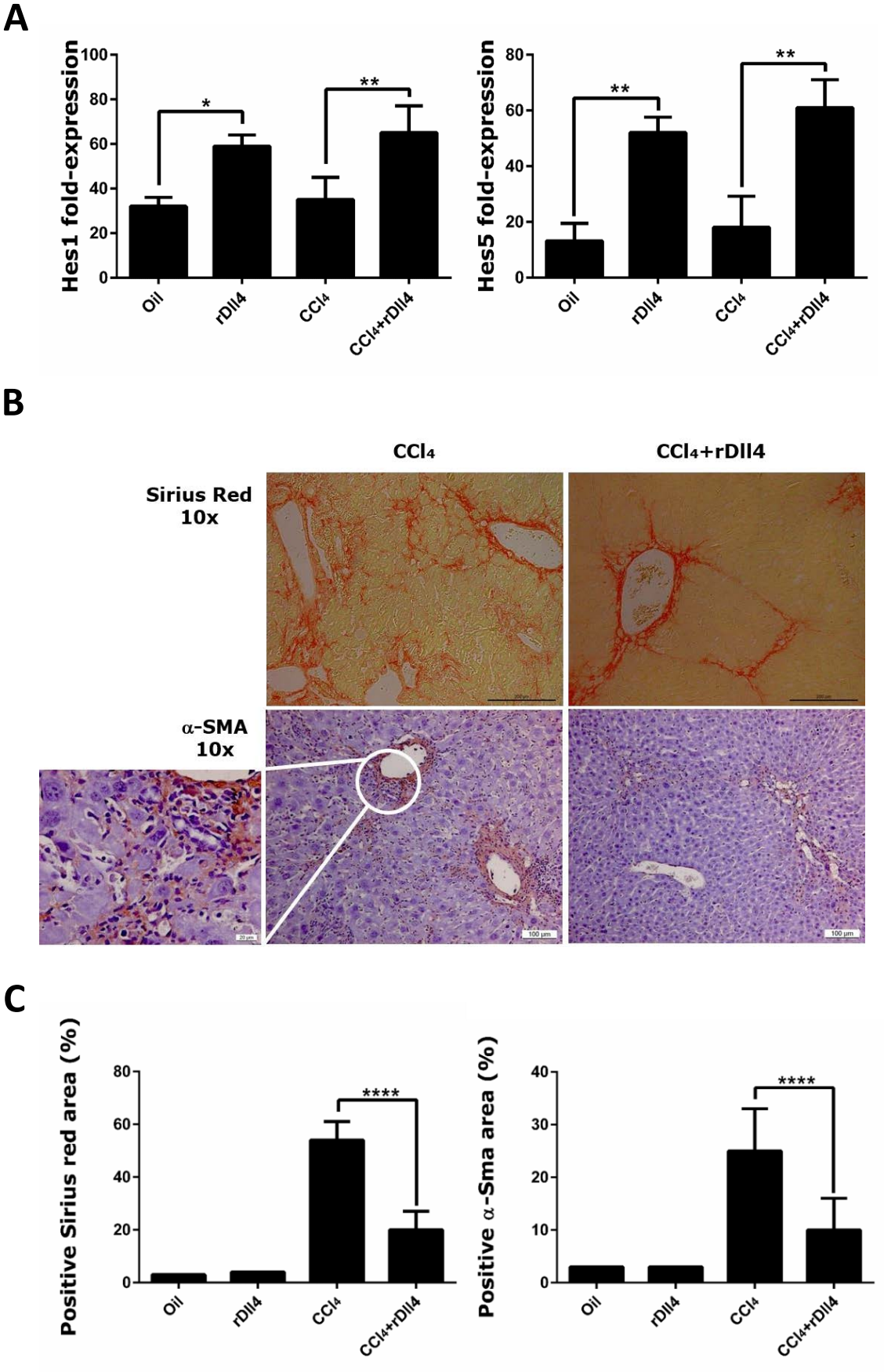

Figure 3.3 Effects of rDll4 on liver fibrosis in CCl_4 animal model (A) mRNA levels of *Hes1* and *Hes5* in mouse liver tissues after various treatments (n=6 per group) (B) Sirius red and α-SMA staining and (C) their semi-quantification. Panel (A) was prepared jointly with Shen et al. Zhejiang University, China.

3.1.4 rDll4 decreased inflammatory cells infiltration and hepatocyte apoptosis in CCl_4-challenged mice

Liver fibrosis is usually accompanied by inflammation and hepatocellular death (Malhi and Gores, 2008). Therefore, the effects of rDll4 on liver inflammation were investigated by H&E staining and IHC staining for F4/80 and CD45, markers of macrophages and leukocytes, respectively. rDll4 administration significantly decreased the recruitment of inflammatory cell to livers after CCl_4 challenge (Figure 3.4 A and B). Furthermore, rDll4 significantly reduced mRNA levels of inflammatory cytokines (e.g. *Tnf-α, Il-6, and Inf-γ*) and chemokines (e.g. *Ccl-2, Ccl-5, and Cxcl-9*) (Figure 3.4 C and D). In addition, hepatocyte apoptosis was measured by IHC for cleaved-caspase-3. rDll4 reduced CCl_4-induced hepatocytes death (Figure 3.4 A and B).

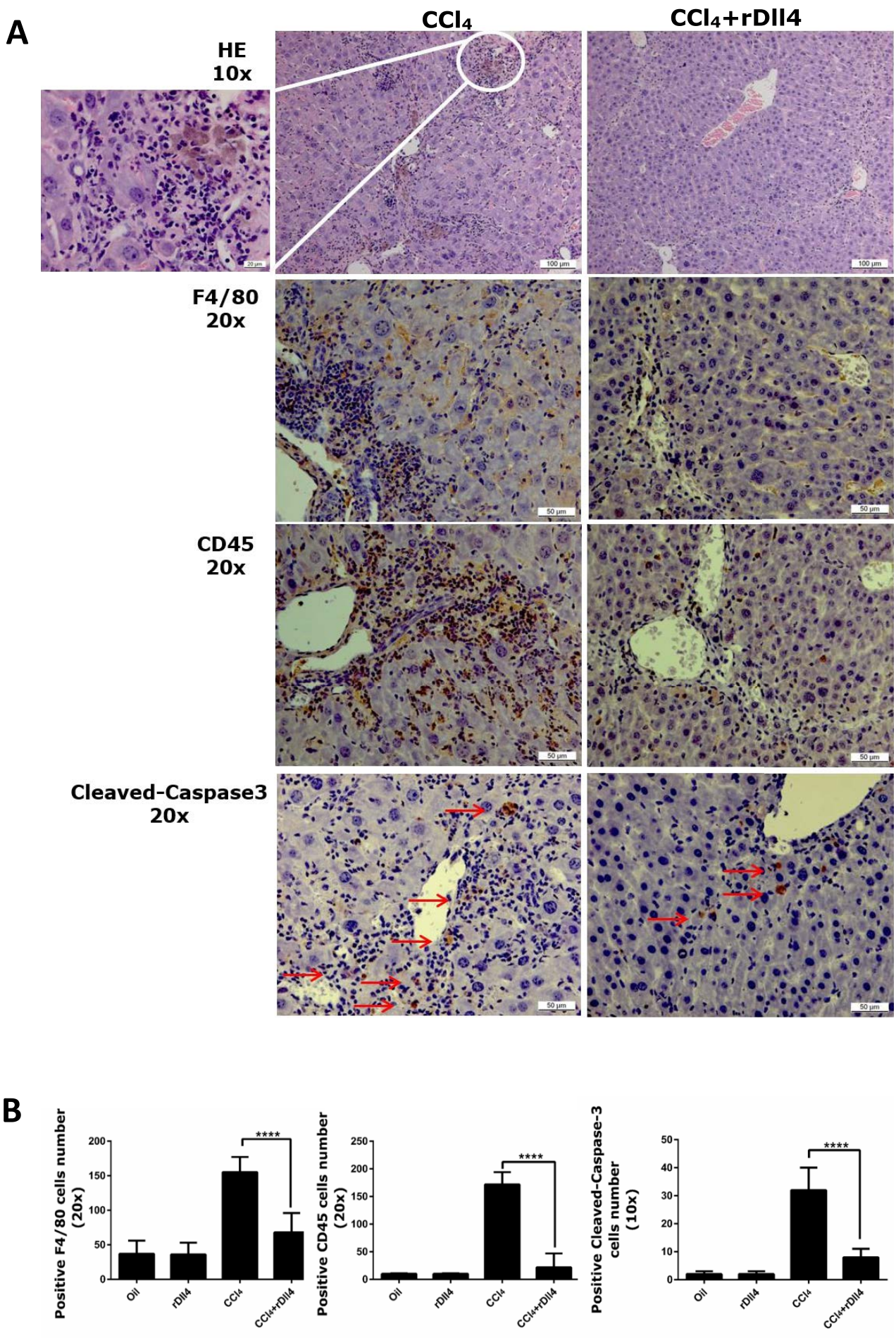
A
CCl4
CCl4+rDll4
HE
10x
F4/80
20x
CD45
20x
Cleaved-Caspase3
20x
B
Positive F4/80 cells number (20x)
Positive CD45 cells number (20x)
Positive Cleaved-Caspase-3 cells number (10x)
Oil
rDll4
CCl4
CCl4+rDll4
****

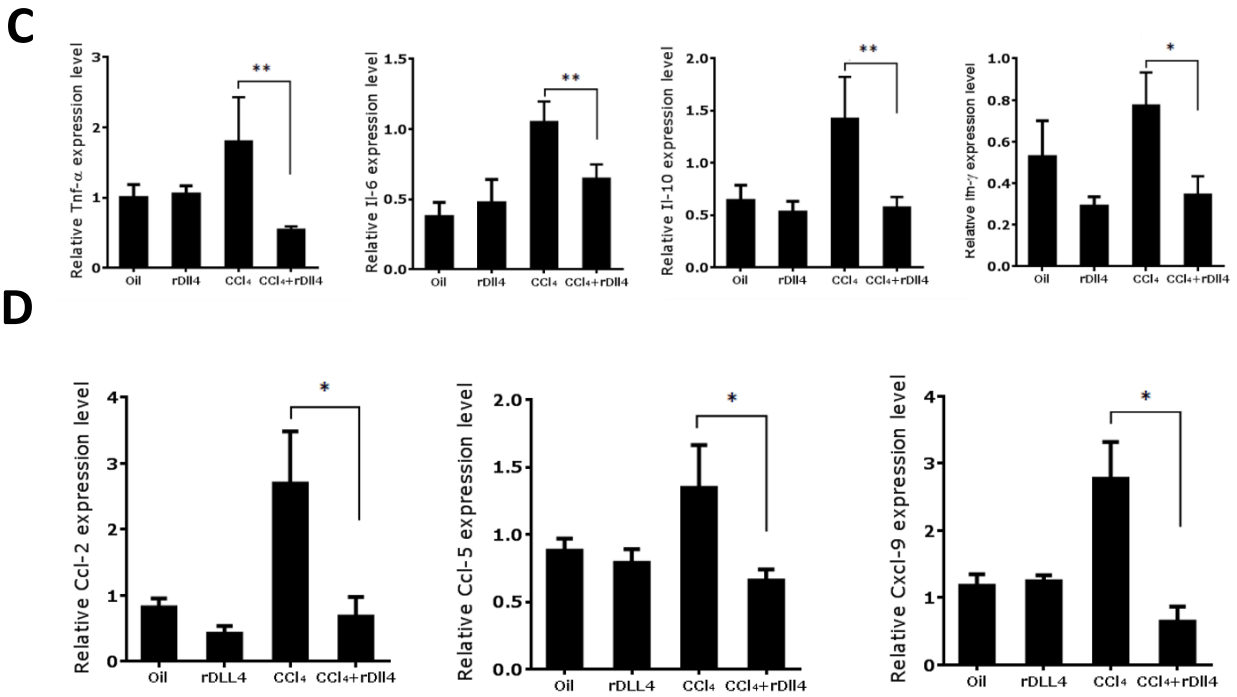

Figure 3.4 Inhibition of Inflammatory cells infiltration and hepatocytes apoptosis by rDll4 (A) H&E staining was performed to measure inflammatory infiltration in mice with different treatments (n=6 each group). F4/80 and CD45 staining were used to examine macrophages and non-macrophage inflammatory cells. Cleaved-caspase-3 was used to detect apoptotic cells as indicated by arrows (B) F4/80, CD45, and cleaved-caspase-3 positive cells were quantified using ImageJ software (C) mRNA levels of inflammatory cytokines and (D) chemokines were quantified by qPCR. Panel C and D were prepared jointly with Shen et al., Zhejiang University, China.

3.1.5 rDll4 induced massive hepatic necrosis in BDL mice

Next, the effects of rDll4 on BDL animal model was investigated. In contrast to CCl_4 model, treatment of BDL mice with rDll4 caused the death of all animals within 1 week (Figure 10.2). We examined bile infarct in liver tissues collected at different time points following BDL in mice with or without rDll4 administration. At 6 h following the operation, there was no obvious bile infarct in all BDL mice. Since 12 h following BDL, robust bile infarcts emerged and became larger with time, particularly in BDL mice with rDll4 injection (Figure 3.5). Figure 3.6 A shows the maximum diameter of bile infarcts (MDB) in BDL mice with or without rDll4 administration. At 4 or 7 d following BDL in mice receiving rDll4 treatment, massive hepatic necrosis appeared in all animals (diffuse panlobular and multilobular necrosis) (Figure 3.6 B).

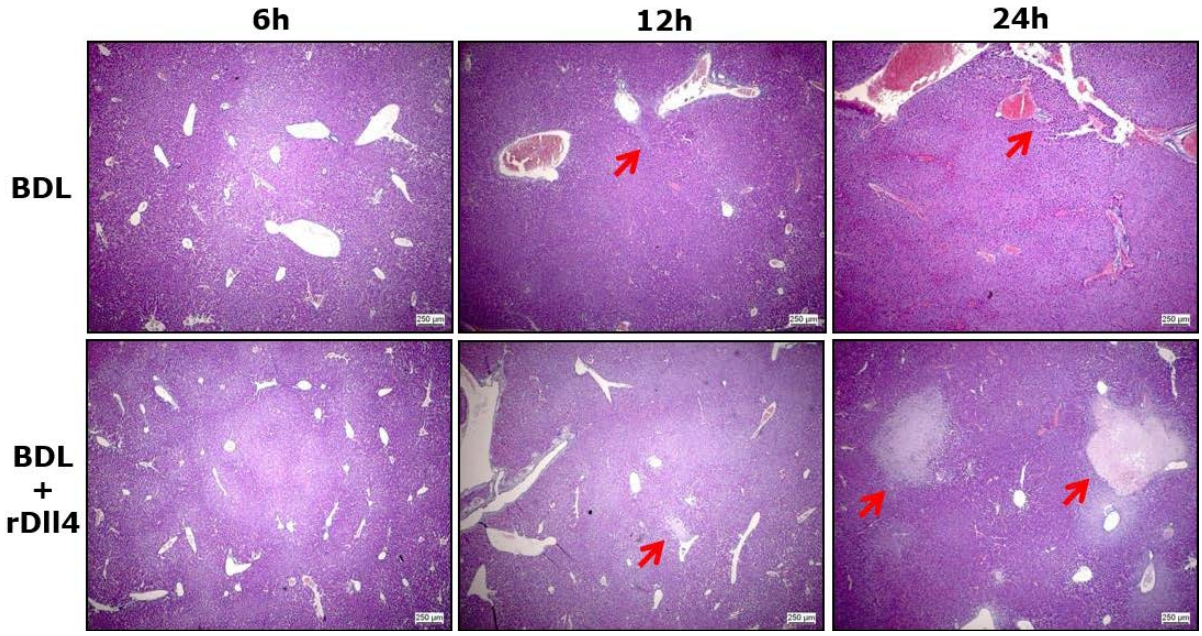

Figure 3.5 H&E staining demonstrating bile infarcts in mice at 6 h, 12 h and 24 h after BDL. Arrows show bile infarcts.

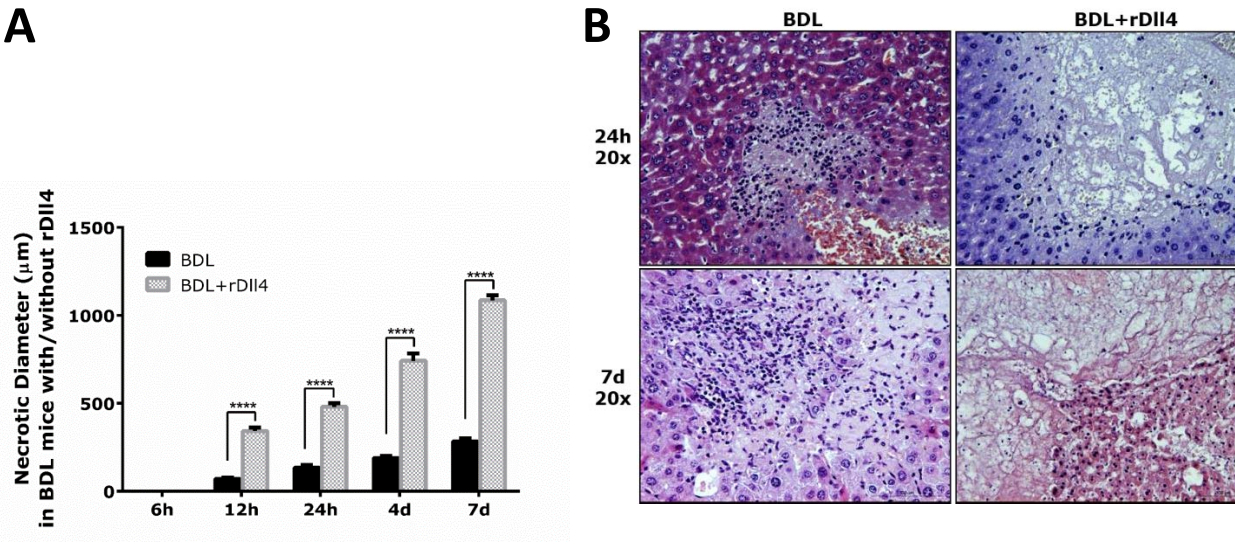

Figure 3.6 Administration of rDll4 induces massive hepatic necrosis in BDL mice (A) Diameters of maximum bile infarcts (3 areas per sample; n=6 per group) were calculated in BDL-mice injected with or without rDll4 injection at different time points following operation. (B) Representative liver tissues show bile infarct with inflammatory cells infiltration in BDL mice.

Noteworthy, H&E staining showed a very weak inflammatory response in BDL mice treated with rDll4 (Figure 3.6 B). The results suggest that rDll4 administration might impact inflammatory cell recruitment in BDL mice. The hypothesis was supported by measurement of CCL2, a key chemokine in charge of inflammatory infiltration. IHC revealed lack of CCL2 expression in BDL mice (Figure 3.7).

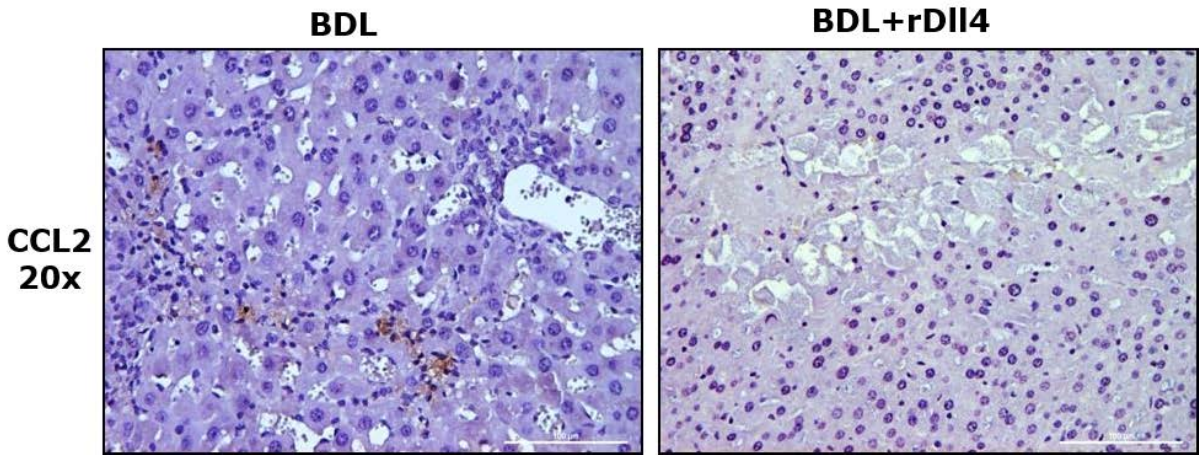

Figure 3.7 IHC staining shows CCL2 expression in BDL and BDL+rDll4 mice 4 days after BDL operation.

3.1.6 rCcl2 administration rescued rDll4-administrated BDL mice

To observe the role of CCL2 in BDL mice, BDL animals were treated with 2 different doses of rCcl2 (1 and 5 μg/kg) 1 d after rDll4 administration. Interestingly, rCcl2 treatment rescued all mice from death (Figure 10.2). In addition, rCcl2 dose-dependently decreased rDll4-induced massive hepatic necrosis in BDL mice (Figure 3.8).

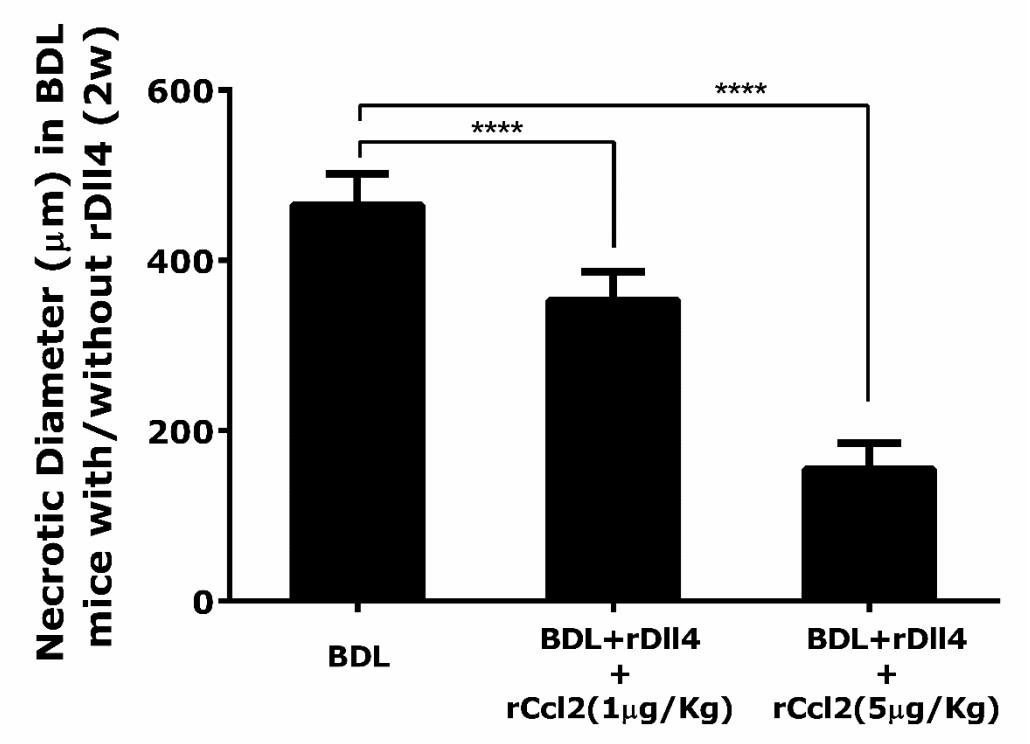

Figure 3.8 The diameters of maximum bile infarcts were calculated in mice 2 weeks following BDL with/without rDll4 and rCcl2 injection (n=6 per group).

H&E staining further showed improved inflammatory cells recruitment after rCcl2 treatments (Figure 3.9).

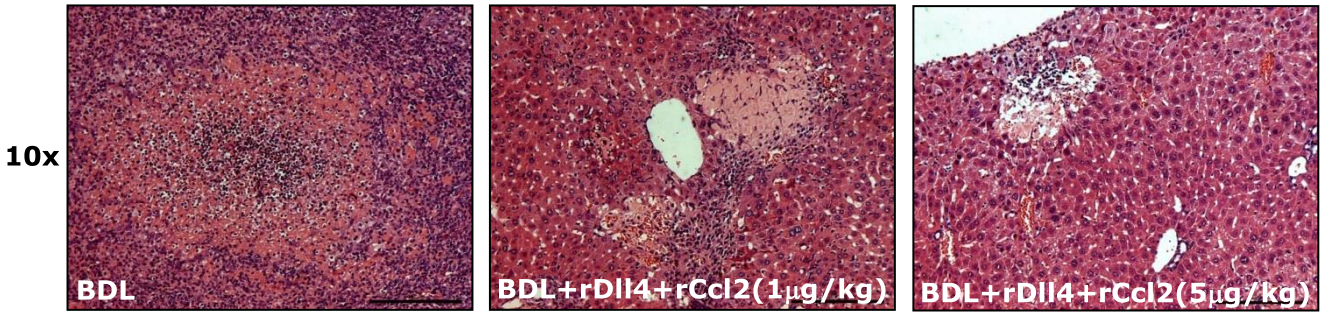

Figure 3.9 Bile infarct and inflammatory cell infiltration in 2 weeks BDL mice with/without rDll4 and rCcl2 treatment.

We performed IHC staining for CD45, myeloperoxidase and F4/80 to identify inflammatory cell types. IHC analyses showed that neutrophils localized in the center of the necrotic area while macrophages existed at the periphery (Figure 3.10).

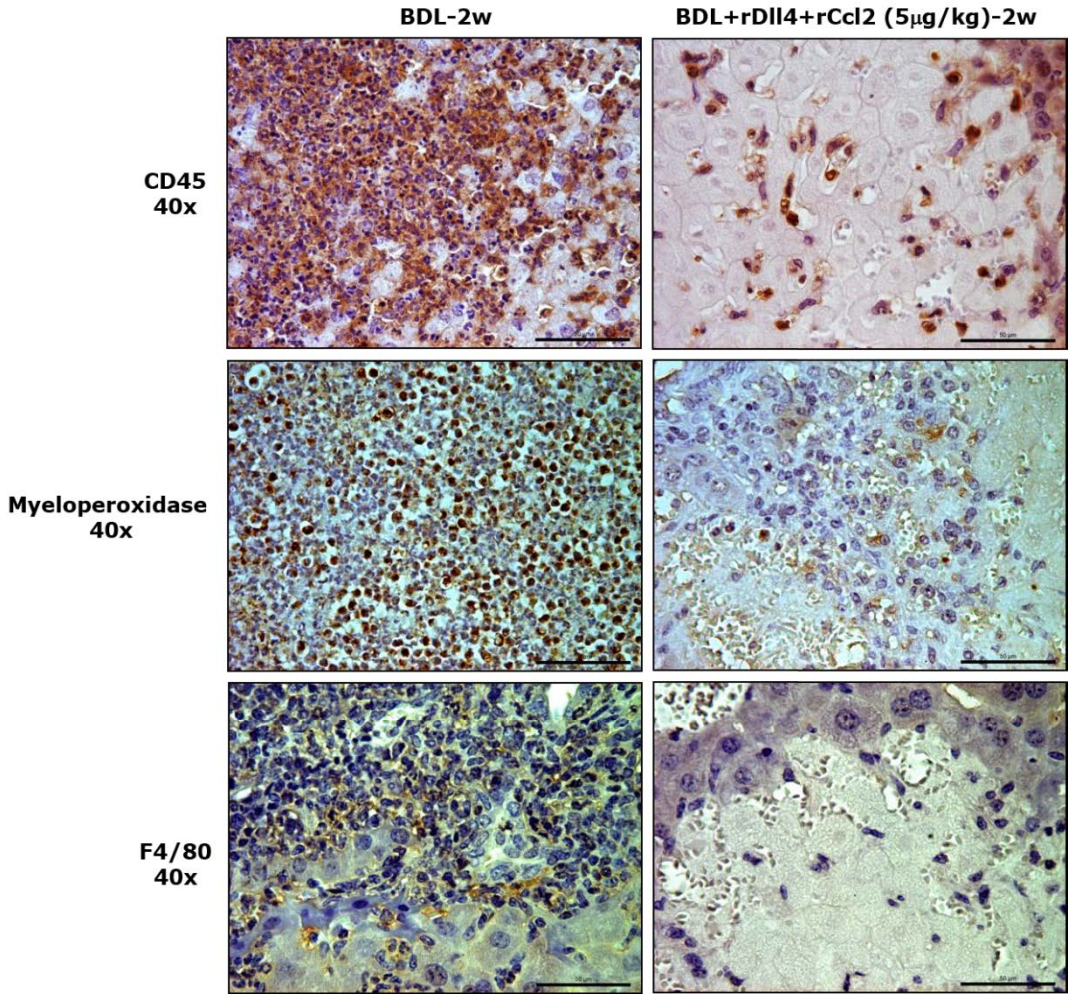

Figure 3.10 Leucocyte, neutrophil and macrophage infiltration in 2 weeks BDL-operated mice with/without rDll4 and rCcl2 injection.

3.1.7 DLL4 expression was inversely correlated with CCL2

Next, we investigated the expression of CCL2 and DLL4 in 26 liver samples from patients with chronic HBV infection (16 with ACLF and 10 with cirrhosis). All ACLF samples showed a strong CCL2 immuno-reactivity whereas DLL4 expression was negative. In cirrhotic samples, 4 patients with quiescent cirrhosis did not have both DLL4 and CCL2 expression. In 6 patients with active cirrhosis, 4 had DLL4 positive, and CCL2 negative cells, whereas 2 had liver cells with negative DLL4, but positive CCL2 expression (Table 3.2 and Figure 3.11)

Table 3.2 DLL4 and CCL2 expression in 26 patients with chronic HBV infection. Sixteen patients with ACLF and 10 with cirrhosis (four with quiescent cirrhosis and 6 with active cirrhosis).

Diseases	Inflammatory grade	DLL4	CCL2
quiescent cirrhosis (n=4)	0	-	-
	0	-	-
	0	-	-
	0	-	-
Active cirrhosis (n=6)	2	**+**	-
	2	**+**	-
	2	**+**	-
	3	**+**	-
	3	-	**+**
	3	-	**+**
ACLF (n=16)	3	-	**+**
	3	-	**+**
	3	-	**+**
	3	-	**+**
	3	-	**+**
	3	-	**+**
	4	-	**+**
	4	-	**+**
	4	-	**+**
	4	-	**+**
	4	-	**+**
	4	-	**+**
	4	-	**+**
	4	-	**+**
	4	-	**+**

(-) negative staining

(**+**) positive staining

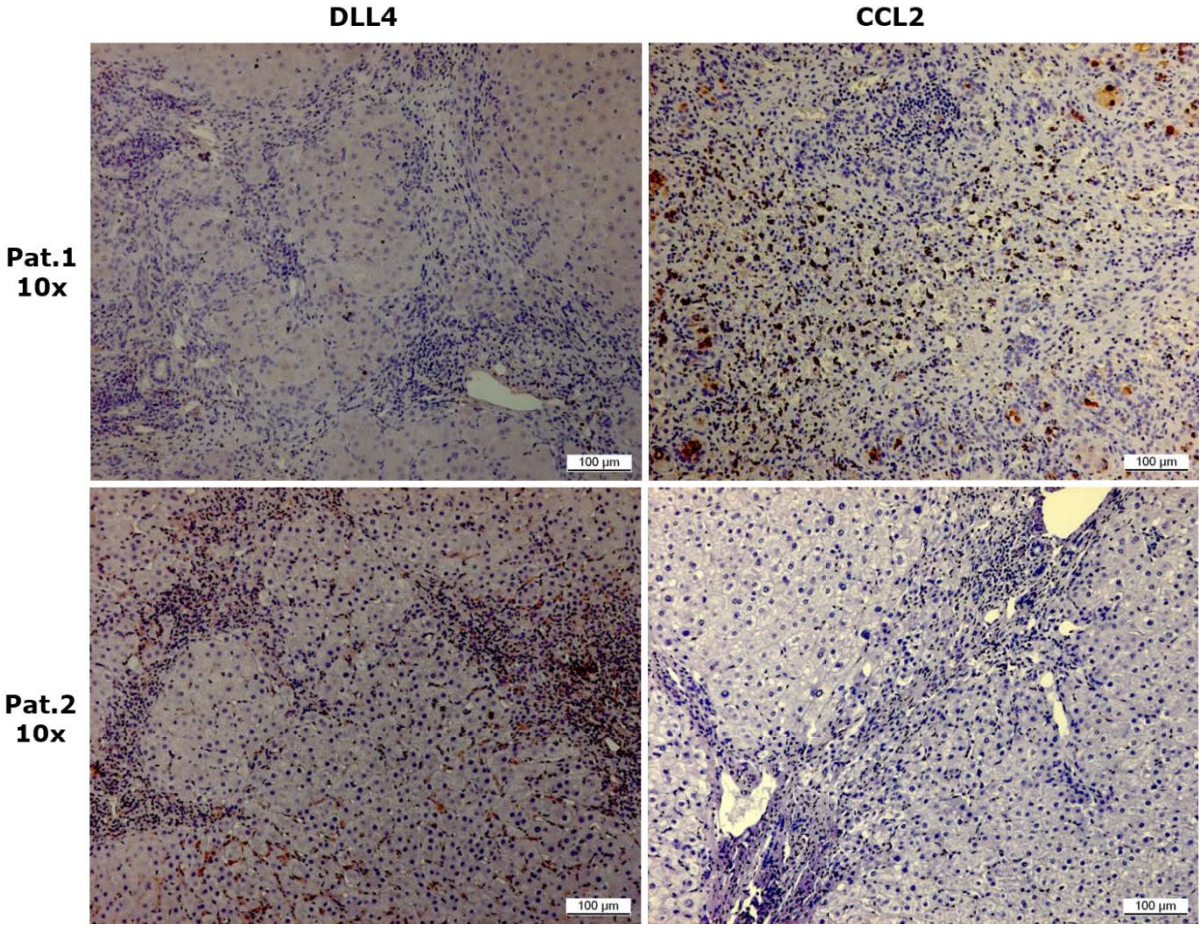

Figure 3.11 DLL4 and CCL2 expression in 2 representative HBV patients with active cirrhosis.

3.2 *In vitro* investigation of rDll4 effects

3.2.1 rDll4 did not affect TGF-β/TNF-α-mediated hepatocyte apoptosis

Primary mouse hepatocytes and AML-12 cell line were incubated with TGF-β and TNF-α with and without rDll4 administration. The assay of caspase-3 activity showed that rDll4 did not affect TGF-β- or TNF-α-mediated hepatocyte apoptosis in both AML-12 (data not shown) and primary hepatocytes (Figure 3.12).

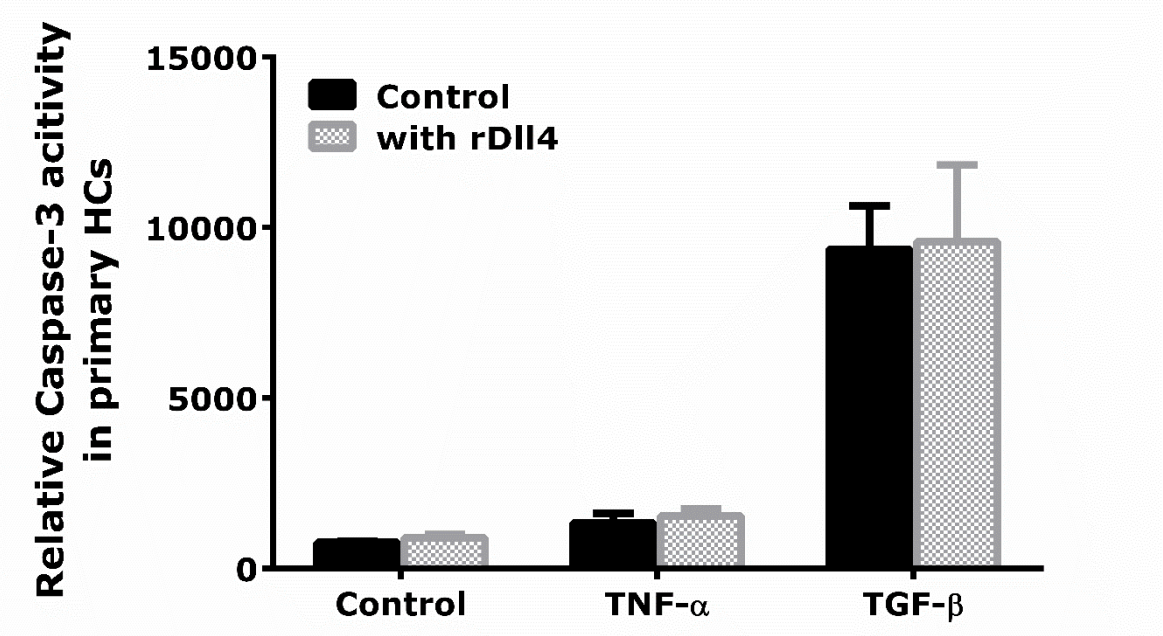

Figure 3.12 Caspase-3 activity assay Primary mouse hepatocytes were treated with TNF-α (20ng/ml) or TGF-β (5 ng/ml) with/without rDll4 (500 ng/ml) for 48 h.

3.2.2 rDll4 did not impact HSCs activation

Incubation of primary HSCs with rDll4 for 3 d did not change mRNA expression of *Col1α1*, *Col1α2*, and *α-Sma* (Figure 3.13 A). Additionally, TGF-β-induced *Col1α1* and *Col1α2* expression was not altered by rDll4 (Figure 3.13 B). Similar results were also obtained in JS-1 cell line (data not shown).

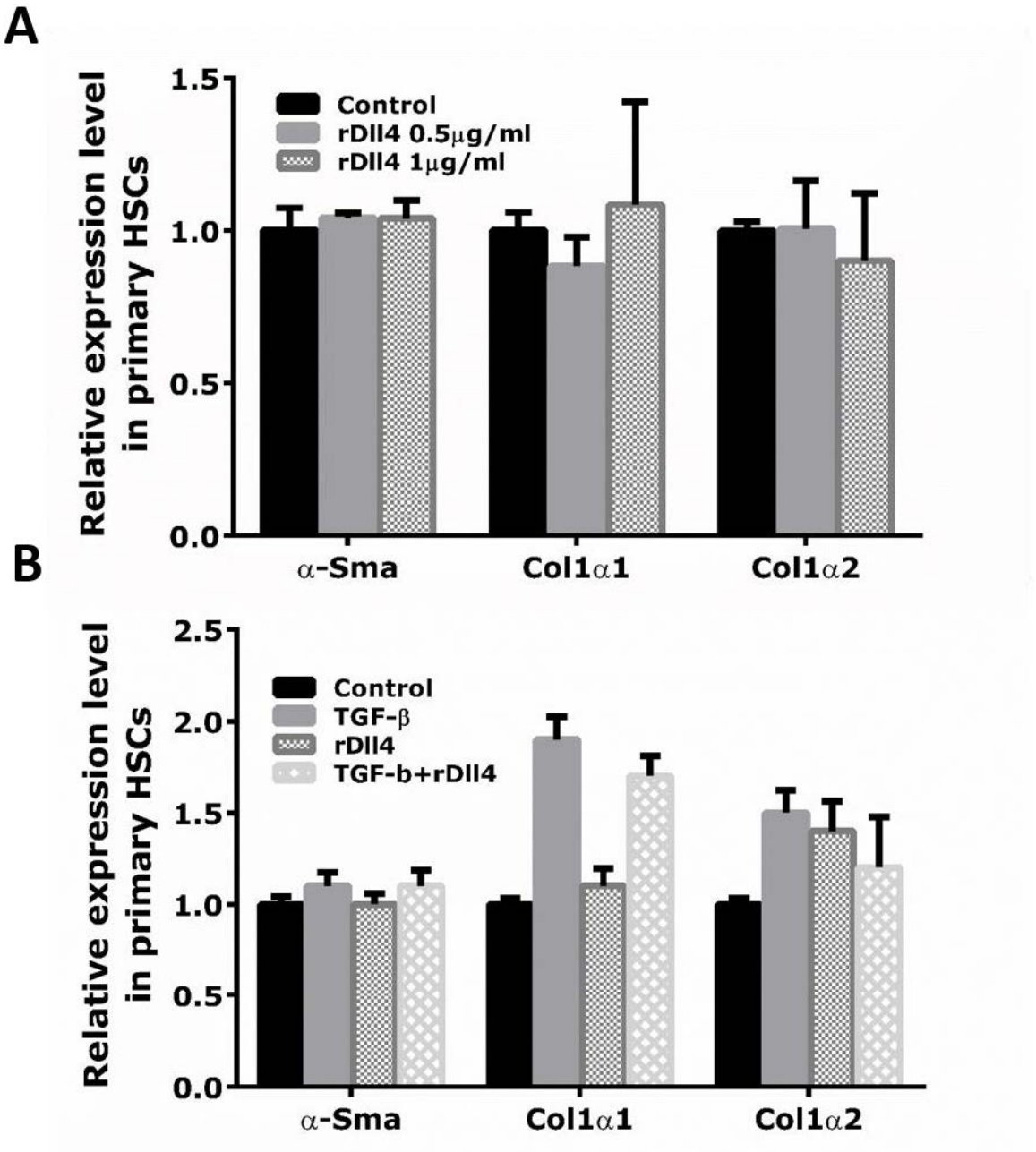

Figure 3.13 Effects of rDll4 on HSCs (A) qPCR was carried out to measure the mRNA levels of α-Sma, Col1α1, and Col1α2 in primary mouse HSCs incubated for 3d with/without two different doses of rDll4 (500 and 1000 ng/ml) (B) rDll4 (500 ng/ml) did not change TGF-β (5 ng/ml)-induced *α-Sma, Col1α1,* and *Col1α2*.

3.2.3 Effects of rDll4 on inflammation

Primary KCs were stimulated with LPS (20 ng/ml) for 16 h before they were treated with rDll4 for 6 h. rDll4 did not affect LPS-induced cytokines levels (*Tnf-α, Il-1α, Il-6 and Il-10, and Tgf-β1*) (data not shown), whereas it significantly reduced LPS-induced chemokines such as *Ccl2, Ccl5, Ccl8, and Ccl9* (Figure 3.14). In JS-1 cell lines, rDll4 only decreased LPS-induced *Ccl2* production (Figure 3.15).

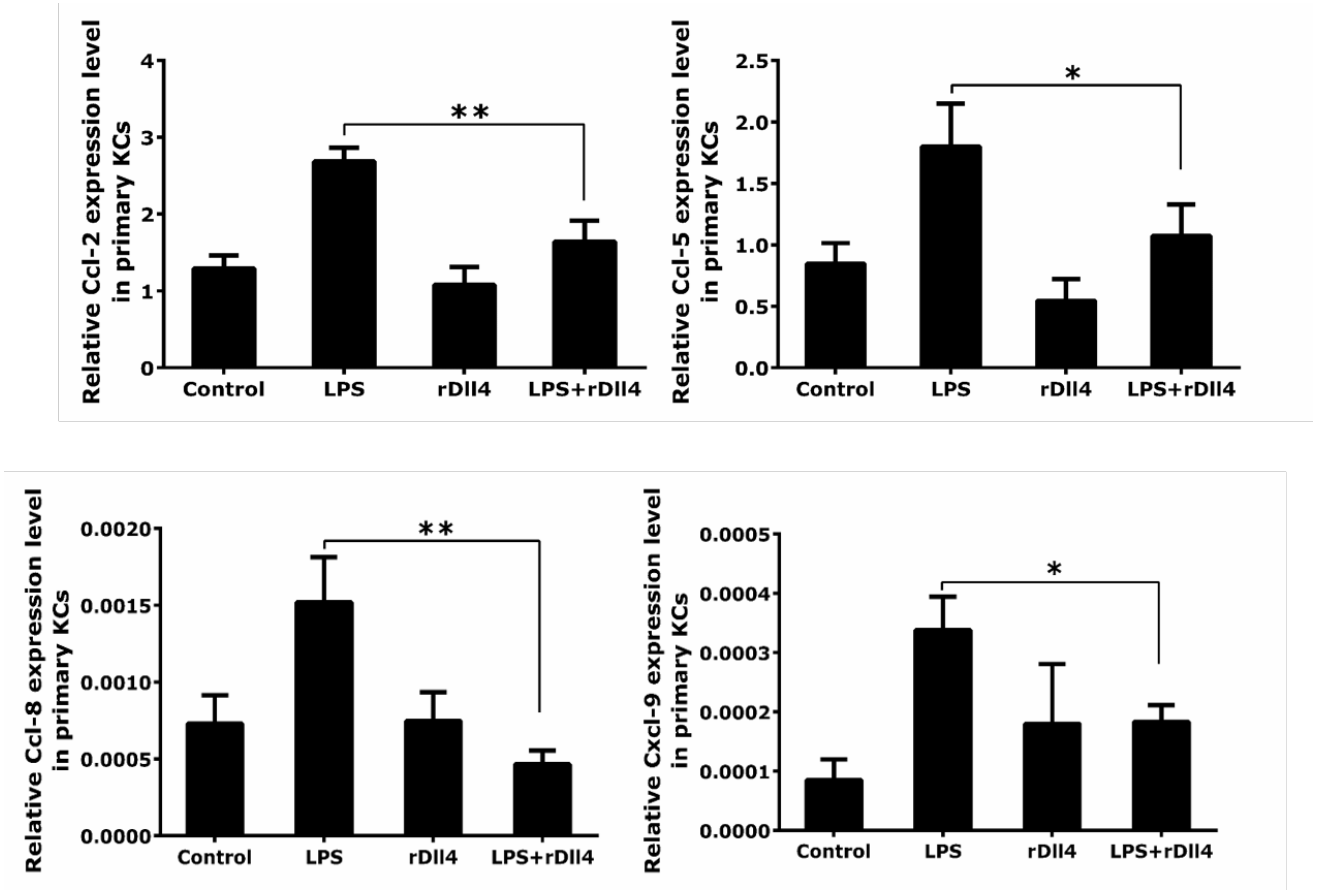

Figure 3.14 Effects of rDll4 on chemokines in KCs Primary KCs treated with LPS (20 n/ml) for 16 h with/without rDll4 (500 ng/ml) during the last 6 h of LPS treatment. mRNA levels of chemokines were quantified with qPCR.

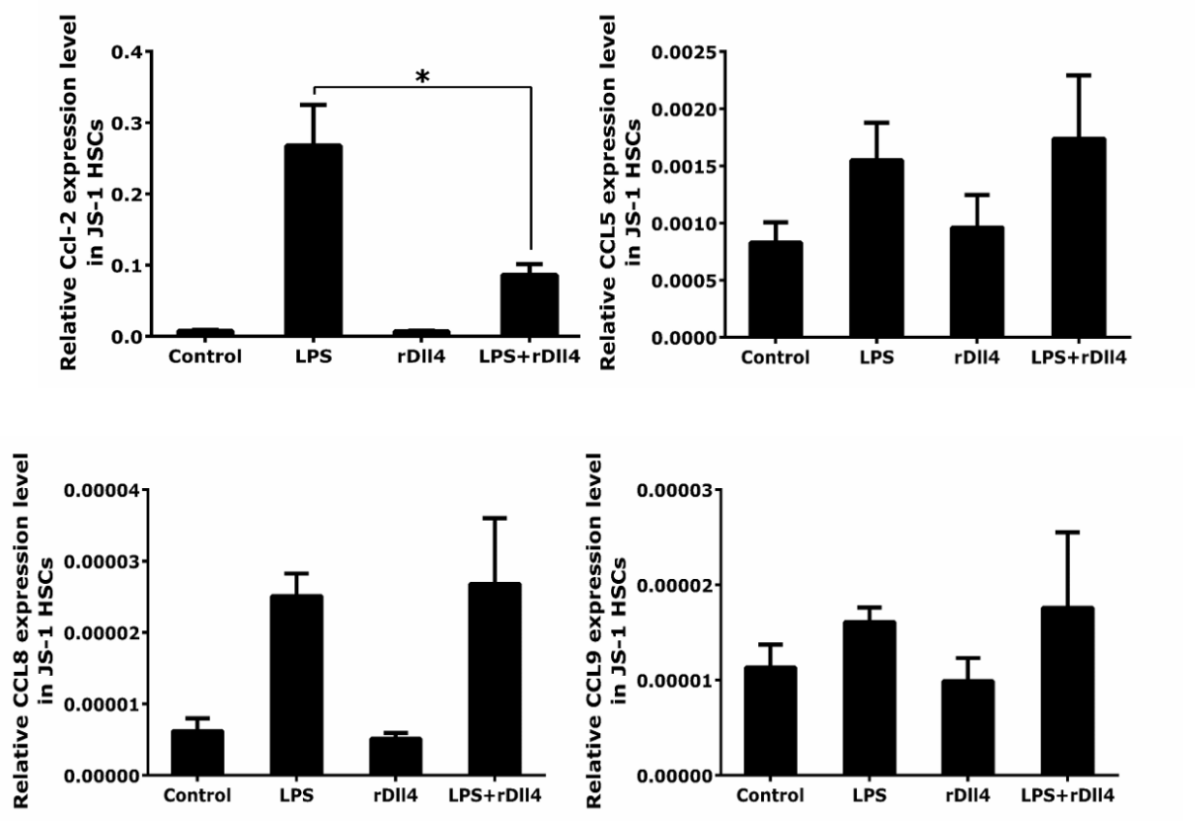

Figure 3.15 Effects of rDll4 on chemokines in JS-1 cells Cells received LPS treatment (100 ng/ml) for 16 h and rDll4 (500 ng/ml) for 6 h. mRNA levels of chemokines were quantified using qPCR.

3.2.4 rDll4 downregulated *Ccl2* expression through inhibition of the NFκB pathway

NFκB plays an important role in controlling the expression of several chemokines during inflammation (Ghosh and Hayden, 2008). Therefore, we investigated its role on *Ccl2* expression in RAW264.7 cells. JSH-23, an NFκB inhibitor, significantly decreased LPS-induced *Ccl2* mRNA levels (Figure 3.16 A) and reduced luciferase activity of *Ccl2* promoter-reporter construct (Figure 3.16 B).

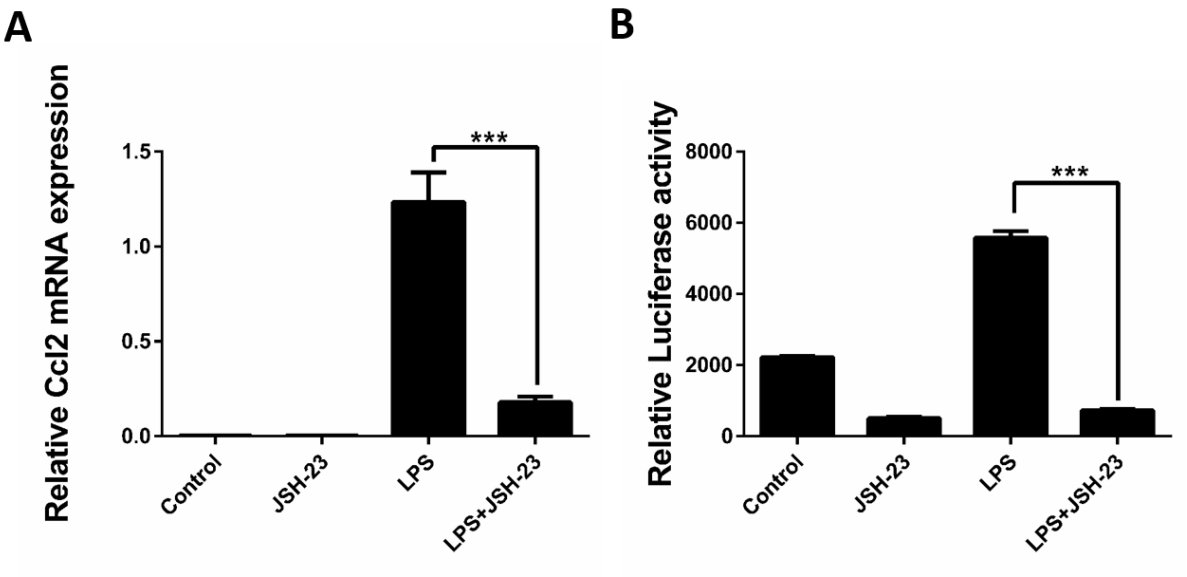

Figure 3.16 Effects of NFκB inhibitor on *Ccl2* in macrophages Treatment of RAW264.7 cells with JSH-23 (100 μM), an NFκB inhibitor, reduced LPS-induced *Ccl2* mRNA levels (A) and the luciferase activity of *Ccl2* promoter reporter construct (B).

Incubation of cells with rDll4 reduced LPS-induced *Ccl2* mRNA level (Figure 3.17 A), CCL2 protein secretion (Figure 3.17 B), and the luciferase activity of *Ccl2* promoter reporter construct (Figure 3.17 C).

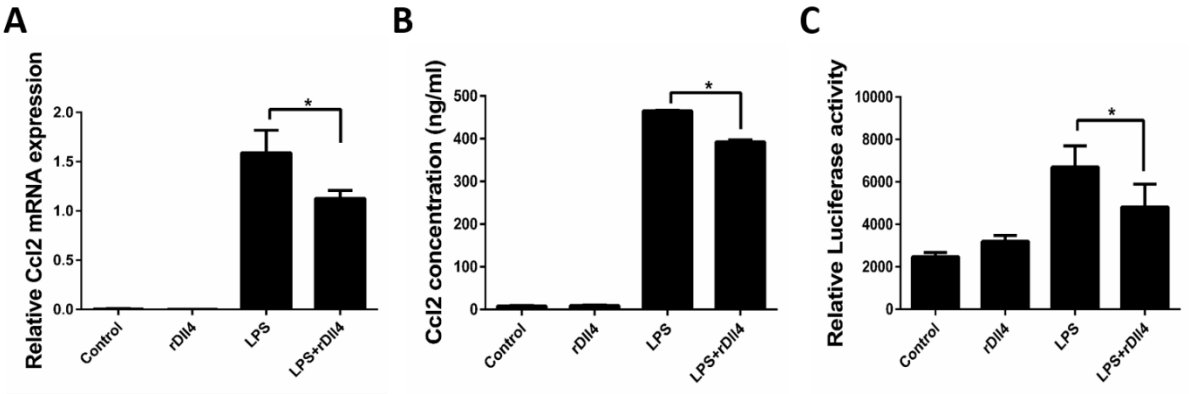

Figure 3.17 Effects of rDll4 on CCL2 in macrophages RAW264.7 cells were treated with LPS for 16 h before they received rDll4 for 6 h. rDll4 reduced (A) *Ccl2* mRNA levels, (B) The protein concentration of CCL2 in the supernatant, and (C) the luciferase activity of *Ccl2* promoter reporter construct.

These results suggest that rDll4 may regulate *Ccl2* by inhibiting NFκB pathway. To confirm this hypothesis, nuclear and cytoplasmic p50 and p65 NFκB subunits were

measured. rDll4 inhibited nuclear translocation of both p50 and p65 NFκB subunits (Figure 3.18 A and B) without affecting cytoplasmic levels (data not shown).

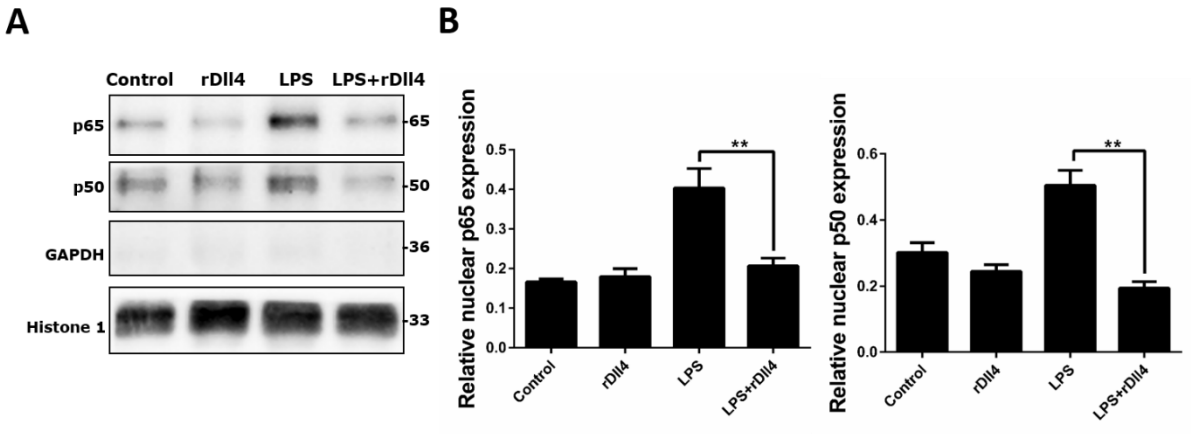

Figure 3.18 Effects of rDll4 on NFκB pathway RAW264.7 cells were treated as indicated; (A) Immunoblot shows nuclear p50 and p65 (B) Immunoblot was quantified using ImageJ software.

In consistent with the *in vitro* findings, p50 (NFκB1) was upregulated in inflammatory cells especially in those surrounding necrotic areas in BDL mice. Treatment with rDll4 decreased NFκB1 expression of BDL mice, which was restored by rCcl2 administration (Figure 3.19).

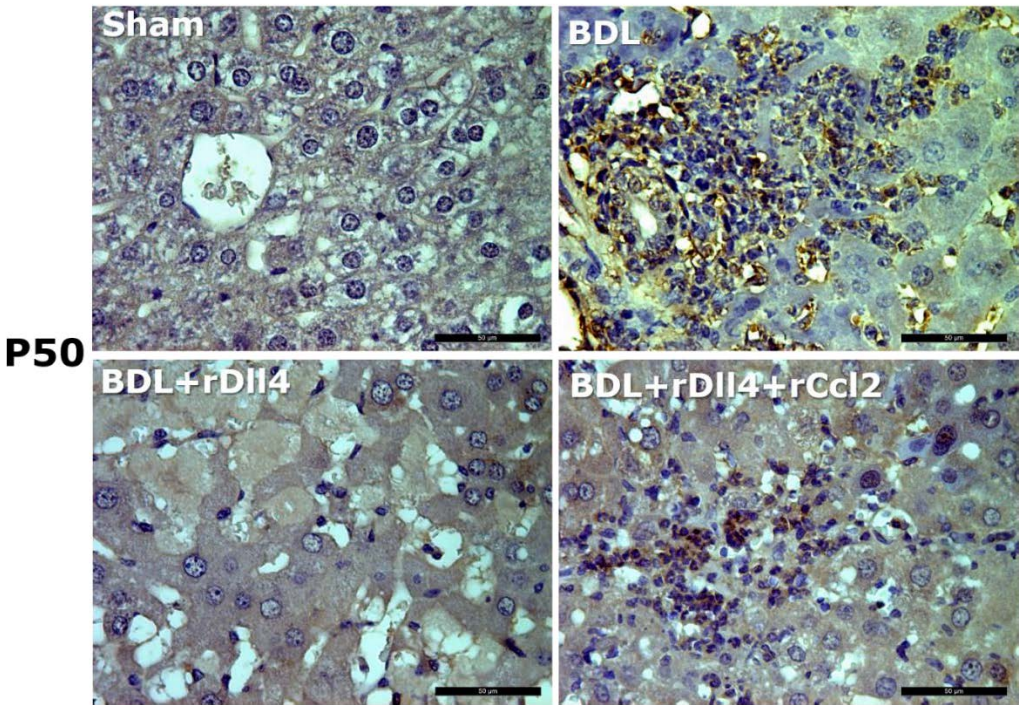

Figure 3.19 P50 IHC staining in different groups of mice as shown. Liver tissues were taken 1 week following BDL.

3.3 Effects of rJag-1

3.3.1 rJag-1 improved liver fibrosis in CCl_4-challenged mice

In addition to Dll4, the role of Jag-1 in liver injury was also investigated in CCl_4 and BDL animal models. In the CCl_4 animal model, rJag-1 reduced liver fibrosis, which was confirmed by Masson's trichrome and α-SMA staining (Figure 3.20).

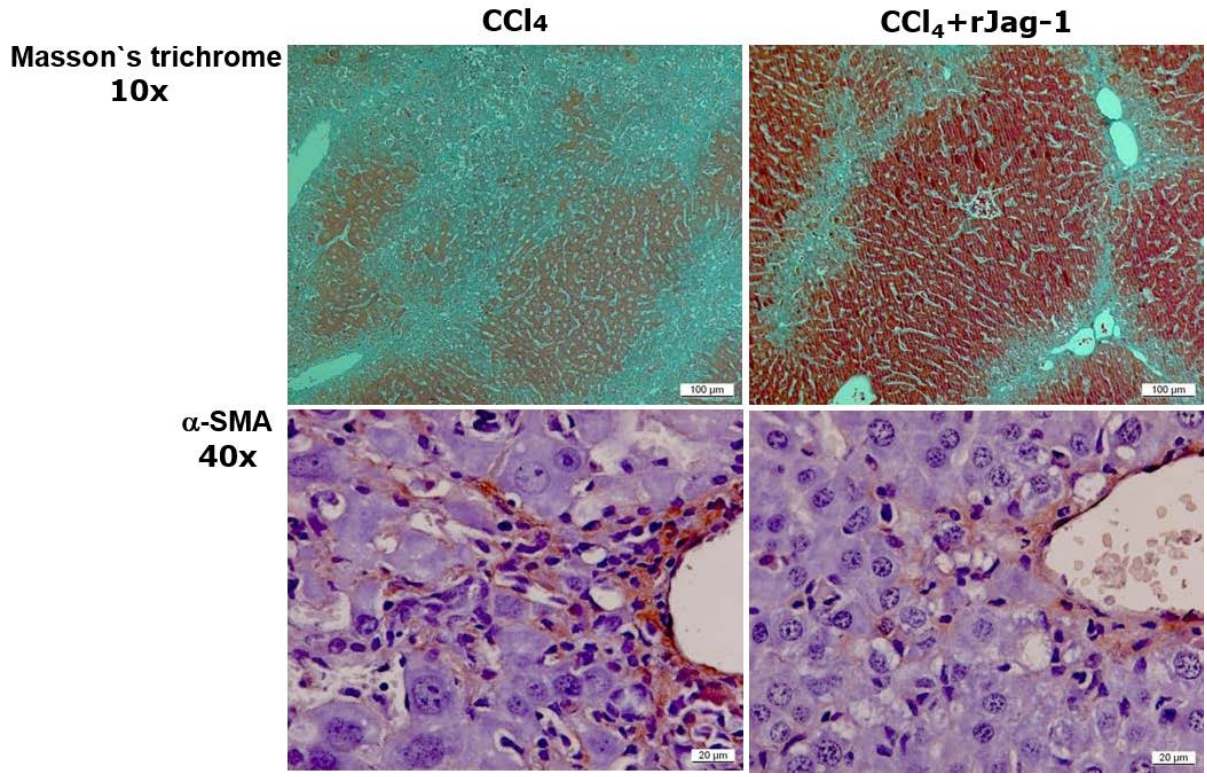

Figure 3.20 Effects of rJag-1 on CCl_4-induced liver fibrosis upper panel shows Masson's trichrome, and the lower panel shows α-SMA staining**.**

3.3.2 rJag-1 reduced hepatocytes apoptosis and inflammatory cell infiltrate in CCl_4-exposed mice

Cleaved-caspase-3 staining showed that rJag-1 treatment reduced CCl_4-induced hepatocytes apoptosis (Figure 3.21).

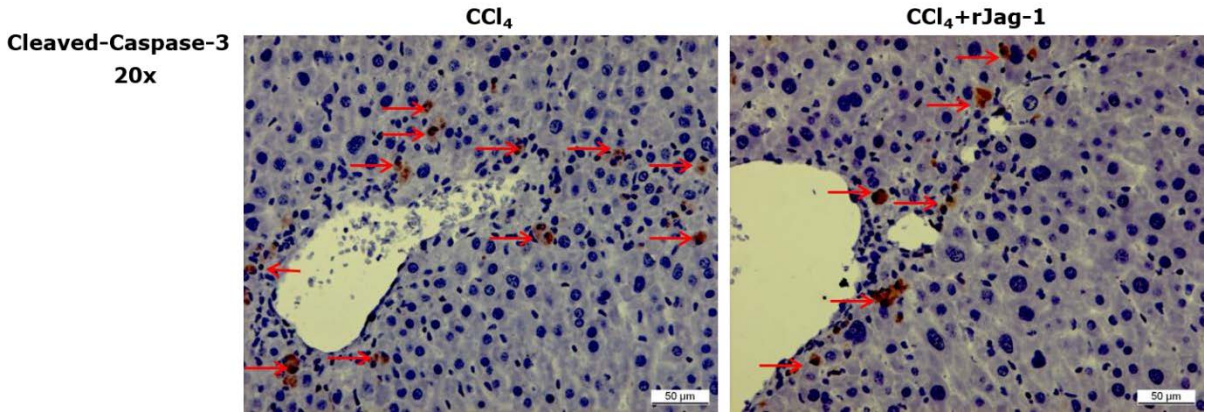

Figure 3.21 Cleaved-Caspase-3 staining in CCl_4 treated mice with/without rJag-1. Arrows highlight apoptotic hepatocytes.

In additions, rJag-1 significantly reduced CCl_4-induced infiltration of inflammatory cells such as macrophages in the liver (Figure 3.22 A, B, and C).

A

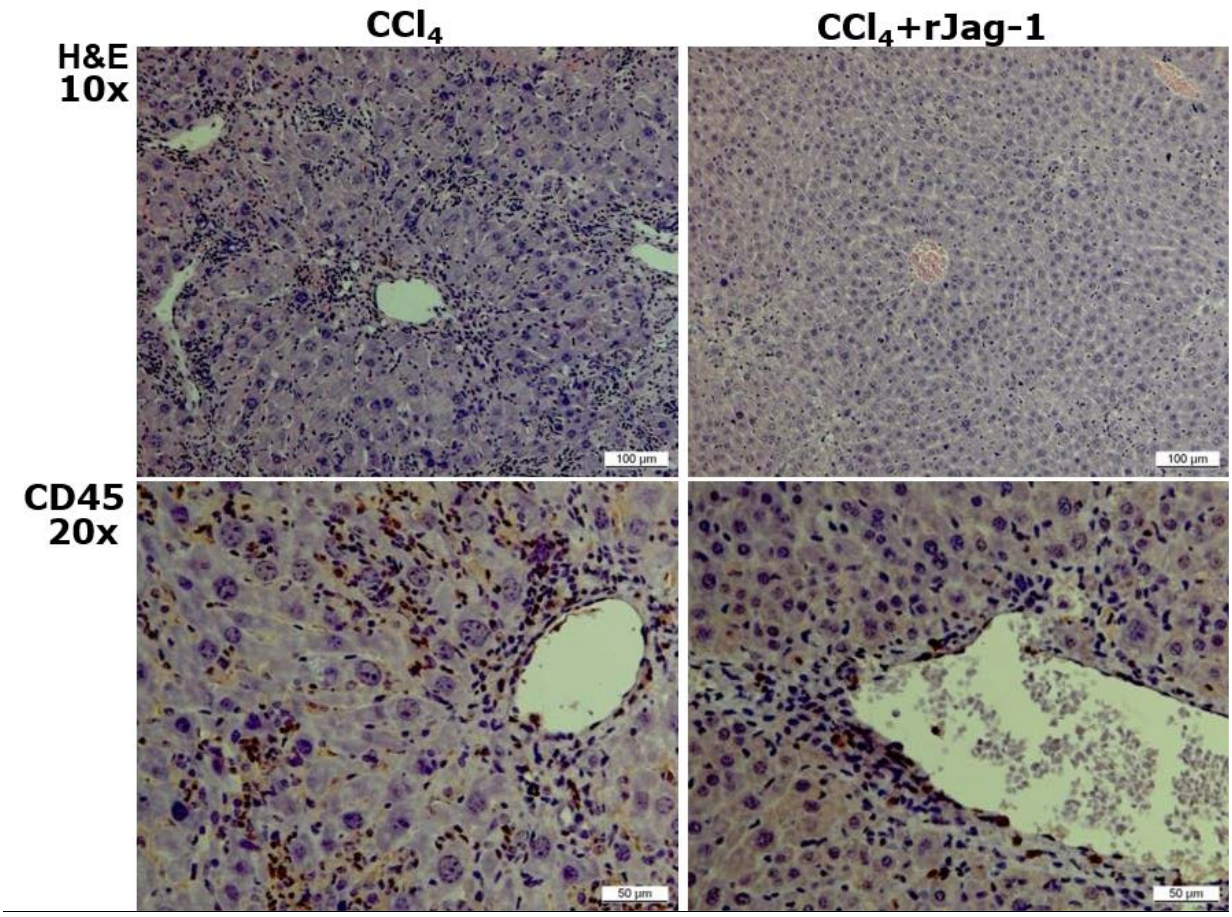

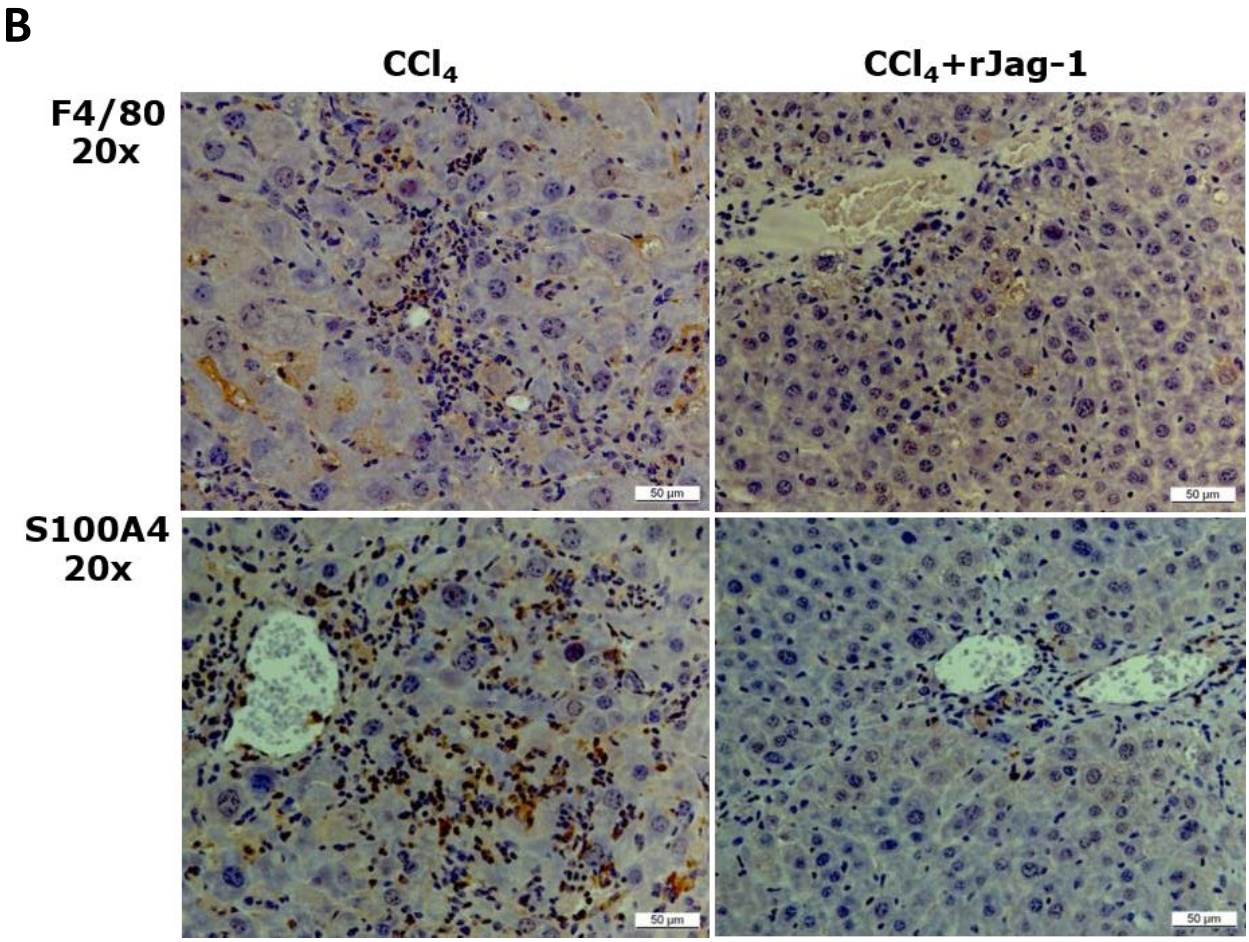

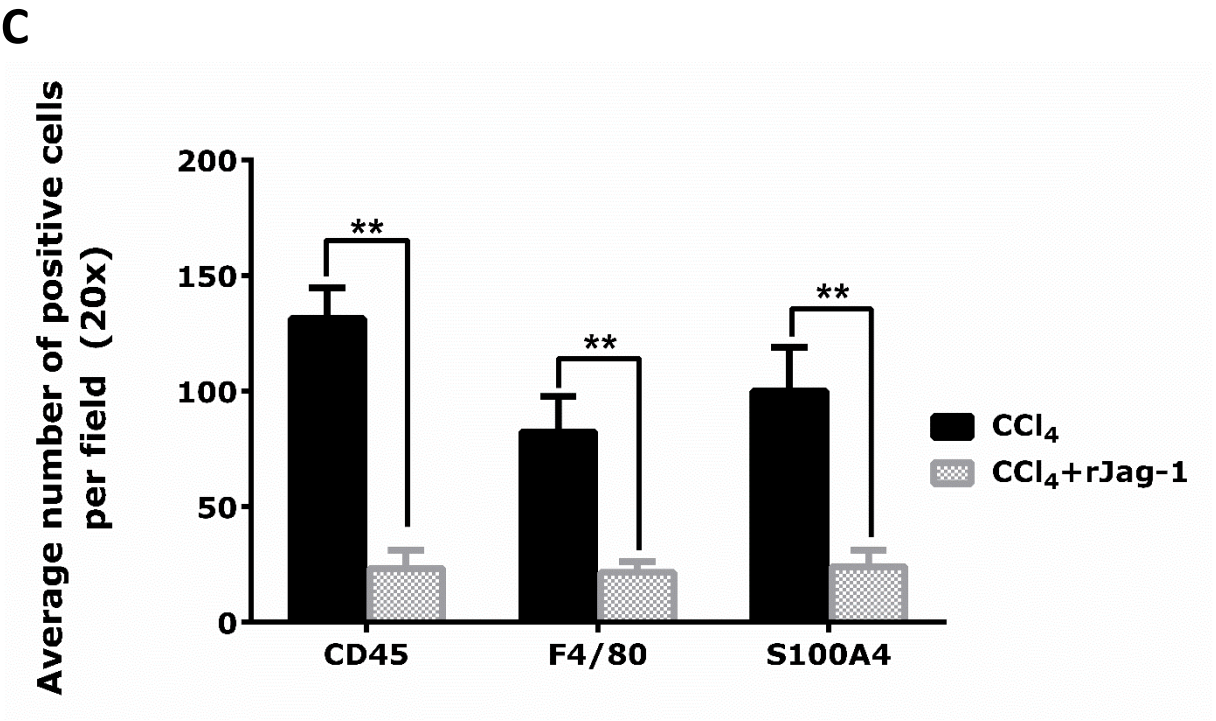

Figure 3.22 Reduction of liver inflammation by rJag-1 in the CCl_4 animal model (A) H&E and CD45 IHC (B) F4/80 and S100A4 IHC (C) Semi-quantification of F4/80, S100A4 and CD45 staining using ImageJ software. S100A4 is a cell marker for macrophages.

3.3.3 rJag-1 aggravated BDL outcome

Similar to rDll4, rJag-1 caused death of all BDL-operated animals within 1 week (Figure 10.2). At early time points, i.e., 6 h, 12 h, and 24 h after BDL operation, there were no difference in bile infarct size between BDL- and BDL+rJag-1-treated mice (Figure 3.23).

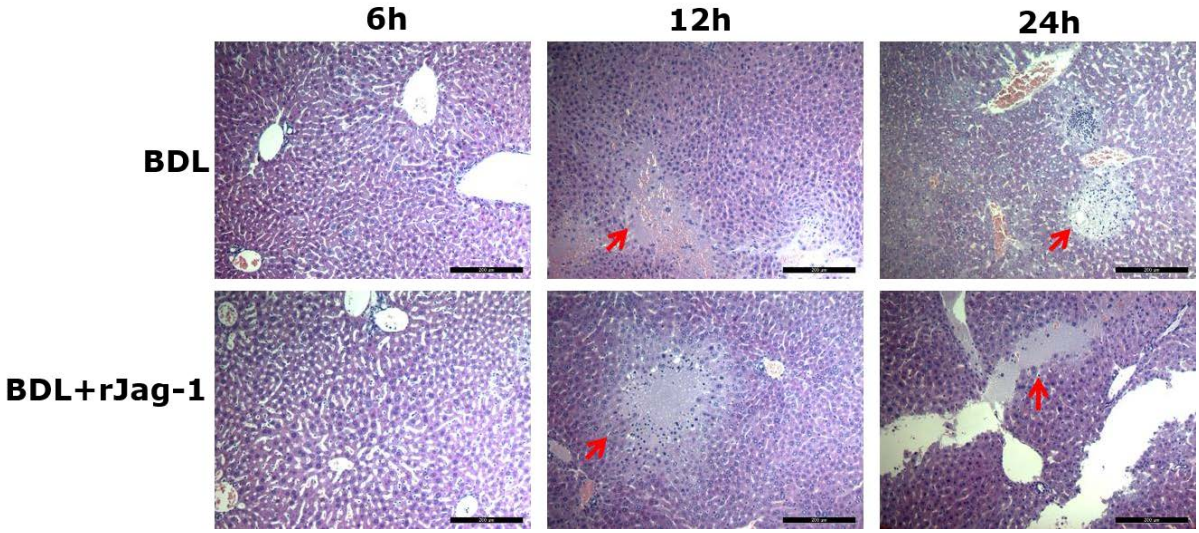

Figure 3.23 Bile infarcts formation (highlighted by red arrows) in BDL and BDL+rJag-1 at 6 h, 12 h and 24 h following BDL surgery.

In contrast to rDll4 which decreased serum levels of alanine aminotransferase (ALT) and aspartate aminotransferase (AST) 6 h following BDL operation, rJag-1 increased the levels of ALT and AST (Figure 10.1). In addition, rJag-1 did not change CCL2 expression (Figure 3.24). Treatment with rJag-1 and rCcl2 increased liver CCL2 expression (Figure 3.24).

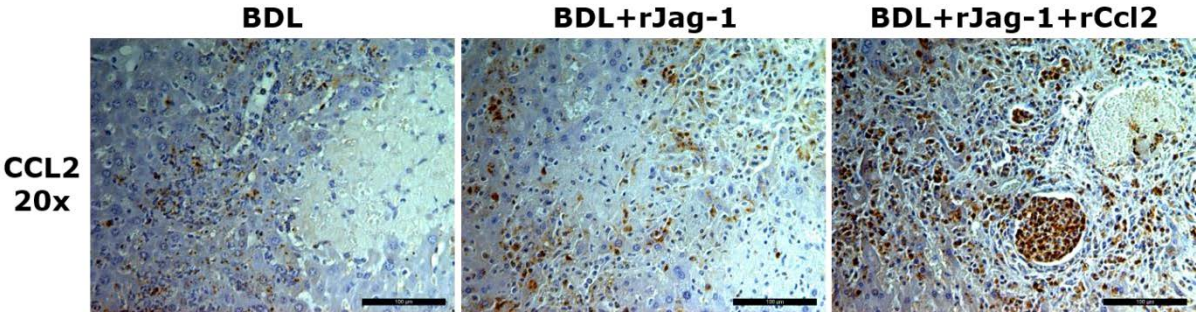

Figure 3.24 CCL2 expression in BDL, BDL+rJag-1, and BDL+rJag-1+rCcl2 groups 5 d after BDL.

3.3.4 rCcl2 did not rescue rJag-1-administrated BDL mice

In contrast to rDll4, treatment of animals with rCcl2 did not prevent rJag1-induced death (Figure 10.2). Treatment with rJag-1 and rCcl2 increased the size of BDL-induced bile infarcts (Figure 3.25), and the infiltration of neutrophils and macrophages (Figure 3.26).

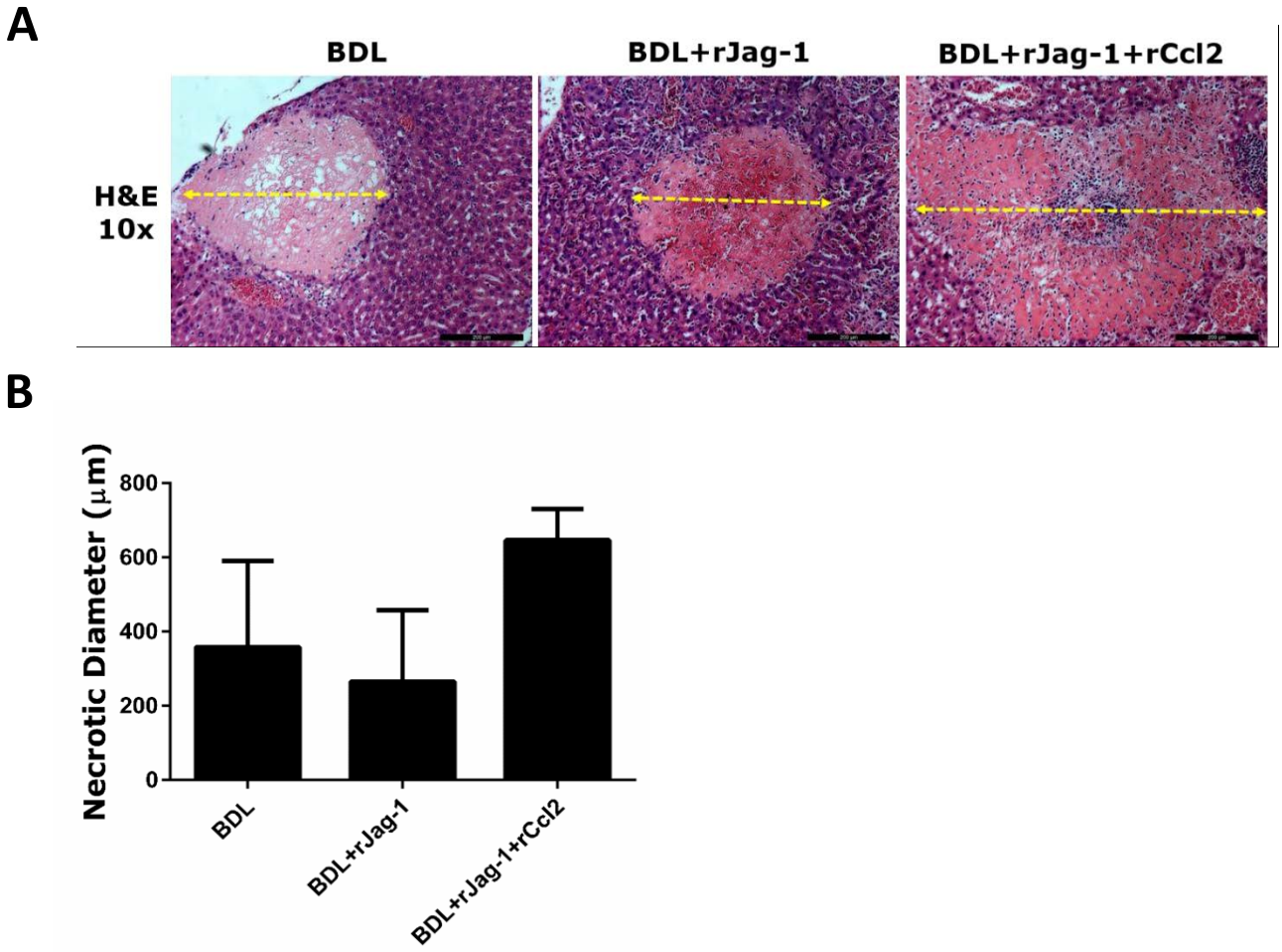

Figure 3.25 (A) H&E staining showing bile infarct 5 d following BDL-operated mice with/without rJag-1 (6.25 μg/kg) and rCcl2 (5 μg/kg) treatment (B) The average maximum diameter of bile infarcts (three different area per mice, n=6 per group).

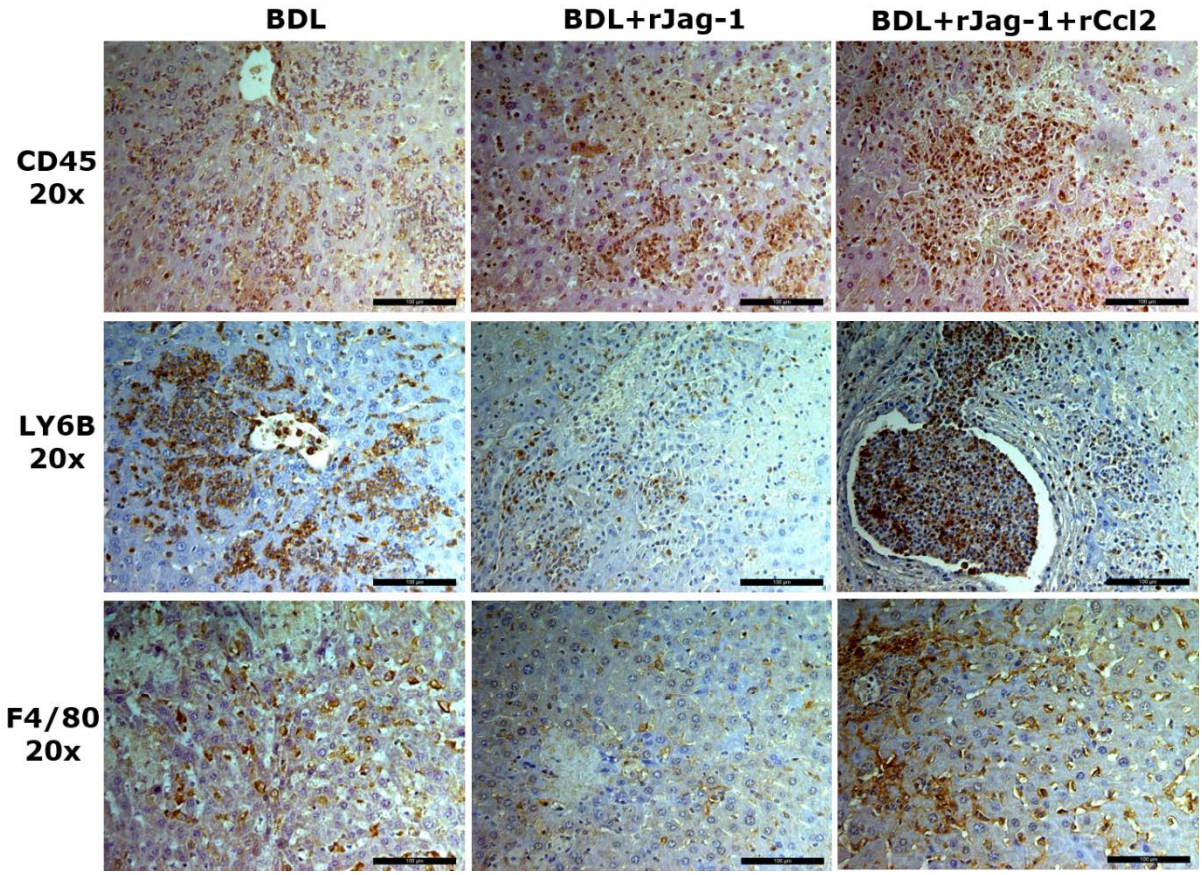

Figure 3.26 IHC for CD45, Ly6B, and F4/80 in BDL-operated mice with/without rJag-1 and rCcl2 treatment 5 d following BDL. LY6B is a cell marker for neutrophils.

3.3.5 rJag-1 administration did not affect hepatocyte apoptosis and chemokines synthesis in KCs and HSCs

Like rDll4, rJag-1 did not impact TNF-α-and TGF-β-induced hepatocyte apoptosis (Figure 3.27).

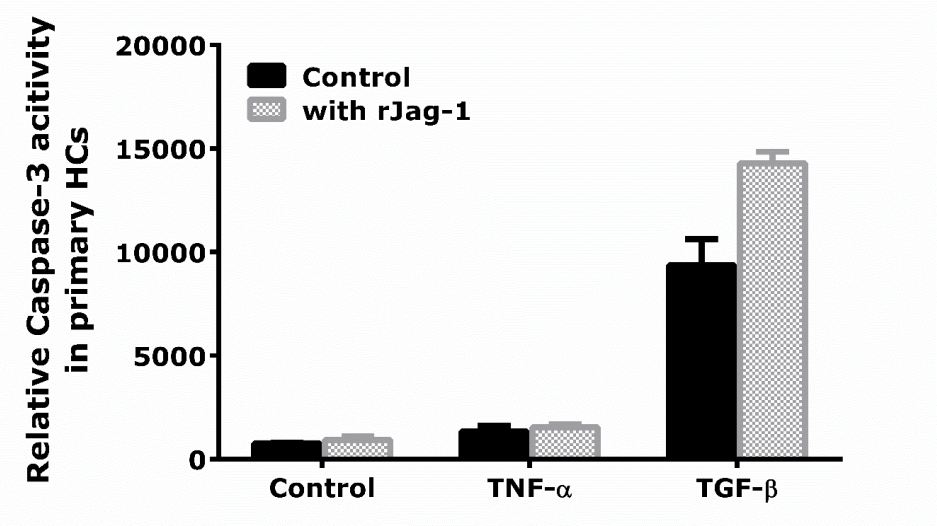

Figure 3.27 Caspase-3 activity assay Primary mouse hepatocytes were treated with TNF-α (20ng/ml) or TGF-β (5 ng/ml) with/without rJag-1 (500 ng/ml) for 48 h.

In addition, rJag-1 did not alter LPS-induced *Ccl2* expression in RAW264.7 and JS-1 cells (Figure 3.28 A and B).

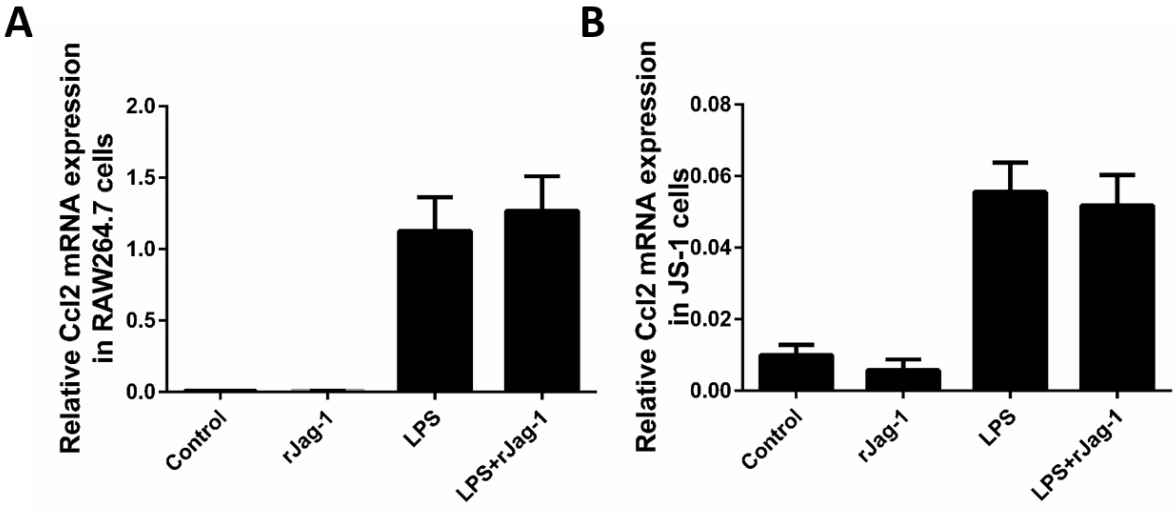

Figure 3.28 Effects of rJag-1 on LPS-induced *Ccl2* mRNA levels in (A) RAW264.7 and (B) JS-1 cells.

3.3.6 rJag-1 did not affect NFκB pathway

In contrast to rDll4, rJag-1 did not inhibit LPS-induced nuclear translocation of p65 (Figure 3.29 A and B).

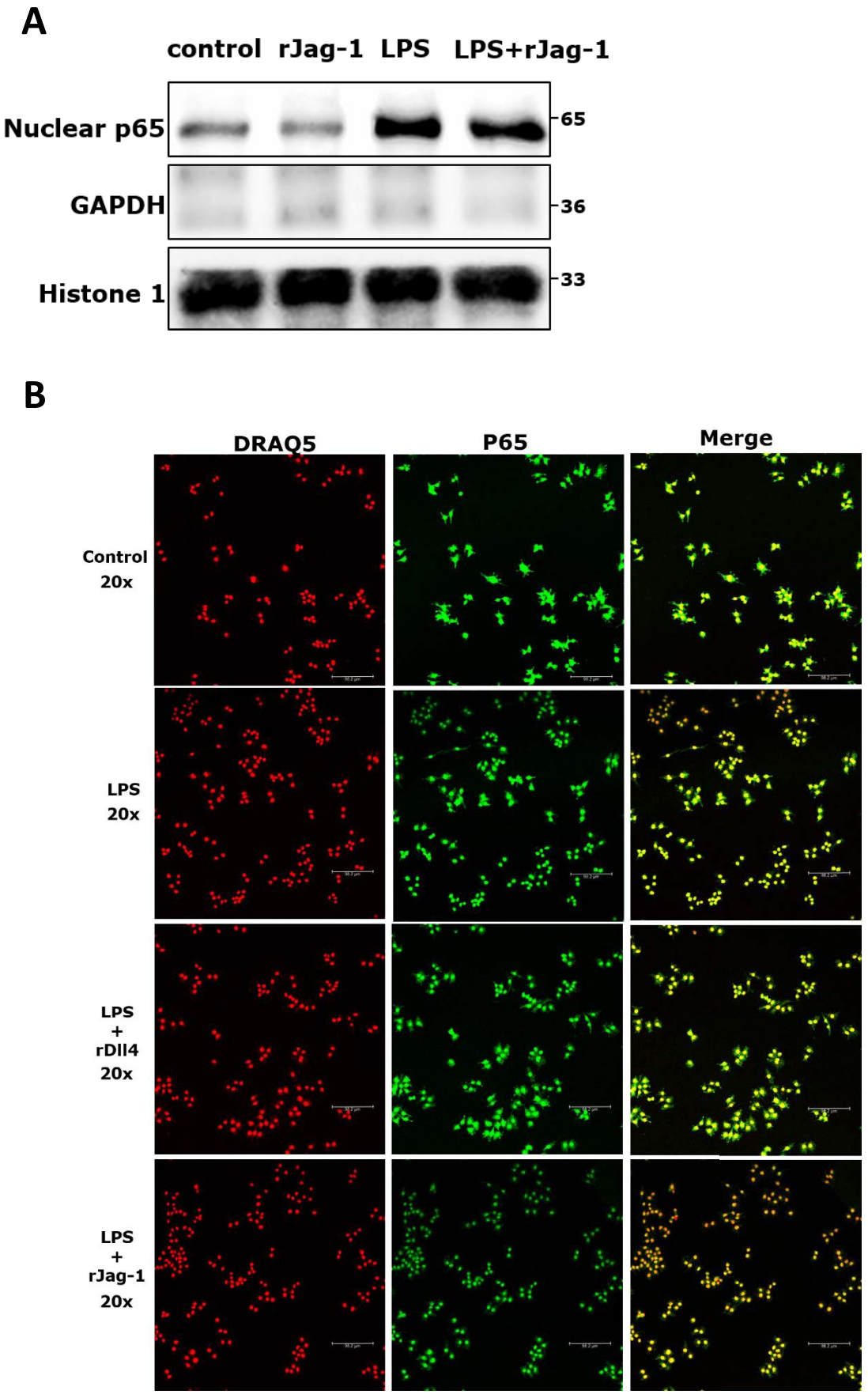

Figure 3.29. rJag-1 did not inhibit LPS-induced nuclear translocation of p65 (A) immunoblot of nuclear fraction (B) IF staining of RAW264.7 cells.

4 DISCUSSION

Previous studies reported the pivotal roles of Notch signaling in acute and chronic liver injuries (Bansal et al., 2015; Hoeft and Kramann, 2017; Yu et al., 2011; Zhang et al., 2016b). However, the roles of individual Notch ligands are still unknown. Underkoffler et al. found that *Jag1* null mutant livers upregulated fibrosis-related genes (Underkoffler et al., 2013). However, Tang et al. showed that *Jag1* knockdown diminished liver fibrosis by suppressing epithelial-mesenchymal transition (EMT) of HSCs in CCl_4-treated rats (Tang et al., 2017).

The current study investigated canonical Notch ligands and receptors in patients with hepatolithiasis and HBV-related cirrhosis. We focused on Notch ligands JAG1 and DLL4, the only ligands expressed in sinusoids of cirrhotic patients. IF staining identified KC and LSECs, but not HSCs, as the sinusoidal cells that express DLL4. The results suggest the potential association of the Notch ligand with liver inflammation, which was supported by additional data that sinusoidal DLL4 expression correlated with inflammation grade in chronic HBV-infected patients (unpublished data).

Under inflammatory conditions, expression of Notch ligands are induced by exogenous factors such as toll-like receptor (TLR) ligands (e.g. LPS) and pathogen (e.g. bacteria and virus) and endogenous inflammatory cytokines such as TNF-α and IL-1β (Shang et al., 2016). Fung and colleagues (2007) showed that human macrophages stimulated with LPS or interleukin (IL)1β increased the expression of DLL4. LPS also induced the expression of JAG1 in primary human and murine macrophages (Foldi et al., 2010). We found that LPS upregulated JAG1 expression, but did not affect DLL4, in RAW264.7 cells (Figure 10.3). This can be explained by different signaling kinetics of Notch family members. Previous studies reported earlier upregulation of JAG1 (12 h) compared to DLL4 (48 h) after LPS treatment of macrophages (Foldi et al., 2010; Fung et al., 2007). In the current experiment, we detected DLL4 and JAG1 24 h following LPS treatment.

Besides Notch ligands, NOTCH1 receptor was overexpressed as well in the sinusoids of cirrhotic patients. The finding is consistent with a previous study showing that *Notch1* mRNA was elevated 10-fold in livers of mice with HBV infection (Wei et al., 2016). In addition, the expression of the NOTCH1 receptor was altered as well in diverse inflammatory microenvironments (Briot et al., 2015; Fazio et al., 2016).

To understand the roles of JAG1 and DLL4 in liver injury, we examined the expression of the two Notch ligands in mice treated with CCl_4. In contrast to patients, JAG1 or DLL4 were not expressed in sinusoids of the animals (data not shown). To observe the effects of DLL4 and JAG1 in this model, we injected recombinant DLL4 and JAG1 into the animals. Several studies demonstrated the biological activity of recombinant Notch ligands *in vivo*. For examples, intraperitoneal injection of rDll4 ameliorated acute kidney failure (Gupta et al., 2010). Following brain ischemia, rDll4 increased expansion of neuronal progenitor cells together with other growth factors (Oya et al., 2008).

In the CCl_4 animal model, both rDll4 and rJag-1 improved liver fibrosis, reduced liver inflammation, and hepatocyte apoptosis. Next, we examined the effects of rDll4 and rJag-1 in BDL animals, additional classic liver injury and fibrosis model. Surprisingly, all BDL mice injected with Notch ligands died within 1 week while saline-treated BDL mice lived up to 2 weeks. Similar to Notch ligands, knockdown of A1 adenosine receptor decreased CCl_4-induced fibrosis, whereas it increased fibrosis in BDL mice (Yang et al., 2010). Iwaisakoa et al. and Yang et al. reported different fibrosis-related genes between these two mouse models (Iwaisako et al., 2014; Yang et al., 2010). These results confirm the notion that these two animal models are different. On the other side, Notch signaling can induce opposite outcomes in different models of cellular proliferation, tumor growth, and organ fibrosis (Hoeft and Kramann, 2017; Schwanbeck et al., 2011). Taken together, disease etiology and cellular context determine the outcome of Notch signaling.

Interestingly, blocking canonical Notch signaling pathway through specific KO of *Rbjκ* in myeloid cells improved fibrosis and diminished infiltration of macrophage and neutrophils cells in the liver of CCl_4-and BDL-treated mice. On the contrary, general deletion of *Rbjκ* aggravated CCl_4-induced hepatic fibrosis (He et al., 2015) highlighting the way of interference with Notch signaling as another determiner of the outcome of Notch signaling.

To elucidate causes underlying BDL mice death, we analyzed liver tissues at early and late time points (6 h, 12 h, 24 h, 4 d, and 7 d) following BDL. We found that rDll4-treated BDL mice had remarkable larger bile infarcts than BDL mice. Furthermore, enhanced bile infarct was accompanied by reduced inflammation. The absence of inflammation in rDll4-treated BDL mice facilitates the development of massive hepatic necrosis.

To clarify how rDll4 inhibited inflammatory cell infiltration, we examined the expression of chemokines in liver tissues and cultured cells. *In vivo*, rDll4 inhibited chemokine expression in both CCl_4 and BDL treated mice. *In vitro*, rDll4 inhibited *Ccl2, Ccl5, Ccl8, Cxcl9* in KCs, as well *Ccl2* in HSCs.

To test whether chemokine plays a crucial protective role in BDL mice, we treated the BDL mice with rCcl2. rCcl2 rescued rDll4-treated BDL mice from death. In rCcl2-treated mice, inflammatory cells increased and size of bile infarcts reduced.

The relationship between DLL4 and CCL2 has been studied in different disease settings by other groups. Aikawa and co-workers studied the interaction between DLL4 and CCL2 chemokines in macrophage RAW264.7 cells. In contrast to our findings, rDll4 increased *Ccl2* expression in these cells, whereas *Dll4* knockdown decreased *Ccl2* expression. Similar results were also demonstrated in 3T3-L1 adipocytes. Furthermore, anti-Dll4 antibody attenuated the expression of *Ccl2* in atherosclerotic lesions (Fukuda et al., 2012). This difference might be explained by the experimental approaches. In the current study, we incubated macrophages with rDll4 directly, whereas Fukuda et al. immobilized rDll4 on the culture plate. Membrane-bound DLL4 and soluble DLL4 have different functional mechanisms as shown by previous studies (Lahmar et al., 2008). In addition, we investigated the impact of rDll4 on cells stimulated by LPS, whereas Fukuda *et al*. (2012) only examined rDll4 in the absence of LPS.

To further investigate the mechanisms of how rDll4 inhibits CCL2, we focused on NFκB signaling pathway, the common downstream signaling exploited by inflammation (Ghosh and Hayden, 2008; Shang et al., 2016). The expression of p65 protein, a primary effector of NFκB signaling pathway, increased in inflammatory cells infiltrating liver of BDL mice. Treatment with rDll4 decreased p65 expression in inflammatory cells. rCcl2 administration restored expression of p65. In RAW264.7 cells, both rDll4 and NFκB inhibitor (JSH-23) inhibited LPS-induced CCL2 expression. Furthermore, LPS-induced nuclear translocation of p65 was inhibited by rDll4 administration. These results suggest that rDll4 inhibits CCL2 expression through interfering with NFκB pathway. In line with our findings, Fukuda et al. also showed that CCL2 expression was increased in macrophages by DLL4 through NFκB pathway (Fukuda et al., 2012).

Interestingly, inhibition of inflammation by rDll4 occurs in both CCl_4 and BDL animal models. However, the Notch ligand produced opposite outcomes, which were

determined by different disease conditions. In the CCl_4 model, rDll4-mediated chemokine inhibition decreases inflammatory cell infiltration and thus attenuates hepatocyte death and fibrosis. However, in the BDL model, limiting bile infarcts requires massive recruitment of inflammatory cells to clear the debris of dead liver cells. CCL2 inhibition by rDll4 blocks recruitment of circulating inflammatory cells into necrotic areas. Consequently, bile infarcts progress into massive hepatic necrosis.

In addition to animal models, we found an inverse association between DLL4 and CCL2 expression in liver tissues of ACLF patients. ACLF is a new disease entity characterized by acute decompensation, dysregulated systemic inflammatory syndrome, and multiorgan failure. ACLF patients undergo systemic inflammatory response syndrome (SIRS) at the early stage of the disease. In such condition, patients suffered from cytokine storm characterized with extremely high levels of different pro-inflammatory cytokines, e.g. TNF-α, IL6, and chemokines including CCL2 (Alam et al., 2017; Khanam et al., 2017; Roth et al., 2009). CCL2 levels were increased in the serum and urine of ACLF patients (Graupera et al., 2016; Roth et al., 2009). The absence of DLL4 expression might be a reason underlying high levels of CCL2 in ACLF.

Several studies reported active Notch signaling in hepatic and extrahepatic inflammatory conditions including primary biliary cirrhosis (Shackel et al., 2001), rheumatoid arthritis (Park et al., 2015), systemic lupus erythematosus (Zhang et al., 2010), and others (Shang et al., 2016). In addition, inhibition of DLL4 activity reduced inflammatory cells infiltration in several diseases (Fukuda et al., 2012; Takeichi et al., 2010). On the other hand, myeloid *Dll4* deficiency did not change the status of hepatic inflammation in low-density lipoprotein receptor KO ($Ldlr^{-/-}$) mouse model of non-alcoholic steatohepatitis, (Jeurissen et al., 2016).

In contrast to rDll4, rJag-1 did not affect *Ccl2* expression *in vitro* and *in vivo*. rCcl2 did not protect rJag-1-treated BDL animals from death. Although the mechanisms of rJag-1-mediated effects remain highly speculative, it is clear that rJag-1-mediated responses are CCL2-independent. Moreover, rJag-1 did not influence LPS-induced *Ccl2* expression or inhibit LPS-induced nuclear translocation of p50 and p65 in macrophages. The results suggest different functional mechanisms between rDll4 and rJag-1, although they showed similar effects in BDL- and CCl_4-induced liver injury. The difference is also reflected in the early changes of ALT and AST in BDL mice: rDll4 decreased, but rJag-1 increased serum ALT and AST levels. Additionally,

rJag-1 did not impact inflammatory cell infiltration in BDL mice compared to rDll4. Therefore, administration of rCcl2 did not benefit the BDL mice treated with rJag-1. By contrast, rCcl2 even led to larger massive bile infarcts than those of BDL mice only treated with rJag-1.

Co-IF analysis of macrophages further showed that rJag-1 increased LPS-induced p65 nuclear translocation in contrast to rDll4. Similarly, JAG1-NOTCH1 signaling increased several NFκB target genes in cultured endothelial cells (Nus et al., 2016). Considering that BDL mice have a higher sensitivity to LPS and NFκB signaling pathway (Harry et al., 1999), further potentiation of this signaling pathway by rJag-1 might be responsible for the rapid death of BDL animals and the early increase in ALT and AST enzymes. Indeed, rJag-1 might increase bacterial translocation from intestine leading to an increase in the serum concentration of LPS thus accelerating the death of BDL mice. In this direction, previous studies already reported crucial roles for Notch signaling in intestinal homeostasis (Pellegrinet et al., 2011) and gut-liver axis (Fowler et al., 2011). However, this interesting hypothesis is beyond the scope of the current study and merits further investigation to confirm it.

The mechanistic differences between rDll4 and rJag-1 confirm the idea that Notch receptors and Notch ligands are not redundant. The same notion was confirmed by different animal phenotypes created by genetic modulation of these genes (Boucher et al., 2012). For example, DLL4 cannot replace DLL1 in myogenic differentiation (Preuße et al., 2015). Distinct biological functions were also reported for JAG1 versus JAG2 in cancer (Choi et al., 2009) and DLL1 versus JAG1 in osteoclastogenesis (Sekine et al., 2012). Similarly, DLL4 and JAG1 respond differently in various pathophysiological contexts. In plaques from patients with peripheral artery diseases, high expression of *DLL4* was associated with upregulation of inflammatory genes such as *CD68, COX2, and VCAM1.* Under such conditions, *JAG1* was downregulated and *vice versa* (Aquila et al., 2017).

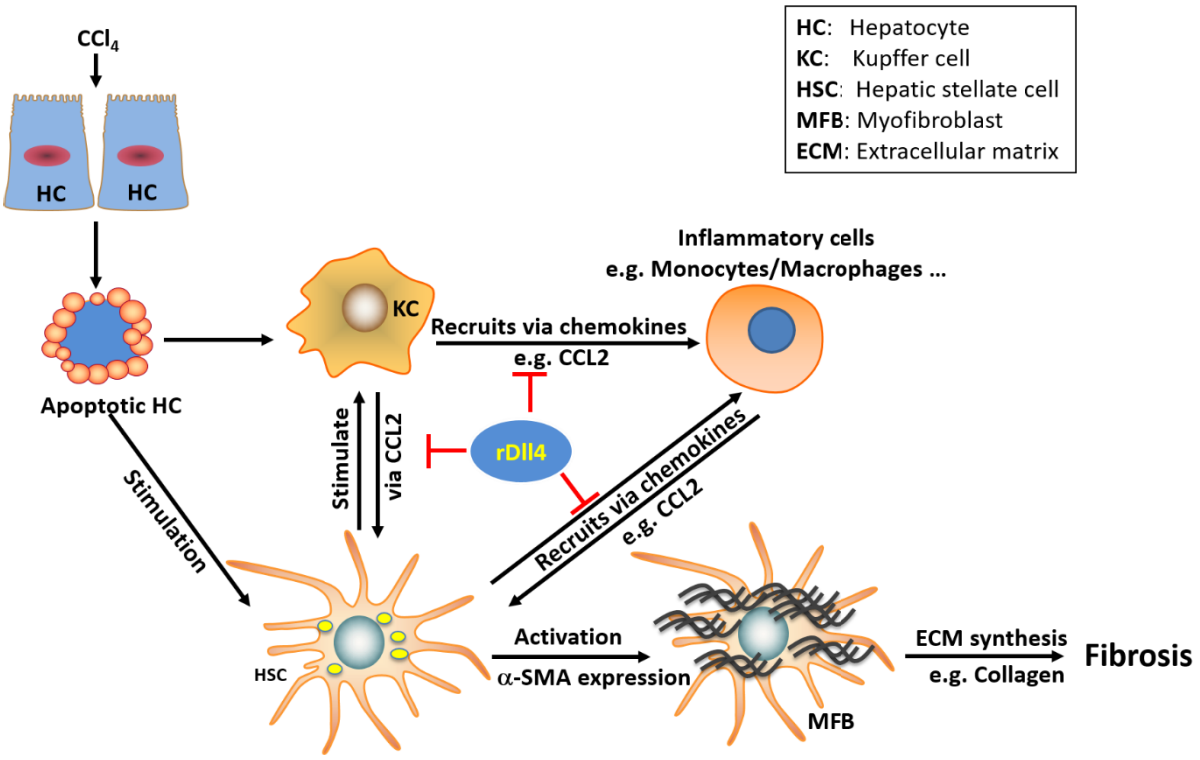

Figure 4.1 A scheme summarizing the effects of rDll4 in CCl_4-dependent liver damage.

Taken together, only DLL4 and JAG1 were overexpressed in sinusoidal cells during HBV-induced liver fibrosis and cirrhosis. rDll4 and rJag-1 reduced CCl_4-induced damage, while they induced quick death of all BDL mice. These results highlight the importance of etiology of liver diseases in determining the outcome of DLL4 and JAG1. rDll4 mediated its action through inhibition of chemokines secretion that leads to a decrease in inflammatory cells infiltration, improvement of liver fibrosis, and hepatocytes apoptosis in the CCl_4 animal model (Figure 4.1). On the other hand, inhibition of chemokines reduced infiltration of inflammatory cells into the liver of BDL mice. Reduced inflammatory reaction led to a compromised wound-healing response and unrestricted growth of bile infarcts to panacinar and multilobular necrosis affecting more than 60-70% of the liver, leading to the death of mice within 1 week after BDL surgery (Figure 4.2 A). Interestingly, the lack of DLL4 expression in the liver of ACLF patients was associated with CCL2 overexpression, which could contribute to cytokine storm associated with ACLF. On the other side, rJag-1 produced similar responses in CCl_4 and BDL animal models. Interestingly, rJag-1-mediated effects were CCL2-independent (Figure 4.2 B). The underlying mechanisms of rJag-1 warrant further investigations.

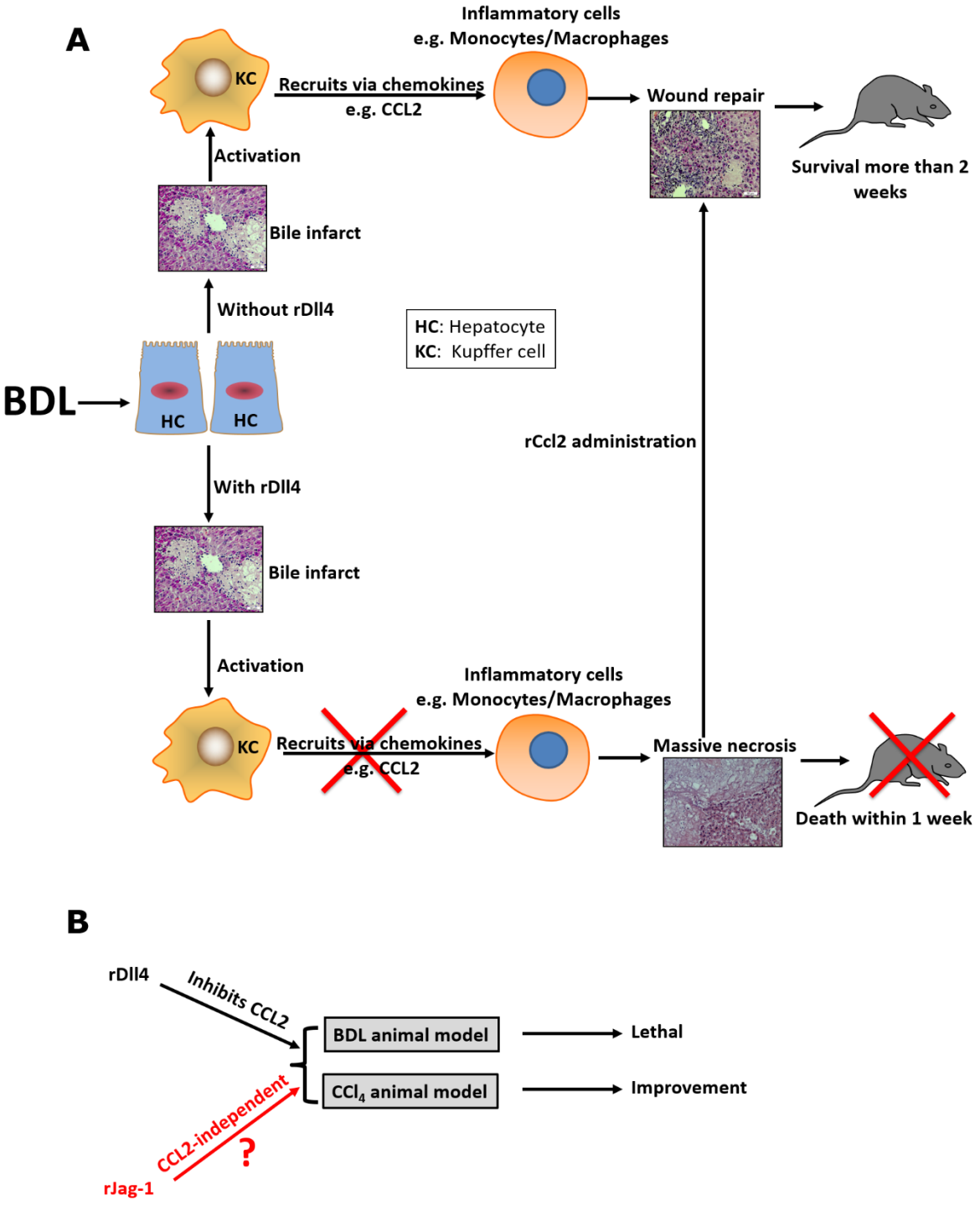

Figure 4.2 Panel (A) summarizing the effects of rDll4 in BDL-dependent liver damage Panel (B) shows similarities and differences between rDll4 and rJag-1.

The current results suggest that Notch ligands could act as a bona fide that either improve or worsen liver injury based on the etiology of liver diseases. Therefore, Well-understanding of etiology of liver diseases and specifying the functions of

individual members of Notch family will assist in the design of more effective Notch-based therapeutics with minimal off-target effects.

5 SUMMARY

Introduction

To date, the roles of individual Notch ligands in liver injury are not well defined. The current study investigated whether and how Notch ligands DLL4 and JAG1 affect liver injury.

Methods

We examined the expression of Notch ligands and receptors by immunohistochemistry (IHC) in the liver samples of 26 patients with HBV-induced liver cirrhosis. The function of recombinant Dll4 (rDll4) and rJag-1 was investigated *in vivo* in carbon tetrachloride (CCl_4) and bile duct ligation (BDL) animal models and *in vitro* in hepatocytes, Kupffer cells (KCs), and hepatic stellate cells (HSCs).

Results

DLL4 and JAG1 were the only Notch ligands expressed in liver sinusoids of examined patients. In the CCl_4 animal model, rDll4 and rJag-1 ameliorated liver fibrosis, decreased infiltration of inflammatory cells, and inhibited apoptosis. On the contrary, rDll4 and rJag-1 caused rapid death of all BDL mice within 1 week. rDll4 inhibited the expression of chemokine ligand 2 (CCL2) and infiltration of inflammatory cells in livers of BDL mice, whereas rJag-1 did not have any impact on inflammatory cells infiltration and CCL2 expression. In macrophages and HSCs, rDll4 inhibited LPS-induced CCL2 expression, whereas rJag-1 did not impact CCL2 expression. Inhibition of inflammation by rDll4 caused unrestricted bile infarct and rapid death of BDL animals. Recombinant Ccl2 (rCcl2) restored the infiltration of inflammatory cells, decreased the size of bile infarcts and rescued rDll4-treated BDL animals from death. In ACLF patients, DLL4 expression was negatively associated with expression of CCL2. In contrast to rDll4-treated BDL animals, rCcl2 did not rescue rJag-1-treated BDL animals.

Conclusion

Etiology determines the effects of DLL4 and JAG1 on liver injury. DLL4 inhibits liver inflammation through inhibiting CCL2, a key chemokine for recruitment of inflammatory cells. How Jag-1 impact liver injury requires further investigation.

6 REFERENCES

Alam, A., Chun Suen, K., and Ma, D. (2017). Acute-on-chronic liver failure: recent update. J. Biomed. Res. *31*, 283–300.

del Álamo, D., Rouault, H., and Schweisguth, F. (2011). Mechanism and significance of cis-inhibition in Notch signalling. Curr. Biol. CB *21*, R40-47.

Andersen, P., Uosaki, H., Shenje, L.T., and Kwon, C. (2012). Non-canonical Notch signaling: emerging role and mechanism. Trends Cell Biol. *22*, 257–265.

Andersson, E.R., and Lendahl, U. (2014). Therapeutic modulation of Notch signalling — are we there yet? Nat. Rev. Drug Discov. *13*, 357–378.

Antfolk, D., Sjöqvist, M., Cheng, F., Isoniemi, K., Duran, C.L., Rivero-Muller, A., Antila, C., Niemi, R., Landor, S., Bouten, C.V.C., et al. (2017). Selective regulation of Notch ligands during angiogenesis is mediated by vimentin. Proc. Natl. Acad. Sci. U. S. A. *114*, E4574–E4581.

Aquila, G., Fortini, C., Pannuti, A., Delbue, S., Pannella, M., Morelli, M.B., Caliceti, C., Castriota, F., de Mattei, M., Ongaro, A., et al. (2017). Distinct gene expression profiles associated with Notch ligands Delta-like 4 and Jagged1 in plaque material from peripheral artery disease patients: a pilot study. J. Transl. Med. *15*, 98.

Artavanis-Tsakonas, S., Muskavitch, M.A., and Yedvobnick, B. (1983). Molecular cloning of Notch, a locus affecting neurogenesis in Drosophila melanogaster. Proc. Natl. Acad. Sci. U. S. A. *80*, 1977–1981.

Aster, J.C., Pear, W.S., and Blacklow, S.C. (2017). The Varied Roles of Notch in Cancer. Annu. Rev. Pathol. Mech. Dis. *12*, 245–275.

Bancroft, J.D., and Layton, C. (2013). Connective and mesenchymal tissues with their stains. Bancrofts Theory Andpractice Histol. Tech. Suvarna SK Layton C Bancroft JD Eds 187–214.

Bansal, R., van Baarlen, J., Storm, G., and Prakash, J. (2015). The interplay of the Notch signaling in hepatic stellate cells and macrophages determines the fate of liver fibrogenesis. Sci. Rep. *5*.

Benedito, R., Roca, C., Sörensen, I., Adams, S., Gossler, A., Fruttiger, M., and Adams, R.H. (2009). The Notch Ligands Dll4 and Jagged1 Have Opposing Effects on Angiogenesis. Cell *137*, 1124–1135.

Best, J., Manka, P., Syn, W.-K., Dollé, L., van Grunsven, L.A., and Canbay, A. (2015). Role of liver progenitors in liver regeneration. Hepatobiliary Surg. Nutr. *4*, 48–58.

Bielesz, B., Sirin, Y., Si, H., Niranjan, T., Gruenwald, A., Ahn, S., Kato, H., Pullman, J., Gessler, M., Haase, V.H., et al. (2010). Epithelial Notch signaling regulates interstitial fibrosis development in the kidneys of mice and humans. J. Clin. Invest. *120*, 4040–4054.

Blair, S.S. (2000). Notch signaling: Fringe really is a glycosyltransferase. Curr. Biol. *10*, R608–R612.

Borggrefe, T., and Liefke, R. (2012). Fine-tuning of the intracellular canonical Notch signaling pathway. Cell Cycle *11*, 264–276.

Boucher, J., Gridley, T., and Liaw, L. (2012). Molecular pathways of notch signaling in vascular smooth muscle cells. Front. Physiol. *3*, 81.

Boulter, L., Govaere, O., Bird, T.G., Radulescu, S., Ramachandran, P., Pellicoro, A., Ridgway, R.A., Seo, S.S., Spee, B., Van Rooijen, N., et al. (2012a). Macrophage derived Wnt signalling opposes Notch signalling in a Numb mediated manner to specify HPC fate in chronic liver disease in human and mouse. Nat. Med. *18*, 572–579.

Boulter, L., Govaere, O., Bird, T.G., Radulescu, S., Ramachandran, P., Pellicoro, A., Ridgway, R.A., Seo, S.S., Spee, B., Van Rooijen, N., et al. (2012b). Macrophage-derived Wnt opposes Notch signaling to specify hepatic progenitor cell fate in chronic liver disease. Nat. Med. *18*, 572–579.

Briot, A., Civelek, M., Seki, A., Hoi, K., Mack, J.J., Lee, S.D., Kim, J., Hong, C., Yu, J., Fishbein, G.A., et al. (2015). Endothelial NOTCH1 is suppressed by circulating lipids and antagonizes inflammation during atherosclerosis. J. Exp. Med. *212*, 2147–2163.

Bulman, M.P., Kusumi, K., Frayling, T.M., McKeown, C., Garrett, C., Lander, E.S., Krumlauf, R., Hattersley, A.T., Ellard, S., and Turnpenny, P.D. (2000). Mutations in the human delta homologue, DLL3, cause axial skeletal defects in spondylocostal dysostosis. Nat. Genet. *24*, 438–441.

Carrieri, F.A., and Dale, J.K. (2017). Turn It Down a Notch. Front. Cell Dev. Biol. *4*.

Cech, T.R., and Steitz, J.A. (2014). The noncoding RNA revolution-trashing old rules to forge new ones. Cell *157*, 77–94.

Ceni, E., Mello, T., Polvani, S., Vasseur-Cognet, M., Tarocchi, M., Tempesti, S., Cavalieri, D., Beltrame, L., Marroncini, G., and Pinzani, M. (2017). The orphan nuclear receptor COUP-TFII coordinates hypoxia-independent proangiogenic responses in hepatic stellate cells. J. Hepatol. *66*, 754–764.

Chen, Y., Zheng, S., Qi, D., Zheng, S., Guo, J., Zhang, S., and Weng, Z. (2012). Inhibition of Notch signaling by a γ-secretase inhibitor attenuates hepatic fibrosis in rats. PloS One *7*, e46512.

Chillakuri, C.R., Sheppard, D., Lea, S.M., and Handford, P.A. (2012). Notch receptor–ligand binding and activation: Insights from molecular studies. Semin. Cell Dev. Biol. *23*, 421–428.

Choi, K., Ahn, Y.-H., Gibbons, D.L., Tran, H.T., Creighton, C.J., Girard, L., Minna, J.D., Qin, F.X.-F., and Kurie, J.M. (2009). Distinct biological roles for the notch ligands Jagged-1 and Jagged-2. J. Biol. Chem. *284*, 17766–17774.

Czaja, A.J. (2014). Hepatic inflammation and progressive liver fibrosis in chronic liver disease. World J. Gastroenterol. WJG *20*, 2515–2532.

Deftos, M.L., He, Y.W., Ojala, E.W., and Bevan, M.J. (1998). Correlating notch signaling with thymocyte maturation. Immunity *9*, 777–786.

Dill, M.T., Tornillo, L., Fritzius, T., Terracciano, L., Semela, D., Bettler, B., Heim, M.H., and Tchorz, J.S. (2013). Constitutive Notch2 signaling induces hepatic tumors in mice. Hepatol. Baltim. Md *57*, 1607–1619.

Fabris, L., Cadamuro, M., Guido, M., Spirli, C., Fiorotto, R., Colledan, M., Torre, G., Alberti, D., Sonzogni, A., Okolicsanyi, L., et al. (2007). Analysis of Liver Repair Mechanisms in Alagille Syndrome and Biliary Atresia Reveals a Role for Notch Signaling. Am. J. Pathol. *171*, 641–653.

Fazio, C., Piazzi, G., Vitaglione, P., Fogliano, V., Munarini, A., Prossomariti, A., Milazzo, M., D'Angelo, L., Napolitano, M., Chieco, P., et al. (2016). Inflammation increases NOTCH1 activity via MMP9 and is counteracted by Eicosapentaenoic Acid-free fatty acid in colon cancer cells. Sci. Rep. *6*, 20670.

Fiorotto, R., Raizner, A., Morell, C.M., Torsello, B., Scirpo, R., Fabris, L., Spirli, C., and Strazzabosco, M. (2013). Notch signaling regulates tubular morphogenesis during repair from biliary damage in mice. J. Hepatol. *59*, 124–130.

Fischer, A., and Gessler, M. (2007). Delta-Notch--and then? Protein interactions and proposed modes of repression by Hes and Hey bHLH factors. Nucleic Acids Res. *35*, 4583–4596.

Fischer, A.H., Jacobson, K.A., Rose, J., and Zeller, R. (2008). Hematoxylin and eosin staining of tissue and cell sections. CSH Protoc. *2008*, pdb.prot4986.

Fiuza, U.-M., and Arias, A.M. (2007). Cell and molecular biology of Notch. J. Endocrinol. *194*, 459–474.

Foldi, J., Chung, A.Y., Xu, H., Zhu, J., Outtz, H.H., Kitajewski, J., Li, Y., Hu, X., and Ivashkiv, L.B. (2010). Autoamplification of Notch signaling in macrophages by TLR-induced and RBP-J-dependent induction of Jagged1. J. Immunol. Baltim. Md 1950 *185*, 5023–5031.

Fowler, J.C., Zecchini, V.R., and Jones, P.H. (2011). Intestinal activation of Notch signaling induces rapid onset hepatic steatosis and insulin resistance. PloS One *6*, e20767.

Friedman, S.L. (2008). Hepatic fibrosis -- overview. Toxicology *254*, 120–129.

Fryer, C.J., White, J.B., and Jones, K.A. (2004). Mastermind recruits CycC:CDK8 to phosphorylate the Notch ICD and coordinate activation with turnover. Mol. Cell *16*, 509–520.

Fu, Y.-P., Edvardsen, H., Kaushiva, A., Arhancet, J.P., Howe, T.M., Kohaar, I., Porter-Gill, P., Shah, A., Landmark-Høyvik, H., Fosså, S.D., et al. (2010). NOTCH2 in breast cancer: association of SNP rs11249433 with gene expression in ER-positive breast tumors without TP53 mutations. Mol. Cancer *9*, 113.

Fukuda, D., Aikawa, E., Swirski, F.K., Novobrantseva, T.I., Kotelianski, V., Gorgun, C.Z., Chudnovskiy, A., Yamazaki, H., Croce, K., Weissleder, R., et al. (2012). Notch ligand Delta-like 4 blockade attenuates atherosclerosis and metabolic disorders. Proc. Natl. Acad. Sci. *109*, E1868–E1877.

Fung, E., Tang, S.-M.T., Canner, J.P., Morishige, K., Arboleda-Velasquez, J.F., Cardoso, A.A., Carlesso, N., Aster, J.C., and Aikawa, M. (2007). Delta-like 4 induces notch signaling in macrophages: implications for inflammation. Circulation *115*, 2948–2956.

Gallahan, D., and Callahan, R. (1997). The mouse mammary tumor associated gene INT3 is a unique member of the NOTCH gene family (NOTCH4). Oncogene *14*, 1883–1890.

Garg, V., Muth, A.N., Ransom, J.F., Schluterman, M.K., Barnes, R., King, I.N., Grossfeld, P.D., and Srivastava, D. (2005). Mutations in NOTCH1 cause aortic valve disease. Nature *437*, 270–274.

Geisler, F., and Strazzabosco, M. (2015). Emerging roles of Notch signaling in liver disease. Hepatology *61*, 382–392.

Geisler, F., Nagl, F., Mazur, P.K., Lee, M., Zimber-Strobl, U., Strobl, L.J., Radtke, F., Schmid, R.M., and Siveke, J.T. (2008). Liver-specific inactivation of Notch2, but not Notch1, compromises intrahepatic bile duct development in mice. Hepatol. Baltim. Md *48*, 607–616.

Ghosh, S., and Hayden, M.S. (2008). New regulators of NF-kappaB in inflammation. Nat. Rev. Immunol. *8*, 837–848.

Giachino, C., Boulay, J.-L., Ivanek, R., Alvarado, A., Tostado, C., Lugert, S., Tchorz, J., Coban, M., Mariani, L., Bettler, B., et al. (2015). A Tumor Suppressor Function for Notch Signaling in Forebrain Tumor Subtypes. Cancer Cell *28*, 730–742.

Gil-García, B., and Baladrón, V. (2016). The complex role of NOTCH receptors and their ligands in the development of hepatoblastoma, cholangiocarcinoma and hepatocellular carcinoma: Role of NOTCH receptors and their ligands in liver cancer. Biol. Cell *108*, 29–40.

Giovannini, C., Baglioni, M., Baron Toaldo, M., Ventrucci, C., D'Adamo, S., Cipone, M., Chieco, P., Gramantieri, L., and Bolondi, L. (2013). Notch3 inhibition enhances sorafenib cytotoxic efficacy by promoting GSK3b phosphorylation and p21 down-regulation in hepatocellular carcinoma. Oncotarget *4*, 1618–1631.

Giovannini, C., Bolondi, L., and Gramantieri, L. (2016a). Targeting Notch3 in Hepatocellular Carcinoma: Molecular Mechanisms and Therapeutic Perspectives. Int. J. Mol. Sci. *18*, 56.

Giovannini, C., Minguzzi, M., Genovese, F., Baglioni, M., Gualandi, A., Ravaioli, M., Milazzo, M., Tavolari, S., Bolondi, L., and Gramantieri, L. (2016b). Molecular and proteomic insight into Notch1 characterization in hepatocellular carcinoma. Oncotarget *7*, 39609–39626.

Graupera, I., Solà, E., Fabrellas, N., Moreira, R., Solé, C., Huelin, P., de la Prada, G., Pose, E., Ariza, X., Risso, A., et al. (2016). Urine Monocyte Chemoattractant Protein-1 Is an Independent Predictive Factor of Hospital Readmission and Survival in Cirrhosis. PloS One *11*, e0157371.

Guest, R.V., Boulter, L., Kendall, T.J., Minnis-Lyons, S.E., Walker, R., Wigmore, S.J., Sansom, O.J., and Forbes, S.J. (2014). Cell lineage tracing reveals a biliary origin of intrahepatic cholangiocarcinoma. Cancer Res. *74*, 1005–1010.

Guo, J., Hong, F., Loke, J., Yea, S., Lim, C.L., Lee, U., Mann, D.A., Walsh, M.J., Sninsky, J.J., and Friedman, S.L. (2010). A DDX5 S480A polymorphism is associated with increased transcription of fibrogenic genes in hepatic stellate cells. J. Biol. Chem. *285*, 5428–5437.

Gupta, S., Li, S., Abedin, M.J., Wang, L., Schneider, E., Najafian, B., and Rosenberg, M. (2010). Effect of Notch activation on the regenerative response to acute renal failure. Am. J. Physiol. Renal Physiol. *298*, F209-215.

Hanlon, L., Avila, J.L., Demarest, R.M., Troutman, S., Allen, M., Ratti, F., Rustgi, A.K., Stanger, B.Z., Radtke, F., Adsay, V., et al. (2010). Notch1 functions as a tumor suppressor in a model of K-ras-induced pancreatic ductal adenocarcinoma. Cancer Res. *70*, 4280–4286.

Harry, D., Anand, R., Holt, S., Davies, S., Marley, R., Fernando, B., Goodier, D., and Moore, K. (1999). Increased sensitivity to endotoxemia in the bile duct-ligated cirrhotic Rat. Hepatol. Baltim. Md *30*, 1198–1205.

Hassed, S.J., Wiley, G.B., Wang, S., Lee, J.-Y., Li, S., Xu, W., Zhao, Z.J., Mulvihill, J.J., Robertson, J., Warner, J., et al. (2012). RBPJ Mutations Identified in Two Families Affected by Adams-Oliver Syndrome. Am. J. Hum. Genet. *91*, 391–395.

Hayashi, T., Gust, K.M., Wyatt, A.W., Goriki, A., Jäger, W., Awrey, S., Li, N., Oo, H.Z., Altamirano-Dimas, M., Buttyan, R., et al. (2016). Not all NOTCH Is Created Equal: The Oncogenic Role of NOTCH2 in Bladder Cancer and Its Implications for Targeted Therapy. Clin. Cancer Res. Off. J. Am. Assoc. Cancer Res. *22*, 2981–2992.

He, F., Guo, F.-C., Li, Z., Yu, H.-C., Ma, P.-F., Zhao, J.-L., Feng, L., Li, W.-N., Liu, X.-W., Qin, H.-Y., et al. (2015). Myeloid-specific disruption of recombination signal binding protein Jκ ameliorates hepatic fibrosis by attenuating inflammation through cylindromatosis in mice. Hepatol. Baltim. Md *61*, 303–314.

Hengstler, J.G., Utesch, D., Steinberg, P., Platt, K.L., Diener, B., Ringel, M., Swales, N., Fischer, T., Biefang, K., Gerl, M., et al. (2000). Cryopreserved primary hepatocytes as a constantly available in vitro model for the evaluation of human and animal drug metabolism and enzyme induction. Drug Metab. Rev. *32*, 81–118.

Hernandez-Gea, V., and Friedman, S.L. (2011). Pathogenesis of liver fibrosis. Annu. Rev. Pathol. *6*, 425–456.

Hoeft, K., and Kramann, R. (2017). Developmental Signaling and Organ Fibrosis. Curr. Pathobiol. Rep. *5*, 133–143.

Hofmann, J.J., Zovein, A.C., Koh, H., Radtke, F., Weinmaster, G., and Iruela-Arispe, M.L. (2010). Jagged1 in the portal vein mesenchyme regulates intrahepatic bile duct development: insights into Alagille syndrome. Dev. Camb. Engl. *137*, 4061–4072.

Hoyne, G.F. (2012). The role of Notch receptors and ligands in regulation of immune responses. Curr. Trends Immunol. *13*.

Hu, J., Srivastava, K., Wieland, M., Runge, A., Mogler, C., Besemfelder, E., Terhardt, D., Vogel, M.J., Cao, L., and Korn, C. (2014). Endothelial cell-derived angiopoietin-2 controls liver regeneration as a spatiotemporal rheostat. Science *343*, 416–419.

Hu, L., Xue, F., Shao, M., Deng, A., and Wei, G. (2013). Aberrant expression of Notch3 predicts poor survival for hepatocellular carcinomas. Biosci. Trends *7*, 152–156.

Huang, M.-T., Dai, Y.-S., Chou, Y.-B., Juan, Y.-H., Wang, C.-C., and Chiang, B.-L. (2009). Regulatory T Cells Negatively Regulate Neovasculature of Airway Remodeling via DLL4-Notch Signaling. J. Immunol. *183*, 4745–4754.

Huang, M.-T., Chen, Y.-L., Lien, C.-I., Liu, W.-L., Hsu, L.-C., Yagita, H., and Chiang, B.-L. (2017). Notch Ligand DLL4 Alleviates Allergic Airway Inflammation via Induction of a Homeostatic Regulatory Pathway. Sci. Rep. *7*, 43535.

Huntzicker, E.G., Hötzel, K., Choy, L., Che, L., Ross, J., Pau, G., Sharma, N., Siebel, C.W., Chen, X., and French, D.M. (2015). Differential effects of targeting Notch receptors in a mouse model of liver cancer. Hepatol. Baltim. Md *61*, 942–952.

Ishiguro, H., Okubo, T., Kuwabara, Y., Kimura, M., Mitsui, A., Sugito, N., Ogawa, R., Katada, T., Tanaka, T., Shiozaki, M., et al. (2017). NOTCH1 activates the Wnt/β-catenin signaling pathway in colon cancer. Oncotarget *8*, 60378–60389.

Iwaisako, K., Jiang, C., Zhang, M., Cong, M., Moore-Morris, T.J., Park, T.J., Liu, X., Xu, J., Wang, P., Paik, Y.-H., et al. (2014). Origin of myofibroblasts in the fibrotic liver in mice. Proc. Natl. Acad. Sci. U. S. A. *111*, E3297-3305.

Jeurissen, M.L.J., Walenbergh, S.M.A., Houben, T., Hendrikx, T., Li, J., Oligschlaeger, Y., van Gorp, P.J., Gijbels, M.J.J., Bitorina, A., Nessel, I., et al. (2016). Myeloid DLL4 Does Not Contribute to the Pathogenesis of Non-Alcoholic Steatohepatitis in Ldlr-/- Mice. PloS One *11*, e0167199.

Jörs, S., Jeliazkova, P., Ringelhan, M., Thalhammer, J., Dürl, S., Ferrer, J., Sander, M., Heikenwalder, M., Schmid, R.M., Siveke, J.T., et al. (2015). Lineage fate of ductular reactions in liver injury and carcinogenesis. J. Clin. Invest. *125*, 2445–2457.

Joshi, I., Minter, L.M., Telfer, J., Demarest, R.M., Capobianco, A.J., Aster, J.C., Sicinski, P., Fauq, A., Golde, T.E., and Osborne, B.A. (2009). Notch signaling mediates G1/S cell-cycle progression in T cells via cyclin D3 and its dependent kinases. Blood *113*, 1689–1698.

Joutel, A., Corpechot, C., Ducros, A., Vahedi, K., Chabriat, H., Mouton, P., Alamowitch, S., Domenga, V., Cécillion, M., Marechal, E., et al. (1996). Notch3 mutations in CADASIL, a hereditary adult-onset condition causing stroke and dementia. Nature *383*, 707–710.

Junqueira, L.C., Bignolas, G., and Brentani, R.R. (1979). Picrosirius staining plus polarization microscopy, a specific method for collagen detection in tissue sections. Histochem. J. *11*, 447–455.

Katoonizadeh, A., Nevens, F., Verslype, C., Pirenne, J., and Roskams, T. (2006). Liver regeneration in acute severe liver impairment: a clinicopathological correlation study. Liver Int. Off. J. Int. Assoc. Study Liver *26*, 1225–1233.

Khanam, A., Trehanpati, N., Riese, P., Rastogi, A., Guzman, C.A., and Sarin, S.K. (2017). Blockade of Neutrophil's Chemokine Receptors CXCR1/2 Abrogate Liver Damage in Acute-on-Chronic Liver Failure. Front. Immunol. *8*, 464.

Klinakis, A., Szabolcs, M., Politi, K., Kiaris, H., Artavanis-Tsakonas, S., and Efstratiadis, A. (2006). Myc is a Notch1 transcriptional target and a requisite for Notch1-induced mammary tumorigenesis in mice. Proc. Natl. Acad. Sci. U. S. A. *103*, 9262–9267.

Kodama, Y., Hijikata, M., Kageyama, R., Shimotohno, K., and Chiba, T. (2004). The role of notch signaling in the development of intrahepatic bile ducts. Gastroenterology *127*, 1775–1786.

Köhler, C., Bell, A.W., Bowen, W.C., Monga, S.P., Fleig, W., and Michalopoulos, G.K. (2004). Expression of Notch-1 and its ligand Jagged-1 in rat liver during liver regeneration. Hepatol. Baltim. Md *39*, 1056–1065.

Kok, S.-H., Hong, C.-Y., Kuo, M.Y.-P., Wang, C.-C., Hou, K.-L., Lin, Y.-T., Galson, D.L., and Lin, S.-K. (2009). Oncostatin M-induced CCL2 transcription in osteoblastic cells is mediated by multiple levels of STAT-1 and STAT-3 signaling: An implication for the pathogenesis of arthritis. Arthritis Rheum. *60*, 1451–1462.

Kopan, R., and Ilagan, M.X.G. (2009). The Canonical Notch Signaling Pathway: Unfolding the Activation Mechanism. Cell *137*, 216–233.

Krejcí, A., Bernard, F., Housden, B.E., Collins, S., and Bray, S.J. (2009). Direct response to Notch activation: signaling crosstalk and incoherent logic. Sci. Signal. *2*, ra1.

Lahmar, M., Catelain, C., Poirault, S., Dorsch, M., Villeval, J.-L., Vainchenker, W., Albagli, O., and Lauret, E. (2008). Distinct effects of the soluble versus membrane-bound forms of the notch ligand delta-4 on human CD34+CD38low cell expansion and differentiation. Stem Cells Dayt. Ohio *26*, 621–629.

Li, L., Krantz, I.D., Deng, Y., Genin, A., Banta, A.B., Collins, C.C., Qi, M., Trask, B.J., Kuo, W.L., Cochran, J., et al. (1997). Alagille syndrome is caused by mutations in human Jagged1, which encodes a ligand for Notch1. Nat. Genet. *16*, 243–251.

Libbrecht, L. (2006). Hepatic progenitor cells in human liver tumor development. World J. Gastroenterol. *12*, 6261–6265.

Liu, Z., Fan, F., Wang, A., Zheng, S., and Lu, Y. (2014). Dll4-Notch signaling in regulation of tumor angiogenesis. J. Cancer Res. Clin. Oncol. *140*, 525–536.

Lobry, C., Oh, P., and Aifantis, I. (2011). Oncogenic and tumor suppressor functions of Notch in cancer: it's NOTCH what you think. J. Exp. Med. *208*, 1931–1935.

Lobry, C., Oh, P., Mansour, M.R., Look, A.T., and Aifantis, I. (2014). Notch signaling: switching an oncogene to a tumor suppressor. Blood *123*, 2451–2459.

Loomes, K.M., Taichman, D.B., Glover, C.L., Williams, P.T., Markowitz, J.E., Piccoli, D.A., Baldwin, H.S., and Oakey, R.J. (2002). Characterization of Notch receptor expression in the developing mammalian heart and liver. Am. J. Med. Genet. *112*, 181–189.

Lukacs-Kornek, V., and Lammert, F. (2017). The progenitor cell dilemma: Cellular and functional heterogeneity in assistance or escalation of liver injury. J. Hepatol. *66*, 619–630.

Mahmood, T., and Yang, P.-C. (2012). Western Blot: Technique, Theory, and Trouble Shooting. North Am. J. Med. Sci. *4*, 429–434.

Malhi, H., and Gores, G.J. (2008). Cellular and Molecular Mechanisms of Liver Injury. Gastroenterology *134*, 1641–1654.

Martignetti, J.A., Tian, L., Li, D., Ramirez, M.C.M., Camacho-Vanegas, O., Camacho, S.C., Guo, Y., Zand, D.J., Bernstein, A.M., Masur, S.K., et al. (2013). Mutations in PDGFRB cause autosomal-dominant infantile myofibromatosis. Am. J. Hum. Genet. *92*, 1001–1007.

Mašek, J., and Andersson, E.R. (2017). The developmental biology of genetic Notch disorders. Development *144*, 1743–1763.

Mazur, P.K., Einwächter, H., Lee, M., Sipos, B., Nakhai, H., Rad, R., Zimber-Strobl, U., Strobl, L.J., Radtke, F., Klöppel, G., et al. (2010). Notch2 is required for progression of pancreatic intraepithelial neoplasia and development of pancreatic ductal adenocarcinoma. Proc. Natl. Acad. Sci. U. S. A. *107*, 13438–13443.

McDaniell, R., Warthen, D.M., Sanchez-Lara, P.A., Pai, A., Krantz, I.D., Piccoli, D.A., and Spinner, N.B. (2006). NOTCH2 Mutations Cause Alagille Syndrome, a Heterogeneous Disorder of the Notch Signaling Pathway. Am. J. Hum. Genet. *79*, 169–173.

Mederacke, I., Dapito, D.H., Affò, S., Uchinami, H., and Schwabe, R.F. (2015). High-yield and high-purity isolation of hepatic stellate cells from normal and fibrotic mouse livers. Nat. Protoc. *10*, 305–315.

Meester, J.A.N., Southgate, L., Stittrich, A.-B., Venselaar, H., Beekmans, S.J.A., den Hollander, N., Bijlsma, E.K., Helderman-van den Enden, A., Verheij, J.B.G.M., Glusman, G., et al. (2015). Heterozygous Loss-of-Function Mutations in DLL4 Cause Adams-Oliver Syndrome. Am. J. Hum. Genet. *97*, 475–482.

Metz, C.W., and Bridges, C.B. (1917). Incompatibility of Mutant Races in Drosophila. Proc. Natl. Acad. Sci. U. S. A. *3*, 673–678.

Miele, L. (2006). Notch Signaling. Clin. Cancer Res. *12*, 1074–1079.

Miyoshi, H., Rust, C., Roberts, P.J., Burgart, L.J., and Gores, G.J. (1999). Hepatocyte apoptosis after bile duct ligation in the mouse involves Fas. Gastroenterology *117*, 669–677.

Monsalve, E., Pérez, M.A., Rubio, A., Ruiz-Hidalgo, M.J., Baladrón, V., García-Ramírez, J.J., Gómez, J.C., Laborda, J., and Díaz-Guerra, M.J.M. (2006). Notch-1 up-regulation and signaling following macrophage activation modulates gene expression patterns known to affect antigen-presenting capacity and cytotoxic activity. J. Immunol. Baltim. Md 1950 *176*, 5362–5373.

Morell, C.M., and Strazzabosco, M. (2014). Notch signaling and new therapeutic options in liver disease. J. Hepatol. *60*, 885–890.

Morell, C.M., Fiorotto, R., Fabris, L., and Strazzabosco, M. (2013). Notch signalling beyond liver development: Emerging concepts in liver repair and oncogenesis. Clin. Res. Hepatol. Gastroenterol. *37*, 447–454.

Morell, C.M., Fiorotto, R., Meroni, M., Raizner, A., Torsello, B., Cadamuro, M., Spagnuolo, G., Kaffe, E., Sutti, S., Albano, E., et al. (2017). Notch signaling and progenitor/ductular reaction in steatohepatitis. PloS One *12*, e0187384.

Murillo, M.M., del Castillo, G., Sánchez, A., Fernández, M., and Fabregat, I. (2005). Involvement of EGF receptor and c-Src in the survival signals induced by TGF-beta1 in hepatocytes. Oncogene *24*, 4580–4587.

Nguyen, T., Nioi, P., and Pickett, C.B. (2009). The Nrf2-Antioxidant Response Element Signaling Pathway and Its Activation by Oxidative Stress. J. Biol. Chem. *284*, 13291–13295.

Nicolas, M., Wolfer, A., Raj, K., Kummer, J.A., Mill, P., van Noort, M., Hui, C., Clevers, H., Dotto, G.P., and Radtke, F. (2003). Notch1 functions as a tumor suppressor in mouse skin. Nat. Genet. *33*, 416–421.

Nijjar, S.S., Crosby, H.A., Wallace, L., Hubscher, S.G., and Strain, A.J. (2001). Notch receptor expression in adult human liver: a possible role in bile duct formation and hepatic neovascularization. Hepatol. Baltim. Md *34*, 1184–1192.

Nistri, S., Sassoli, C., and Bani, D. (2017). Notch Signaling in Ischemic Damage and Fibrosis: Evidence and Clues from the Heart. Front. Pharmacol. *8*.

Noguera-Troise, I., Daly, C., Papadopoulos, N.J., Coetzee, S., Boland, P., Gale, N.W., Lin, H.C., Yancopoulos, G.D., and Thurston, G. (2006). Blockade of Dll4 inhibits tumour growth by promoting non-productive angiogenesis. Nature *444*, 1032–1037.

Nowell, C.S., and Radtke, F. (2017). Notch as a tumour suppressor. Nat. Rev. Cancer *17*, 145–159.

Nus, M., Martínez-Poveda, B., MacGrogan, D., Chevre, R., D'Amato, G., Sbroggio, M., Rodríguez, C., Martínez-González, J., Andrés, V., Hidalgo, A., et al. (2016). Endothelial Jag1-RBPJ signalling promotes inflammatory leucocyte recruitment and atherosclerosis. Cardiovasc. Res.

Oda, T., Elkahloun, A.G., Pike, B.L., Okajima, K., Krantz, I.D., Genin, A., Piccoli, D.A., Meltzer, P.S., Spinner, N.B., Collins, F.S., et al. (1997). Mutations in the human Jagged1 gene are responsible for Alagille syndrome. Nat. Genet. *16*, 235–242.

Okamoto, M., Matsuda, H., Joetham, A., Lucas, J.J., Domenico, J., Yasutomo, K., Takeda, K., and Gelfand, E.W. (2009). Jagged1 on Dendritic Cells and Notch on CD4+ T Cells Initiate Lung Allergic Responsiveness by Inducing IL-4 Production. J. Immunol. *183*, 2995–3003.

Osipo, C., Golde, T.E., Osborne, B.A., and Miele, L.A. (2008). Off the beaten pathway: the complex cross talk between Notch and NF-κB. Lab. Invest. *88*, 11–17.

Outtz, H.H., Wu, J.K., Wang, X., and Kitajewski, J. (2010). Notch1 deficiency results in decreased inflammation during wound healing and regulates vascular endothelial growth factor receptor-1 and inflammatory cytokine expression in macrophages. J. Immunol. Baltim. Md 1950 *185*, 4363–4373.

Oya, S., Yoshikawa, G., Takai, K., Tanaka, J.-I., Higashiyama, S., Saito, N., Kirino, T., and Kawahara, N. (2008). Region-specific proliferative response of neural progenitors to exogenous stimulation by growth factors following ischemia. Neuroreport *19*, 805–809.

Palomero, T., Lim, W.K., Odom, D.T., Sulis, M.L., Real, P.J., Margolin, A., Barnes, K.C., O'Neil, J., Neuberg, D., Weng, A.P., et al. (2006). NOTCH1 directly regulates c-MYC and activates a feed-forward-loop transcriptional network promoting leukemic cell growth. Proc. Natl. Acad. Sci. U. S. A. *103*, 18261–18266.

Palomero, T., Sulis, M.L., Cortina, M., Real, P.J., Barnes, K., Ciofani, M., Caparros, E., Buteau, J., Brown, K., Perkins, S.L., et al. (2007). Mutational loss of PTEN induces resistance to NOTCH1 inhibition in T-cell leukemia. Nat. Med. *13*, 1203–1210.

Park, J.-S., Kim, S.-H., Kim, K., Jin, C.-H., Choi, K.Y., Jang, J., Choi, Y., Gwon, A.-R., Baik, S.-H., Yun, U.J., et al. (2015). Inhibition of notch signalling ameliorates experimental inflammatory arthritis. Ann. Rheum. Dis. *74*, 267–274.

Park, J.T., Li, M., Nakayama, K., Mao, T.-L., Davidson, B., Zhang, Z., Kurman, R.J., Eberhart, C.G., Shih, I.-M., and Wang, T.-L. (2006). Notch3 gene amplification in ovarian cancer. Cancer Res. *66*, 6312–6318.

Pellegrinet, L., Rodilla, V., Liu, Z., Chen, S., Koch, U., Espinosa, L., Kaestner, K.H., Kopan, R., Lewis, J., and Radtke, F. (2011). Dll1- and dll4-mediated notch signaling are required for homeostasis of intestinal stem cells. Gastroenterology *140*, 1230-1240.e1-7.

Preuße, K., Tveriakhina, L., Schuster-Gossler, K., Gaspar, C., Rosa, A.I., Henrique, D., Gossler, A., and Stauber, M. (2015). Context-Dependent Functional Divergence of the Notch Ligands DLL1 and DLL4 In Vivo. PLoS Genet. *11*, e1005328.

Rangarajan, A., Talora, C., Okuyama, R., Nicolas, M., Mammucari, C., Oh, H., Aster, J.C., Krishna, S., Metzger, D., Chambon, P., et al. (2001). Notch signaling is a direct determinant of keratinocyte growth arrest and entry into differentiation. EMBO J. *20*, 3427–3436.

Restivo, G., Nguyen, B.-C., Dziunycz, P., Ristorcelli, E., Ryan, R.J.H., Özuysal, Ö.Y., Di Piazza, M., Radtke, F., Dixon, M.J., Hofbauer, G.F.L., et al. (2011). IRF6 is a mediator of Notch pro-differentiation and tumour suppressive function in keratinocytes. EMBO J. *30*, 4571–4585.

Rostama, B., Peterson, S.M., Vary, C.P.H., and Liaw, L. (2014). Notch signal integration in the vasculature during remodeling. Vascul. Pharmacol. *63*, 97–104.

Roth, G.A., Faybik, P., Hetz, H., Ankersmit, H.J., Hoetzenecker, K., Bacher, A., Thalhammer, T., and Krenn, C.G. (2009). MCP-1 and MIP3-alpha serum levels in acute liver failure and molecular adsorbent recirculating system (MARS) treatment: a pilot study. Scand. J. Gastroenterol. *44*, 745–751.

Sawitza, I., Kordes, C., Reister, S., and Häussinger, D. (2009). The niche of stellate cells within rat liver. Hepatol. Baltim. Md *50*, 1617–1624.

Schmittgen, T.D., and Livak, K.J. (2008). Analyzing real-time PCR data by the comparative C(T) method. Nat. Protoc. *3*, 1101–1108.

Schwanbeck, R., Martini, S., Bernoth, K., and Just, U. (2011). The Notch signaling pathway: molecular basis of cell context dependency. Eur. J. Cell Biol. *90*, 572–581.

Segarra, M., Williams, C.K., Sierra, M. de la L., Bernardo, M., McCormick, P.J., Maric, D., Regino, C., Choyke, P., and Tosato, G. (2008). Dll4 activation of Notch signaling reduces tumor vascularity and inhibits tumor growth. Blood *112*, 1904–1911.

Seki, E., and Schwabe, R.F. (2015). Hepatic inflammation and fibrosis: functional links and key pathways. Hepatol. Baltim. Md *61*, 1066–1079.

Sekine, C., Koyanagi, A., Koyama, N., Hozumi, K., Chiba, S., and Yagita, H. (2012). Differential regulation of osteoclastogenesis by Notch2/Delta-like 1 and Notch1/Jagged1 axes. Arthritis Res. Ther. *14*, R45.

Sekiya, S., and Suzuki, A. (2012). Intrahepatic cholangiocarcinoma can arise from Notch-mediated conversion of hepatocytes. J. Clin. Invest. *122*, 3914–3918.

Shackel, N.A., McGuinness, P.H., Abbott, C.A., Gorrell, M.D., and McCaughan, G.W. (2001). Identification of novel molecules and pathogenic pathways in primary biliary cirrhosis: cDNA array analysis of intrahepatic differential gene expression. Gut *49*, 565–576.

Shang, Y., Smith, S., and Hu, X. (2016). Role of Notch signaling in regulating innate immunity and inflammation in health and disease. Protein Cell *7*, 159–174.

Shin, H.M., Minter, L.M., Cho, O.H., Gottipati, S., Fauq, A.H., Golde, T.E., Sonenshein, G.E., and Osborne, B.A. (2006). Notch1 augments NF-kappaB activity by facilitating its nuclear retention. EMBO J. *25*, 129–138.

Siebel, C., and Lendahl, U. (2017). Notch Signaling in Development, Tissue Homeostasis, and Disease. Physiol. Rev. *97*, 1235–1294.

Simpson, M.A., Irving, M.D., Asilmaz, E., Gray, M.J., Dafou, D., Elmslie, F.V., Mansour, S., Holder, S.E., Brain, C.E., Burton, B.K., et al. (2011). Mutations in NOTCH2 cause Hajdu-Cheney syndrome, a disorder of severe and progressive bone loss. Nat. Genet. *43*, 303–305.

Southgate, L., Sukalo, M., Karountzos, A.S.V., Taylor, E.J., Collinson, C.S., Ruddy, D., Snape, K.M., Dallapiccola, B., Tolmie, J.L., Joss, S., et al. (2015). Haploinsufficiency of the NOTCH1 Receptor as a Cause of Adams-Oliver Syndrome With Variable Cardiac Anomalies. Circ. Cardiovasc. Genet. *8*, 572–581.

Sparks, E.E., Huppert, K.A., Brown, M.A., Washington, M.K., and Huppert, S.S. (2010). Notch signaling regulates formation of the three-dimensional architecture of intrahepatic bile ducts in mice. Hepatol. Baltim. Md *51*, 1391–1400.

Spee, B., Carpino, G., Schotanus, B.A., Katoonizadeh, A., Vander Borght, S., Gaudio, E., and Roskams, T. (2010). Characterisation of the liver progenitor cell niche in liver diseases: potential involvement of Wnt and Notch signalling. Gut *59*, 247–257.

Strazzabosco, M., and Fabris, L. (2013). The balance between Notch/Wnt signaling regulates progenitor cells' commitment during liver repair: mystery solved? J. Hepatol. *58*, 181–183.

Tag, C.G., Sauer-Lehnen, S., Weiskirchen, S., Borkham-Kamphorst, E., Tolba, R.H., Tacke, F., and Weiskirchen, R. (2015). Bile Duct Ligation in Mice: Induction of Inflammatory Liver Injury and Fibrosis by Obstructive Cholestasis. J. Vis. Exp. JoVE.

Takeichi, N., Yanagisawa, S., Kaneyama, T., Yagita, H., Jin, Y.-H., Kim, B.S., and Koh, C.-S. (2010). Ameliorating effects of anti-Dll4 mAb on Theiler's murine encephalomyelitis virus-induced demyelinating disease. Int. Immunol. *22*, 729–738.

Tang, G., Weng, Z., Song, J., and Chen, Y. (2017). Reversal effect of Jagged1 signaling inhibition on CCl4-induced hepatic fibrosis in rats. Oncotarget *8*, 60778–60788.

Tseng, Y.-C., Tsai, Y.-H., Tseng, M.-J., Hsu, K.-W., Yang, M.-C., Huang, K.-H., Li, A.F.-Y., Chi, C.-W., Hsieh, R.-H., Ku, H.-H., et al. (2012). Notch2-induced COX-2 expression enhancing gastric cancer progression. Mol. Carcinog. *51*, 939–951.

Tun, T., Hamaguchi, Y., Matsunami, N., Furukawa, T., Honjo, T., and Kawaichi, M. (1994). Recognition sequence of a highly conserved DNA binding protein RBP-J kappa. Nucleic Acids Res. *22*, 965–971.

Underkoffler, L.A., Carr, E., Nelson, A., Ryan, M.J., Schulz, R., Schultz, R., and Loomes, K.M. (2013). Microarray data reveal relationship between Jag1 and Ddr1 in mouse liver. PloS One *8*, e84383.

Vacca, A., Felli, M.P., Palermo, R., Di Mario, G., Calce, A., Di Giovine, M., Frati, L., Gulino, A., and Screpanti, I. (2006). Notch3 and pre-TCR interaction unveils distinct NF-kappaB pathways in T-cell development and leukemia. EMBO J. *25*, 1000–1008.

Villanueva, A., Alsinet, C., Yanger, K., Hoshida, Y., Zong, Y., Toffanin, S., Rodriguez-Carunchio, L., Solé, M., Thung, S., Stanger, B.Z., et al. (2012). Notch signaling is

activated in human hepatocellular carcinoma and induces tumor formation in mice. Gastroenterology *143*, 1660-1669.e7.

Wakabayashi, N., Skoko, J.J., Chartoumpekis, D.V., Kimura, S., Slocum, S.L., Noda, K., Palliyaguru, D.L., Fujimuro, M., Boley, P.A., Tanaka, Y., et al. (2014). Notch-Nrf2 axis: regulation of Nrf2 gene expression and cytoprotection by notch signaling. Mol. Cell. Biol. *34*, 653–663.

Wang, M.M. (2011). Notch signaling and Notch signaling modifiers. Int. J. Biochem. Cell Biol. *43*, 1550–1562.

Wang, C., Qi, R., Li, N., Wang, Z., An, H., Zhang, Q., Yu, Y., and Cao, X. (2009). Notch1 signaling sensitizes tumor necrosis factor-related apoptosis-inducing ligand-induced apoptosis in human hepatocellular carcinoma cells by inhibiting Akt/Hdm2-mediated p53 degradation and up-regulating p53-dependent DR5 expression. J. Biol. Chem. *284*, 16183–16190.

Wang, X.-P., Zhou, J., Han, M., Chen, C.-B., Zheng, Y.-T., He, X.-S., and Yuan, X.-P. (2017). MicroRNA-34a regulates liver regeneration and the development of liver cancer in rats by targeting Notch signaling pathway. Oncotarget *8*, 13264–13276.

Wei, X., Wang, J.-P., Hao, C.-Q., Yang, X.-F., Wang, L.-X., Huang, C.-X., Bai, X.-F., Lian, J.-Q., and Zhang, Y. (2016). Notch Signaling Contributes to Liver Inflammation by Regulation of Interleukin-22-Producing Cells in Hepatitis B Virus Infection. Front. Cell. Infect. Microbiol. *6*.

Weng, A.P., Ferrando, A.A., Lee, W., Morris, J.P., Silverman, L.B., Sanchez-Irizarry, C., Blacklow, S.C., Look, A.T., and Aster, J.C. (2004). Activating mutations of NOTCH1 in human T cell acute lymphoblastic leukemia. Science *306*, 269–271.

Weng, H.-L., Liu, Y., Chen, J.-L., Huang, T., Xu, L.-J., Godoy, P., Hu, J.-H., Zhou, C., Stickel, F., Marx, A., et al. (2009). The etiology of liver damage imparts cytokines transforming growth factor beta1 or interleukin-13 as driving forces in fibrogenesis. Hepatol. Baltim. Md *50*, 230–243.

Xu, H., Zhu, J., Smith, S., Foldi, J., Zhao, B., Chung, A.Y., Outtz, H., Kitajewski, J., Shi, C., Weber, S., et al. (2012). Notch-RBP-J signaling regulates the transcription factor IRF8 to promote inflammatory macrophage polarization. Nat. Immunol. *13*, 642–650.

Yamaguchi, N., Oyama, T., Ito, E., Satoh, H., Azuma, S., Hayashi, M., Shimizu, K., Honma, R., Yanagisawa, Y., Nishikawa, A., et al. (2008). NOTCH3 signaling pathway plays crucial roles in the proliferation of ErbB2-negative human breast cancer cells. Cancer Res. *68*, 1881–1888.

Yang, P., Han, Z., Chen, P., Zhu, L., Wang, S., Hua, Z., and Zhang, J. (2010). A contradictory role of A1 adenosine receptor in carbon tetrachloride- and bile duct ligation-induced liver fibrosis in mice. J. Pharmacol. Exp. Ther. *332*, 747–754.

Ye, Q.-F., Zhang, Y.-C., Peng, X.-Q., Long, Z., Ming, Y.-Z., and He, L.-Y. (2012). siRNA-mediated silencing of Notch-1 enhances docetaxel induced mitotic arrest and apoptosis in prostate cancer cells. Asian Pac. J. Cancer Prev. APJCP *13*, 2485–2489.

Yin, Q., Wang, W., Cui, G., Nan, H., Yan, L., Zhang, W., Zhang, S., and Wei, J. (2017). The expression levels of Notch-related signaling molecules in pulmonary microvascular endothelial cells in bleomycin-induced rat pulmonary fibrosis. Physiol. Res. *66*, 305–315.

Yu, H.-C., Qin, H.-Y., He, F., Wang, L., Fu, W., Liu, D., Guo, F.-C., Liang, L., Dou, K.-F., and Han, H. (2011). Canonical notch pathway protects hepatocytes from ischemia/reperfusion injury in mice by repressing reactive oxygen species production through JAK2/STAT3 signaling. Hepatol. Baltim. Md *54*, 979–988.

Zhang, M., Biswas, S., Qin, X., Gong, W., Deng, W., and Yu, H. (2016a). Does Notch play a tumor suppressor role across diverse squamous cell carcinomas? Cancer Med. *5*, 2048–2060.

Zhang, W., Xu, W., and Xiong, S. (2010). Blockade of Notch1 signaling alleviates murine lupus via blunting macrophage activation and M2b polarization. J. Immunol. Baltim. Md 1950 *184*, 6465–6478.

Zhang, X., Du, G., Xu, Y., Li, X., Fan, W., Chen, J., Liu, C., Chen, G., Liu, C., Zern, M.A., et al. (2016b). Inhibition of notch signaling pathway prevents cholestatic liver fibrosis by decreasing the differentiation of hepatic progenitor cells into cholangiocytes. Lab. Investig. J. Tech. Methods Pathol. *96*, 350–360.

Zhu, F., Li, T., Qiu, F., Fan, J., Zhou, Q., Ding, X., Nie, J., and Yu, X. (2010). Preventive effect of Notch signaling inhibition by a gamma-secretase inhibitor on peritoneal dialysis fluid-induced peritoneal fibrosis in rats. Am. J. Pathol. *176*, 650–659.

Zong, Y., Panikkar, A., Xu, J., Antoniou, A., Raynaud, P., Lemaigre, F., and Stanger, B.Z. (2009). Notch signaling controls liver development by regulating biliary differentiation. Dev. Camb. Engl. *136*, 1727–1739.

7 LIST OF TABLES

8 RESUME

Personal Information

Name and first name:	Dewidar, Bedair
Date of birth:	24.05.1984
Place of birth:	Al-Mahalla El-Kubra, Egypt
Marital status:	Married
Father:	Ibrahim Dewidar
Mother:	Sabra Mottaw

Education

04.2014– Current	Heidelberg University, Germany PhD student at Department of Medicine II, Medical Faculty Mannheim (Under supervision of Prof. Dr. Steven Dooley).
08.2012	Tanta University, Egypt Master Degree of Pharmaceutical Sciences at Department of Pharmacology and Toxicology, Faculty of Pharmacy.
05.2006	Tanta University, Egypt Bachelor Degree of Pharmaceutical Sciences with grade excellence with honor, Faculty of Pharmacy.

Publications

Zhang, Y., Kim, D.-K., Lu, Y., Jung, Y.S., Lee, J.-M., Kim, Y.-H., Lee, Y.S., Kim, J., **Dewidar, B.**, Jeong, W.-I., et al. (2017). Orphan nuclear receptor ERRγ is a key regulator of human fibrinogen gene expression. PloS One 12, e0182141.

Shen, Z., Liu, Y., **Dewidar, B.**, Hu, J., Park, O., Feng, T., Xu, C., Yu, C., Li, Q., Meyer, C., et al. (2016). Delta-Like Ligand 4 Modulates Liver Damage by Down-Regulating Chemokine Expression. Am. J. Pathol. 186, 1874–1889.

Fabregat, I., Moreno-Càceres, J., Sánchez, A., Dooley, S., **Dewidar, B.**, Giannelli, G., Ten Dijke, P., and IT-LIVER Consortium (2016). TGF-β signalling and liver disease. FEBS J. 283, 2219–2232.

Dewidar, B., Soukupova, J., Fabregat, I., and Dooley, S. (2015). TGF-β in Hepatic Stellate Cell Activation and Liver Fibrogenesis: Updated. Curr. Pathobiol. Rep. 3, 291–305.

El-Mahdy, N.A., El-Sisi, A.E., **Dewidar, B.I.**, and El-Desouky, K.I. (2013). Histamine protects against the acute phase of experimentally-induced hepatic ischemia/re-perfusion. J. Immunotoxicol. 10, 9–16.

International Conferences

FALK (January 29-30, 2015; Munich, Germany): a poster entitled “Delta like ligand4 modulates chemokine ligand 2 through impacting the NFkB pathway”.

GASL (January 30-31, 2015; Munich, Germany): an oral presentation entitled “Delta like ligand4 ameliorates liver fibrogenesis through inhibiting chemokines”.

EASL (April 22-26, 2015; Vienna, Austria): a poster entitled “Delta like ligand 4 drives liver damage through regulating chemokines”.

EASL monothematic conference (June 17-18, 2016; Porto, Portugal) a poster entitled “TGF-beta2 inhibition in endothelial cells ameliorates liver fibrogenesis and inflammation”.

Falk/GASL conference (January 19-21, 2017; Essen, Germany): two posters entitled “ABCB5+ mesenchymal stem cell transplantation in a chronic liver disease mouse model” and “Anti-fibrotic and anti-inflammatory consequences of TGF-β2 silencing in biliary liver disease”, respectively.

DGVS (September 15-16, 2017; Dresden, Germany): an oral presentation entitled “Jagged-1 expression in stressed hepatocytes enhances phagocytic activity of Kupffer cells”.

SBMC (July 04-05, 2018; Bremen, Germany): a poster entitled “CD271 antibody-labeled magnetic beads for isolation of murine hepatic stellate cells.

9 ACKNOWLEDGEMENTS

First and foremost, I wish to express my sincere gratitude to my academic advisor Prof. Steven Dooley for accepting me in his group and giving me all required support, encouragement, and guidance during the pursuit of this project.

I am also indebted to Dr. Weng Honglei for his patience, kind supervision, fruitful discussion, and insightful comments.

I would like to thank my colleagues at the Department of Molecular Hepatology, Medical Faculty Mannheim, the University of Heidelberg for their friendship and great cooperation especially Dr. Teng Feng for helping me with the experimental setup of isolated cells.

Thanks to Dr. Junhao Hu for teaching me the protocol of isolation of primary Kupffer cells, and to Mrs. Alexander Müller and Mr. Christof Dormann for their technical assistance during cell isolation.

I am grateful to our Chinese collaboration group (especially Dr. Zhe Shen and Dr. Youming Li, Zhejiang University, Hangzhou, China) for providing me with the needed liver samples.

I would also like to thank my Egyptian government, DAAD, University of Heidelberg, and Prof. Steven Dooley. Without their financial support, this work would not be possible.

Thanks also extend to Prof. Matthias Ebert and in general to the hospital of Medical Faculty Mannheim for giving me access to all laboratory instruments and tools used to finish the current study.

Warm thanks to my supportive wife Mervat Mehesen and my lovely children Khaled and Omar, who provide me with endless power, motivation and inspiration.

Finally, I would like to add personal thanks to my sisters, Mom and Dad for their love and tireless enthusiasm.

10 APPENDIX

10.1 Buffers / Solutions

10.1.1 IHC

10.1.1.1 EDTA retrieval solution

EDTA (disodium salt)..... 0.37 g
Distilled water to ..... 1000 mL
Mix, adjust pH to 8.0 with 1N NaOH.

10.1.1.2 Citrate retrieval solution

Tri-sodium citrate (dihydrate) ..... 2.94 g
Distilled water to ..... 1000 mL
Mix, adjust pH to 6.0 with 1N HCl, and add 0.5 mL of Tween 20.

10.1.1.3 Picro-sirius red solution

Sirius red (Sigma)..... 0.5 g
Saturated aqueous solution of picric acid (Sigma) to..... 500 mL

10.1.1.4 Masson's trichrome staining buffers

Buffer A:
Acid fuchsin ..... 0.5 g
Ponceau Xylidine..... 0.5 g
Distilled water ..... 99 mL
Glacial acetic acid (Sigma-Aldrich) ..... 1 mL
Buffer B:
Phosphomolybdic acid (5%) ..... 25 mL
Phosphotungstic acid (5%)..... 25 mL
Buffer C:
Light green..... 2 g
Glacial acetic acid (Sigma-Aldrich) ..... 2 mL
Distilled water to ..... 100 mL
Weigert's iron hematoxylin solution:
Prepared according to Weigert by mixing equal parts of solution A and solution B (Table 2.1)

10.1.2 IF/ICC

10.1.2.1 BSA (3 %)

Bovine serum albumin (Serve) ..... 15 g
Distilled water to ..... 500 mL
Mix well, add 250 µl Tween 20, aliquot and store at -20 C°. Thaw at RT before use. This buffer was used for blocking non-specific binding during IF staining.

10.1.2.2 BSA (0.5 %)

BSA ..... 2.5 g
Distilled water to ..... 500 mL
Mix well, add 250 µl Tween 20 mL Tween 20, aliquot and store at -20 C°. Thaw at RT before use. This buffer was used for diluting primary and secondary antibodies during IF staining.

10.1.2.3 Wash buffer for ICC

BSA ..... 0.1 g
PBS to ..... 100 mL
Mix well and store at 4 C°.

10.1.2.4 Blocking buffer for ICC

BSA ..... 1 g
Triton-X-100..... 0.5 mL
PBS to ..... 100 mL
Mix well and store at 4 C°.

10.1.3 ELISA

10.1.3.1 Wash buffer

Weigh 9.55 g PBS powder for each liter. After dissolving in distilled water, adjust pH to 7.2-7.4, and filter solution through 0.22 µM filter. Then, add 0.5 mL Tween 20, mix the solution, and store at 4 C°.

10.1.3.2 Diluent buffer

BSA ..... 10 g
PBS (pH=7.2-7.4; 0.22 µM filtered) to..... 1000 mL
Mix well, and store at 4 C°.

10.1.4 Subcellular fractionation

10.1.4.1 Harvest buffer

HEPES 7.9 (100 mM) ..... 5 mL
NaCl (1 M) ..... 5 mL
Sucrose ..... 8.56 g
EDTA (10mM)..... 0.5 mL
Triton-X-100..... 250 µL
DTT (1000 mM) ..... 50 µL
Protease inhibitors..... 1 tablet
Phosphatase inhibitors (100X)..... 500 µL
Distilled water to ..... 50 mL
Mix well, aliquot, and store at -20 C°.

10.1.4.2 Buffer A

HEPES 7.9 (100 mM) ..... 5 mL
KCl (100 mM) ..... 5 mL
EDTA (10 mM)..... 0.5 mL
EGTA (5 mM) ..... 1 mL
DTT (1 M) ..... 50 µL
Protease inhibitors..... 1 tablet
Phosphatase inhibitors (100X)..... 500 µL
Distilled water to ..... 50 mL
Mix well, aliquot, and store at -20 C°.

10.1.4.3 Buffer C

HEPES 7.9 (100 mM) ..... 5 mL
NaCl (1 M) ..... 25 mL
EDTA (10 mM)..... 0.5 mL
EGTA (5 mM) ..... 1 mL
NP-40 ..... 50 µL
DTT (1 M) ..... 50 µL
Protease inhibitors..... 1 tablet
Phosphatase inhibitors (100X)..... 500 µL
Distilled water to ..... 50 mL
Mix well, aliquot, and store at -20 C°.

10.1.5 Immunoblotting

10.1.5.1 Loading buffer 5x

B-Mercaptoethanol ..... 2.5 mL
SDS ..... 2 g
Bromo phenol blue ..... 10 mg
Tris HCl (Ph=6.8, 1M)..... 6 mL
EDTA (500mM)..... 200 µl
Glycerin (99%)..... 10 mL
Distilled water ..... 1.3 mL
Mix well, aliquot and store at -20 C°.

10.1.5.2 Gel composition

Separating gel (12%)
For preparing four gels, the following is added:
Distilled water ..... 6 mL
Acr-Bis (29:1) 30% ..... 12 mL
Tris (1M, pH=8.8)..... 11.4 mL
SDS (10%)..... 0.3 mL
APS (10%)..... 0.3 mL
TEMED ..... 0.012 mL
Stacking gel (5%)
The mount needed to prepare four gels:
Distilled water ..... 5.5 mL
Acr-Bis (29:1) 30% ..... 1.3 mL
Tris (1M, pH=6.8)..... 1 mL
SDS (10%)..... 0.08 mL
APS (10%)..... 0.08 mL
TEMED ..... 0.008 mL

10.1.5.3 Running buffer 10x

Glycine..... 144 g
Tris base..... 30.34 g
SDS (10% sol.) ..... 100 mL
Distilled water to ..... 1000 mL

10.1.5.4 Transfer buffer 10x

Glycine..... 144 g
Tris base..... 30.2 g

Distilled water to ..... 1000 mL
For 1L (1X) transfer buffer solution, mix 100 mL transfer buffer (10x), 100 mL methanol, and 800 mL distilled water.

10.1.5.5 TBS 10x buffer

Tris base..... 12.1 g
NaCl..... 87.66 g
Distilled water to ..... 1000 mL
Adjust pH to 7.6. For 1x TBST wash buffer, mix 100 mLl TBS buffer (10x), 900 mL distilled water, and 1 mL Tween 20.

10.1.5.6 Enhanced chemiluminescence (ECL) solution

Solution A
TRIS buffer (0.1M, pH = 8,5) ..... 5 mL
Luminol (250 mM)..... 50 µl
p-coumaric acid (90 mM) ..... 22 µl
Solution B
TRIS buffer (0.1M, pH = 8,5) ..... 5 mL
H_2O_2 30 % (w/w)..... 3 µl
Mix solution A and B in equal ratio directly before use, incubate the washed membrane for 1 min in the ECL solution, dry the membrane and measure the luminescence.

10.1.6 Activated caspase-3 assay

Cell lysis buffer
HEPES (100mM) ..... 50 mL
NaCl (750 mM) ..... 13.3 mL
CHAPS ..... 0.1 g
DTT (1 M) ..... 100 µL
EDTA (100 mM)..... 100 µL
Distilled water to ..... 100 mL
Assay buffer
HEPES (100mM) ..... 50 mL
NaCl (750 mM) ..... 13.3 mL
CHAPS ..... 0.1 g
DTT (1 M) ..... 1 mL
EDTA (100 mM)..... 100 µL
Glycerol ..... 10 mL
Distilled water to ..... 100 mL

10.1.7 Cell isolation

10.1.7.1 Percoll solution

To obtain density of 1,063 g/mL, mix 47.74 mL Easycoll® and 51.26 mL PBS in sterile 250 ml flask according to the following formula:

$$V(\%) = \frac{(\text{‘D} - D\%) \times 10^2}{\text{‘‘D} - D\%}$$

‘D Final required density

‘‘D Density of starting Percoll

D% Density of iso-osmotic diluting solution (PBS)

V(%) The percent needed volume from starting Percoll

10.1.7.2 MACs buffer

BSA ..... 0.5 g
EDTA (0.5 M)..... 0.4 mL
PBS to ..... 100 mL

10.1.7.3 Glucose solution

D-Glucose..... 9 g
Distilled water to 1L
Mix and filter through 0.22 µm filter

10.1.7.4 KH buffer

NaCl..... 60 g
KCl..... 1.75 g
KH_2PO_4..... 1.6 g
Distilled water to ..... 1000 mL
Mix, adjust pH to 7.6, and filter through 0.22 µm filter

10.1.7.5 HEPES buffer 8.5

HEPES ..... 30 g
Distilled water to ..... 500 mL
Mix, adjust pH to 8.5, and filter through 0.22 µm filter

10.1.7.6 HEPES buffer 7.6

HEPES ..... 30 g
Distilled water to ..... 500 mL
Mix, adjust pH to 7.6, and filter through 0.22 µm filter

10.1.7.7 EGTA solution

EGTA..... 475 mg
Distilled water to ..... 10 mL
Mix, adjust pH to 7.6, and filter through 0.22 µm filter

10.1.7.8 $CaCl_2.2\ H_2O$ solution

$CaCl_2.2\ H_2O$..... 1.9 g
Distilled water to ..... 100 mL
Mix and filter through 0.22 µm filter

10.1.7.9 $MgSO_4 .7\ H_2O$ solution

$MgSO_4.7\ H_2O$ ..... 1.23 g
Distilled water to ..... 50 mL
Mix and filter through 0.22 µm filter

10.1.7.9 Amino acids solution

L-Alanine ..... 0.27 g
L-Aspartic Acid ..... 0.14 g
L-Asparagine ..... 0.4 g
L-Citrullin ..... 0.27 g
L-Cysteine ..... 0.14 g
L-Histidine..... 1 g
L-Glutamic Acid ..... 1 g
L-Glycine ..... 1 g
L-Isoleucine ..... 0.4 g
L-Leucine..... 0.8 g
L-Lysine..... 1.3 g
L-Methionine..... 0.55 g
L-Ornithine..... 0.65 g
L-Phenylalanine..... 0.55 g
L-Proline ..... 0.55 g
L-Serine..... 0.65 g
L-Threonine ..... 1.35 g
L-Tryptophan ..... 0.65 g
L-Tyrosine..... 0.55 g
L-Valine ..... 0.8 g
Distilled water to ..... 1000 mL
Mix, adjust pH to 7.6, filter through 0.22 µm filter, aliquot and store at -20 C°.

10.1.7.10 Glutamine solution

Glutamine ..... 0.07 g
Distilled water to ..... 20 mL
Mix and filter through 0.22 µm filter. Always prepare freshly.

10.1.7.11 EDTA buffer

Glucose solution ..... 124 mL
KH buffer ..... 20 mL
HEPES buffer 8.5 ..... 20 mL
Amino acids solution..... 30 mL
Glutamine solution..... 2 mL
EGTA solution ..... 0.8 mL
Mix, warm at 37C° before infusion, and always prepare freshly. The amount can scaled up and down depending on the number of mice used for cells isolation.

10.1.7.12 Collagenase buffer for HCs and KCs

Glucose solution ..... 155 mL
KH buffer ..... 25 mL
HEPES buffer 8.5 ..... 25 mL
Amino acids solution..... 38 mL
Glutamine solution..... 2.5 mL
$CaCl_2.2\ H_2O$ solution ..... 10 mL

Dissolve collagenase (18675 IU) in 40 mL collagenase buffer, filter and complete to 130 mL with collagenase buffer, warm at 37C° before infusion, and always prepare freshly. The amount can be scaled up and down depending on the number of mice used for cells isolation.

10.1.7.13Suspension buffer for HCs

Glucose solution ..... 310 mL
KH buffer ..... 50 mL
Amino acids solution..... 75 mL
Glutamine solution..... 5 mL
$CaCl_2.2\ H_2O$ solution ..... 4 mL
HEPES buffer 7.6 ..... 50 mL
$MgSO_4.7H_2O$ solution ..... 2 mL
BSA ..... 1 g
Mix, and store at 4 C°. The amount can be scaled up and down depending on the number of mice used for cell isolation.

10.1.7.14HSCs isolation buffers

EGTA Buffer
NaCl..... 8 g
KCl ..... 400 mg
$NaH_2PO_4.\ H_2O$..... 88.17 mg
Na_2HPO_4 ..... 120.45 mg
HEPES ..... 2380 mg
$NaHCO_3$..... 350 mg
EGTA..... 190 mg
Glucose ..... 900 mg
Distilled water to ..... 1000 mL
Collagenase buffer
NaCl..... 8 g
KCl ..... 400 mg
$NaH_2PO_4.\ H_2O$..... 88.17 mg
Na_2HPO4..... 120.45 mg
HEPES ..... 2380 mg
$NaHCO_3$..... 350 mg
$CaCl_2.\ 2H_2O$..... 560 mg
Distilled water TO ..... 1000 mL
GBSS/A (Gey's balanced salt solution)
KCl..... 370 mg
$MgCl_2.\ 6H_2O$ ..... 210 mg
$MgSO_4.\ 7H_2O$ ..... 70 mg
Na_2HPO4..... 59.6 mg
KH_2PO_4..... 30 mg
Glucose ..... 991 mg
$NaHCO_3$..... 2270 mg
$CaCl_2.\ 2H_2O$..... 225 mg
Distilled water to ..... 1000 mL

Nycodenz solution
Nycodenz..... 32 g
GBSS/A to ..... 110 mL
Mix well, filter through o.22 µm, and store at 4C°. Adjust pH to 7.38 before use.
Pronase solution
Pronase E..... 90 mg
Collagenase buffer ..... 150 mL
Adjust pH to 7.38 before use:
Collagenase D solution
Collagenase D ..... 63 mg
Collagenase buffer ..... 200 mL
Adjust pH to 7.38 before use.
Stirring solution
Collagenase D ..... 50 mg
Pronase E..... 50 mg
Collagenase buffer ..... 100 mL
DNase (1mg/mL) ..... 200 µL
Adjust pH to 7.38 before use.

10.2 Mediums

Table 10.1 Culture mediums and conditions

Cells	Medium
Primary cells	
Hepatocytes	**Medium 1**: William E, 10% FBS, 2mM L-Glutamine (Glut), penicillin/streptomycin (P/S) (100 U/ml and 0.1 mg/ml respectively), and Dexamethasone (10^{-7} M). Used for the first 4 h after cells seeding to help cell attachment, then replaced by medium 2 for another 4 h. **Medium 2**: as medium 1 but without FBS **Medium 3**: as medium 2 but without Dexamethasone. The cells were treated in medium 3.
Hepatic stellate cells	**Growth medium**: DMEM high glucose, 10 % FBS, 2mM L-Glut, and P/S (100 U/ml and 0.1 mg/ml respectively). **Starvation medium**: same as growth medium but without FBS
Kupffer cells	**Growth medium**: DMEM high glucose, 10 % FBS, 2mM L-Glut, and P/S (100 U/ml and 0.1 mg/ml respectively). **Starvation medium**: same as growth medium but without FBS
Cell lines	
JS-1 (mouse HSC)	**Growth medium**: DMEM high glucose, 10 % FBS, 2mM L-Glut, and P/S (100

	U/ml and 0.1 mg/ml respectively). **Starvation medium**: same as growth medium but without FBS
AML-12 (mouse hepatocytes)	**Growth medium**: DMEM/F12, 10 % FBS, 2mM L-Glut, P/S (100 U/ml and 0.1 mg/ml respectively), ITS (1X), and Dexamethasone (10^{-7} M) **Starvation medium**: Same as growth medium but without FBS.
RAW264.7	**Growth medium**: DMEM high glucose, 10 % FBS, 2mM L-Glut, and P/S (100 U/ml and 0.1 mg/ml respectively). **Starvation medium**: same as growth medium but with 1% FBS

10.3 Supplementary results

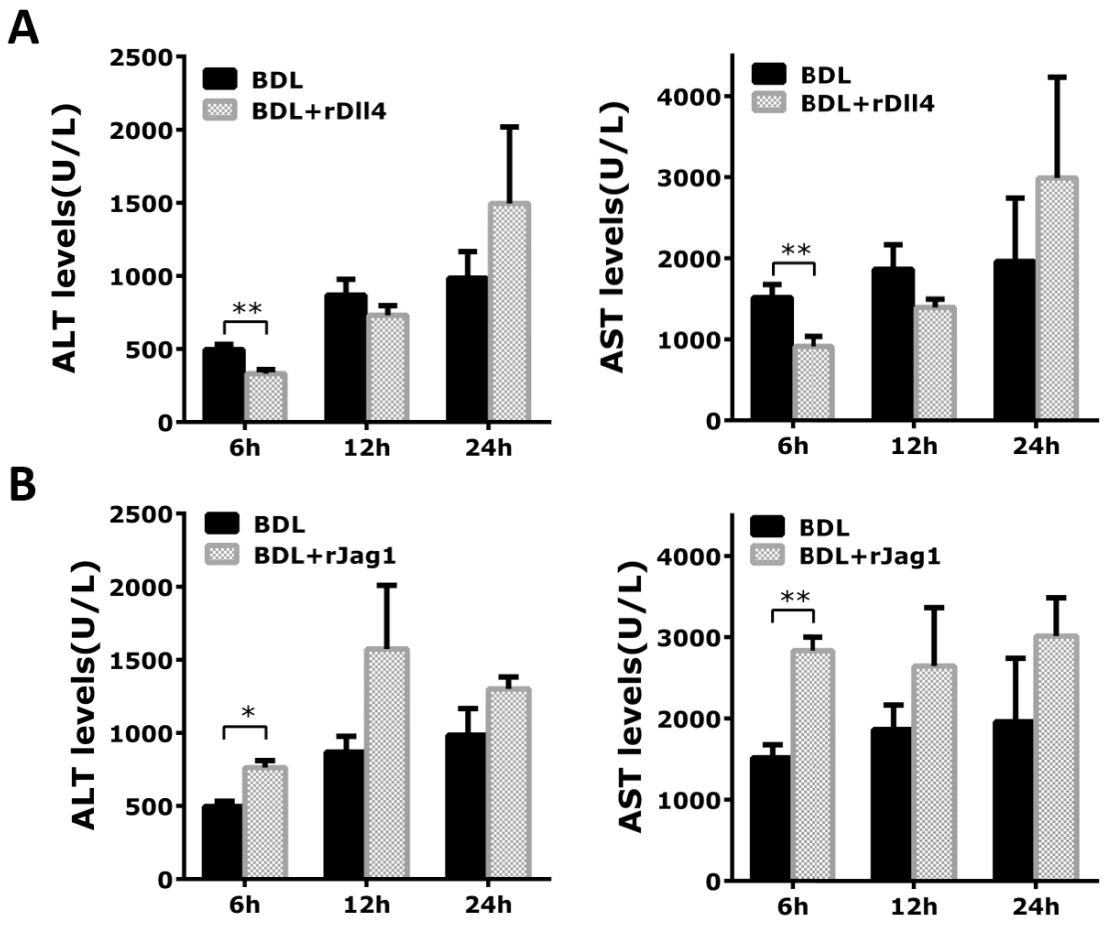

Figure 10.1 Serum alanine aminotransferase (ALT) and aspartate aminotransferase (AST) levels were quantified with a Hitachi 7600-110 automatic analyzer (Tokyo, Japan) in BDL mice treated with or without rDll4 (A) and rJag-1 (B) at different time points after BDL operation (n=6 per group). Results were generated by collaboration with Shen et al., Zhejiang University, China.

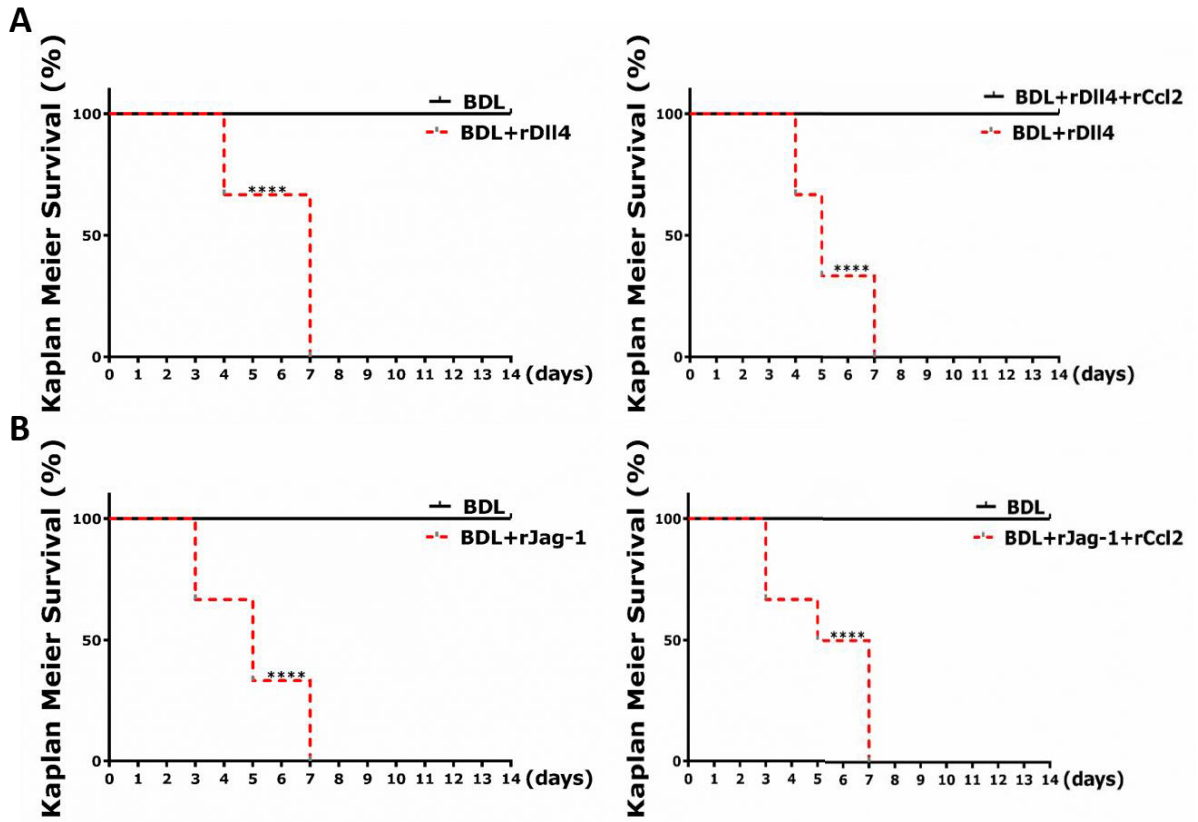

Figure 10.2 Kaplan-Meier survival curve showing mortality of BDL mice after treatment with/without (A) rDll4 and rDll4+rCcl2 (B) rJag-1 and rJag-1+rCcl2. The experiment was repeated 3 times (n=6 per group). Results were generated in collaboration with Shen et al., Zhejiang University, China.

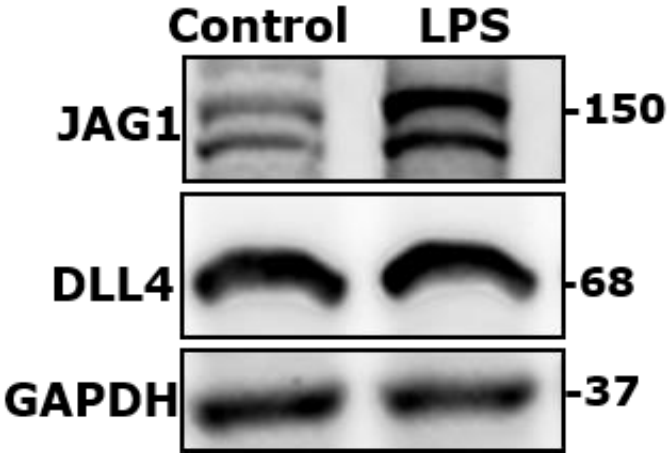

Figure 10.3 Expression of JAG1 and DLL4 after treatment of RAW264.7 cells with LPS (20 ng/ml) for 24 h.